The Design and Assembly of 3D Liver Mimetic Cellular Architectures

Yeonhee Kim

Dissertation Submitted to the Faculty of the Virginia Polytechnic Institute and State University
in partial fulfillment of the requirements for the degree of

Doctor of Philosophy
In
Chemical Engineering

Padmavathy Rajagopalan, Chair
Richey M. Davis
Yong W. Lee
T.M. Murali
Abby W. Morgan

September 7, 2010
Blacksburg, VA

Keywords: liver mimics, polyelectrolyte multilayers, gene expression, DNA microarray, cytochrome P450, intercellular communications

The Design and Assembly of 3D Liver Mimetic Cellular Architectures

Yeonhee Kim

ABSTRACT

We report the assembly of three-dimensional (3D) liver sinusoidal mimics comprised of primary rat hepatocytes, human or rat liver sinusoidal endothelial cells denoted as hLSECs and rLSECs respectively, and an intermediate chitosan-hyaluronic acid (HA) polyelectrolyte multilayer (PEM). The height of the PEMs ranged from 30-55nm and exhibited a shear modulus of ~ 100kPa. Primary rat hepatocytes coated with 5 and 15 PE layers exhibited stable urea and albumin production over a seven day period and these values were either comparable or superior to that in a collagen sandwich (CS). Hepatocyte-PEM-hLSEC liver mimics exhibited stable urea production and increasing albumin secretion over the culture period in comparison to hepatocyte-LSEC samples. In the 3D liver mimics, hLSEC phenotype was maintained and verified by the uptake of acetylated low-density lipoprotein (AcLDL). A sixteen-fold increase in CYP1A1/2 activity was observed for hepatocyte-PEM-10,000 hLSEC samples, thereby, suggesting that interactions between hepatocytes and hLSECs play a key role in enhancing hepatic phenotypes in *in vitro* cultures. As the first step towards elucidating key signaling pathways involved in cell-cell communications, global genome-wide transcriptional profiles of primary hepatocytes cultured in CS and hepatocyte monolayers (HMs) were performed over an eight-day period using DNA microarray measurements and Gene Set Enrichment Analysis (GSEA) in order to derive biologically meaningful information at the level of gene sets. The gene expression in CS cultures steadily diverged from that in HMs. Gene sets up-regulated in CS are those linked to liver metabolic and synthetic functions, such as lipid, fatty acid, alcohol and carbohydrate metabolism, urea production, and synthesis of bile acids. Monooxygenases such as CYP enzymes were significantly up-regulated starting on day 3 in CS cultures. These results serve as a baseline for further investigation into the systems biology of engineered liver tissues. 3D hepatic constructs were also assembled with primary rat hepatocytes and rLSECs, and a chitosan-HA PEM. In these hepatic models, the phenotype of hepatocytes and rLSECs were maintained. rLSEC phenotype was verified over a twelve-day period through immunostaining with the sinusoidal endothelial-1 (SE-1) antibody. In contrast, rLSECs cultured as monolayers lost their phenotype within 3 days. A two-fold increase in albumin production was observed only in the 3D liver models. rLSEC-

PEM-hepatocyte cultures exhibited three- to six-fold increased CYP1A1/2 and CYP3A enzymatic activity. Well-defined bile canaliculi were observed in only 3D hepatic constructs. In summary, these results indicate that the layered rLSEC-PEM-hepatocyte constructs can be used as liver models for future studies.

Acknowledgements

I would like to thank my advisor, Dr. Padma Rajagopalan, for her great guidance throughout my graduate career, and her tremendous support for me to grow as an independent scientist. I really appreciate her patience and willingness in allowing me to pursue the research and experiments that I found interesting and providing endless opportunities to present my research at several conferences. Without her support, these research projects could not have been accomplished. I am also grateful to Dr. T.M. Murali for providing the opportunity to participate in the gene expression project and his invaluable advice and assistance in the field of computational analysis. I would like to thank Dr. Richey M. Davis for his critical input and advice on characterization of biomaterials and his willingness to serve on my graduate committee. I also thank Dr. YongWoo Lee and Dr. Abby W. Morgan for their valuable time and critical comments on my research and their service on my graduate committee.

I am grateful to fellow graduate students and labmates, Dr. Christopher J. Detzel, Adam L. Larkin, Christopher D. Lasher, Adedayo Adeniran, Hale Cigdem Arca, and Nathan Hale for their friendly support and assistance within and outside the lab. Their enthusiasm and hard work were a tremendous source of inspiration and encouragement. I would like to thank Adam Larkin for taking the time to conduct measurements of physical properties of PEM reported in Chapter 2 and to Christopher D. Lasher for his computational analysis reported in Chapter 3. I would also like to thank the undergraduate students who helped and worked with me, Christine Sargent, Logan Milford, Aruna Nagarajan, and Reisha Parham.

I would like to thank my friends, Eunna Chung, Albert Kwansa, and Yujung Dong for helping me open up my mind, having a time to listen to me, and giving me invaluable advice when I need it.

I would like to thank my family for their endless love, support, and encouragement. Most importantly, I am indebted to my husband, Sangil Han, for his unconditional love and support through the ups and downs of my graduate life. Without his patience this would not have been possible.

I gratefully acknowledge the financial support provided by the National Institutes of Health, the National Science Foundation, Thomas F. and Kate Miller Jeffress Foundation, the Institute for Critical Technology and Applied Sciences (ICTAS) at Virginia Tech.

Table of Contents

List of Figures

Chapter 1

Chapter 2

Chapter 3

Chapter 4

List of Tables

List of Abbreviations

3,3'-diotadecylindocarbocyanine	DiI
3-methylcholanthrene	3MC
4-(2-hydroxyethyl) piperazine-1-ethanesulfonic acid	HEPES
Acetylated low-density lipoprotein	AcLDL
Benzyloxyresorufin *o*-dealkylase	BROD
Bovine serum albumin	BSA
Collagen sandwich	CS
Cytochrome-P450	CYP
Di-peptidyl peptidase IV	DPP IV
Dulbecco's modified eagle medium	DMEM
Earle's balanced salt solution	EBSS
Engelbreth-Holm-Swarm	EHS
Enzyme-linked immunosorbent assay	ELISA
Ethoxyresorufin *o*-deakylase	EROD
Ethylene diamine tetra acetic acid	EDTA
Extracellular matrix	ECM
Fluorescein isothiocyanate	FITC
Gene set enrichment analysis	GSEA
Hank's buffered salt solution	HBSS
Hepatic stellate cells	HSCs
Hepatocyte growth factor	HGF
Hepatocyte monolayers	HMs
Human aortic endothelial cells	HAECs
Human liver sinusoidal endothelial cells	hLSECs
Human umbilical vein endothelial cells	HUVECs
Hyaluronic acid	HA
Immunoglobulin G	IgG
Linear models for microarray data	LIMMA
Liver sinusoidal endothelial cells	LSECs

Liver X receptor	LXR
Peroxisome proliferation-activated receptor alpha	PPARα
Phosphate-buffered saline	PBS
Platelet derived growth factor	PDGF
Platelet endothelial cell adhesion molecule	CD31
Poly (*N*-isopropylacrylamide)	NiPAAM
Polyelectrolyte	PE
Polyelectrolyte multilayer	PEM
Polyelectrolyte multilayer	PEM
Quartz crystal microbalance with dissipation	QCM-D
Rat liver sinusoidal endothelial cells	rLSECs
Retinoid X receptor	RXR
Sinusoidal Endothelial-1	SE-1
Sodium dodecyl sulfate	SDS
Three-dimensional	3D
Transforming growth factor beta	TGF-β
Vascular endothelial cell growth factor	VEGF

Chapter 1. Introduction and Background

1.1 Liver Function and Structure

As one of the largest and most important organs in our bodies, the liver carries out a broad range of essential functions such as carbohydrate, lipid, and amino acid metabolism, plasma and protein synthesis, biotransformation of xenobiotics, drugs, and toxins, and bile production. The liver is known to have a remarkable capability for regeneration (1-4). The liver plays a major role in glucose homeostasis (1-4). Excess carbohydrates are stored as glycogen, which can be converted back to glucose for energy (1-4). It is the major organ for synthesis and secretion of serum lipoproteins. It also plays important roles in cholesterol and steroid metabolism and in the metabolism of the fat-soluble vitamins such as vitamins A and D (1-4). The liver is the main source for biosynthesis of plasma proteins such as albumin, globulin, fibrinogen, and prothrombin (1-4). In the case of deamination of amino acids, liver cells have all the necessary enzymes to complete their conversion to urea. The liver is responsible for metabolizing xenobiotics, drugs and toxins (1-4). The smooth endoplasmic reticulum in the liver cells is a cellular component which is responsible for drug metabolism involved in the inactivation process through phase I enzymes such as cytochrome P450 1A, 2B and 3A isoforms, and phase II enzymes such as sulfotransferases, UDP-glucuronosyltransferases and glutathione S-transferases (1-4). On a daily basis, the liver produces and secretes bile which plays a critical role in the metabolism of cholesterol and in the emulsification of fats (1-4). Pigments resulting from the breakdown of aged erythrocytes, such as bilirubin, are excreted into the bile canaliculi through which the bile secreted by the hepatocytes is transferred out of the liver.

Liver zonation is characterized by regional variations in terms of oxygen tension along the liver sinusoids from the portal vein (pO_2: 60-70 mmHg) to the central vein (pO_2: 30-35 mmHg) (5-8). The acinus, a microcirculatory unit of the liver, extends from a terminal portal venule and a terminal hepatic arteriole, which delivers blood into the sinusoids, and subsequently to the central and hepatic veins (5-8). The upstream region around the terminal portal vein is called the periportal zone; the area around the central vein is known as the perivenous, pericentral, or centrilobular zone (5-8). In the liver parenchyma, the key enzymes of various metabolic pathways and their concentrations are distributed asymmetrically. The capacity for oxidative energy metabolism, glucose formation, urea production, plasma protein synthesis, and

bile formation is greater in the periportal region while the capacity for glucose uptake, glutamine formation, and xenobiotic metabolism is higher in the perivenous area (5, 6, 8, 9).

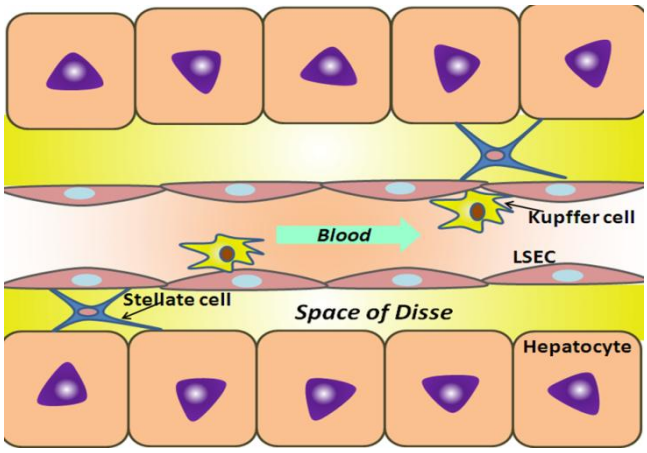

Figure 1.1 Schematic of a liver sinusoid

The primary parenchymal cells found in the liver are called hepatocytes (**Figure 1.1**). Within the parenchyma, hepatocytes have three polarized domains: the apical domains form bile canaliculi that are involved in the transport of bile acids and xenobiotic metabolites; the basal domain is in contact with the extracellular matrix (ECM) region known as the Space of Disse; and the lateral domain is characterized by tight junctions with neighboring hepatocytes (1). The Space of Disse is the interfacial region between the hepatocytes and the hepatic microvasculature (also known as the liver sinusoids). The ECM is highly organized and composed of proteins (collagen type I, II, IV, and V), glycoproteins (fibronectin, laminin, tenascin, and osteonectin), proteoglycans (heparin sulfate, and chondroitin sulfate), and glycosaminoglycans (hyaluronan) (5). The sinusoids are lined with liver sinusoidal endothelial cells (LSECs), which possess fenestrae. These are pores that play a critical role in regulating the exchange of fluids, solutes, and particles (10). The fenestrae are approximately 100-200nm in diameter and allow the passage of small molecules and other metabolites to the hepatocytes through the Space of Disse (10). For these reasons, the Space of Disse is often referred to as a "molecular sieve." Kupffer cells are the resident macrophages and these cells reside within the vasculature. In their capacity as macrophages, these cells are mainly involved in clearing endotoxins from the bloodstream and the phagocytosis of foreign bodies or waste particles (11). Hepatic stellate cells, referred to as

fat-storing cells, play an important role in remodeling the ECM, in the storage of retinoids, and in the secretion of various cytokines (**Figure 1.1**) (12-14).

1.2 Cell Types Found in the Liver

1.2.1 Hepatocytes

Hepatocytes are the principal parenchymal cells found in the liver, and account for 60-80% of the total volume of the liver (1). These cells are responsible for several liver-specific functions. They perform carbohydrate, lipid and amino acid metabolism, detoxification of xenobiotics and drugs. In addition, they are involved in the biosynthesis of plasma proteins such as albumin, transferrin, and α-fetoprotein, regulation of urea, and bile synthesis (1-4). Hepatocytes exhibit a polarized structure that is manifested at multiple levels: in their overall cell shape, in the organization of their cytoskeleton, and through the presence of functionally defined domains in their plasma membrane (1, 14). Hepatocytes exhibit a polygonal morphology, with f-actin localized in the peripheral regions. Cellular polarization is necessary for the maintenance of hepatic phenotypic functions (1, 2, 15). Since hepatocyte-specific phenotypic functions decrease significantly once the cells are detached from the organ, a wide range of culture conditions have been developed over the years to optimize *in vitro* cultures (1, 2, 16, 17).

Some of the strategies employed to preserve phenotypic function are providing a compatible ECM-based substrate, the addition of soluble factors such as hormones to the culture medium and the optimization of the cell-environment interactions (2, 14, 16-18).

1.2.2 Liver Sinusoidal Endothelial Cells (LSECs)

LSECs account for approximately 10-20% of cells found in the liver (19). LSECs form a sinusoidal wall, also called the endothelium, or endothelial lining (1, 10). The liver sinusoids are regarded as unique capillaries that differ from those found in other organs due to the presence of nanoscale pores, also called fenestrae (10). In general, the size of endothelial fenestrae is approximately 150–200 nm in diameter, and they can be clustered to form grouped fenestrae that act as a dynamic filter or as a sieve (10, 19). These fenestrae can contract or expand in response to a wide range of cues such as hormones, drugs, toxins, and diseases. In addition, they enable or prevent the entry of metabolites, pathogens, or circulating cancerous cells (10, 19, 20).

LSECs are capable of significant receptor-mediated endocytosis (20). These cells are often classified as "scavenger" cells since they possess several high affinity endocytotic receptors that enable the endocytosis of collagen, hyaluronate, mannose, and cholesterol (20-28). A unique marker of LSECs is receptor-mediated endocytosis of acetylated low-density lipoprotein (AcLDL), a metabolite formed as a result of lipid metabolism (29, 30). Through a combination of endocytosis and transcytosis, LSECs can transport macromolecules from the bloodstream to the Space of Disse (10, 19). Therefore, LSECs can also be regarded as a selective barrier for macromolecules and as a scavenger system by removing several waste products from the bloodstream and the liver.

1.2.3 Kupffer Cells

Kupffer cells are the liver's macrophage cells. Approximately 20% of the nonparenchymal liver cells are comprised of Kupffer cells (1). These cells play a critical role in mediating the acute and chronic responses of the liver to toxic compounds and in maintaining hepatic homeostasis (9). Kupffer cells are present in the liver vasculature and reside within the lumen of the hepatic sinusoids. Therefore, they are the first cells to be exposed to toxins absorbed from the gastrointestinal tract (31). The primary functions of Kupffer cells include phagocytosis of foreign bodies, removal of endotoxins, antigen presentation, production of pro-inflammatory cytokines, and the modulation of immune and inflammatory responses (1, 9, 31-37). Kupffer cells that are activated by pathogenic agents release inflammatory signaling molecules such as cytokines, nitric oxide, chemokines, growth factors, and reactive oxygen species (31). In a non-inflamed liver, Kupffer cells secrete anti-inflammatory mediators, such as interleukine-10, endogenous prostanoids and TGF-β (11, 31). These cells can pass through the Space of Disse, in order to make a direct contact with hepatocytes and to phagocytose apoptotic hepatocytes (9, 31, 36, 37).

1.2.4 Stellate Cells (Ito Cells or Fat Storing Cells)

Hepatic stellate cells (HSCs), also referred to as Ito cells, fat-storing cells, vitamin A-storing cells or lipocytes, are located in the perisinusoidal Space of Disse and account for approximately 5-8% of the liver (11, 36, 38). These cells are responsible for retinoid storage in order to maintain normal cell proliferation, differentiation, a healthy immune system and vision

(36, 39), and for the reorganization of the ECM by the production of ECM components such as type I, III, IV, VI collagen, fibronectin, laminin, proteoglycans and matrix metalloproteinases (12). They are also involved in the production of growth factors, cytokines, and control the contraction and expansion of the sinusoidal lumen in response to vasoconstricting peptides (12, 13). HSCs exhibit two distinct phenotypes: 'quiescent' and 'activated'. In their quiescent state, HSCs exhibit characteristics such as cytoplasmic lipid droplets and long dendritic-like cytoplasmic prolongations that wrap the sinusoids (12, 14). In the activated state, HSCs lack lipid droplets and display proliferative myofibroblast-like morphology (12). The expression of α-smooth muscle actin and intermediate filaments such as vimentin and desmin are regarded as markers for quiescent HSCs (12).

1.3 *In Vitro* Hepatocyte Culture Systems

When hepatocytes are isolated from the liver and cultured in conventional 2D culture conditions, liver-specific functions such as protein synthesis, lipid, amino acid and carbohydrate metabolism, and xenobiotics biotransformation rapidly decrease within 48h (1, 2, 16, 17, 40). There have been extensive efforts to mimic the *in vivo* hepatic environment by controlling cell-ECM interactions (16, 17, 41), homotypic and heterotypic cell-cell interactions (18, 40, 42-53), and through the addition of hormones and other soluble factors (2, 54).

In vitro culture systems commonly used are, monolayers of cells, collagen sandwiches and Matrigel^{TM} substrates (16, 17, 41). In general, hepatocytes cultured as a monolayer attached to ECM proteins such as collagen or laminin do not exhibit optimal liver-specific function (16, 17, 41). When cultured in a collagen sandwich configuration, hepatocyte morphology, cytoskeletal structure, and a wide range of liver-specific functions have been shown to be maintained over long time periods (16, 17, 41). Matrigel^{TM}, a basement membrane extract from Engelbreth-Holm-Swarm (EHS) mouse sarcoma, enables the formation of spheroids and thereby increases cell-cell contacts (16). Cells cultured on Matrigel^{TM} have been shown to exhibit stable hepatic phenotype as well. However, culturing of only hepatocytes does not recapitulate the 3D hepatic environment found *in vivo* where complex homotypic and heterotypic cellular interactions promote and preserve liver functions.

In an effort to introduce heterotypic cell-cell interactions, hepatocytes have been cultured in 2D systems with other cells types such as fibroblasts or endothelial cells (45-48, 53). Liver-derived cell types include liver epithelial cells (42, 43), sinusoidal endothelial cells (44, 45), rat stellate cells (46), Kupffer cells (47, 48) and the entire 'nonparenchymal' fraction of isolated liver cells (49). As non-liver-derived cell types, embryonic murine 3T3 cells (50), rat dermal fibroblasts(51), and bovine aortic endothelial cells (51, 52) and human fibroblasts(18) have also been investigated. The effects of cell-cell communication have been shown to benefit both the parenchymal and the non-parenchymal cells (40). Co-culturing of hepatocytes with fibroblasts on micropatterned surfaces enables heterotypic cell-cell interactions that lead to the enhancement of hepatic functions(53). Hepatocytes co-cultured with LSECs (45) or Kupffer cells (47, 48) have exhibited the maintenance of hepatocyte-specific phenotype and long-term survival. Although 2D co-culture systems can maintain hepatic phenotype over time, these cultures do not mimic the 3D multi-cellular features found *in vivo*.

More recently, methods to develop 3D layered tissue constructs using temperature-responsive polymers and magnetite particles have been reported (55-59). Poly (*N*-isopropylacrylamide) (NiPAAM), a thermo-responsive polymer, has been used to culture cell layers. Since NiPAAM reverts to its monomeric forms at 20°C, cells can be lifted off as a cell sheet. This feature of NiPAAM was used to culture and list a sheet of human aortic endothelial cells (HAECs). This cell sheet was subsequently placed above a confluent layer of hepatocytes (55-57). In another study, HAECs were exposed to magnetite cationic liposomes and through the use of a magnetic field these cells were layered onto hepatocytes (58, 59). Although such cell-layering approaches have the potential to mimic the 3D stratified aspects of liver structure they pose severe limitations. The effects of a toxic monomer, the destruction of cell sheets and the long-term effect of magnetic particles render such approaches infeasible for practical applications.

1.4 Research Objectives

The research objectives of this thesis are motivated by the need to assemble multi-cellular hepatic architectures that mimic *in vivo* liver structure. Such hepatic constructs can be used to systematically study the effects of a wide range of cues that will enable the elucidation of several

hepatic pathways and in understanding liver physiology. 3D liver-mimetic cellular architectures will be assembled using primary hepatocytes, an intermediate polyelectrolyte multilayer (PEM) that mimics the Space of Disse, and LSECs. Hepatocyte-specific functions will be investigated for the 3D liver mimics and compared to cells cultured as monolayers or in collagen sandwich cultures. Heterotypic cell-cell interactions will be probed using a combination of DNA microarrays and proteomics.

The research objectives of this thesis are:

1. Assemble 3D *in vitro* hepatic architectures comprised of primary hepatocytes, an intermediate PEM consisting of chitosan and hyaluronic acid, and LSECs.
2. Investigate phenotypic functions in the 3D constructs and compare results to hepatocytes cultured in monolayers and in collagen sandwiches.
3. Conduct genome-wide transcriptional profiles of primary hepatocytes cultured in a collagen sandwich and a monolayer.

1.5 Experimental Plan

1.5.1 Aim 1: Design and Assemble 3D Liver Sinusoidal Mimics

The first task was to assemble 3D liver sinusoidal mimics comprised of primary rat hepatocytes, a nano-scale polyelectrolyte multilayer (PEM), and human LSECs (hLSECs). PEM sconsisting of alternating layers of chitosan and hyaluronic acid were assembled to mimic the Space of Disse that is a protein-rich interface between two cell types. The optimal PE layers that exhibited optimal hepatic functions were determined by measurement of urea and albumin production. The mechanical properties of PEM were measured using quartz crystal microbalance with dissipation (QCM-D). The 3D hepatic constructs were assembled by layering hLSECs on hepatocyte-PEM samples. Hepatocyte-PEM-hLSEC cellular constructs were maintained for up to 10 days. Hepatocyte phenotypic functions in the 3D liver mimics were monitored by measurement of urea and albumin production, immunostaining of bile canaliculi, and cytochrome-P450 (CYP) 1A1/2 enzyme activity. hLSEC phenotype was monitored by receptor-mediated endocytosis of acetylated low-density lipoprotein (AcLDL).

1.5.2 Aim 2: Genome-Wide Transcriptional Profiles of Primary Hepatocytes Cultured in CS and Monolayers

Primary hepatocytes were cultured in two widely used culture systems: collagen sandwich (CS) and hepatocyte monolayers (HMs). Each culture system was maintained for a eight-day period. On days 1, 2, 3 and 8 after the deposition of second layer of collagen, total RNA was extracted and purified. The RNA samples were used to conduct DNA microarray measurements. The DNA microarray data were analyzed *via* Gene Set Enrichment Analysis (GSEA) which is a powerful tool to summarize the differential expression of genes at the level of pre-defined gene sets.

1.5.3 Aim 3: Construction of 3D Liver Mimetic Cellular Architectures Comprised of Primary Rat Hepatocytes and Rat LSECs

The third task was to construct 3D liver mimetic cellular architectures comprised of primary rat hepatocytes and rat LSECs (rLSECs), and a chitosan-hyaluronic acid PEM as an interface. Primary rLSECs were isolated and purified *via* a density gradient centrifugation method. rLSECs were used to assemble the 3D hepatic models as described in Chapter 2. rLSECs-PEM-Hepatocyte cellular architectures were visualized by staining rLSECs with non-toxic cell-permeable dye prior to seeding on hepatocytes coated with 5 or 15 PE layers. The 3D hepatic cultures were maintained over a 12-day culture period. rLSEC phenotype was monitored by immunostaining for the sinusoidal endothelial-1 (SE-1) rLSEC marker over 12-day period. Separation of rLSECs and hepatocytes was conducted using SE-1 antibody-tagged Dynabeads® in order to normalize hepatocyte functions to the actual number of hepatocytes present in each sample. Hepatocyte-specific functions were measured by urea and albumin production and CYP1A1/2 and CYP3A enzyme activity. Cell polarity of hepatocytes was verified by immunostaining of bile canaliculi.

Reprinted from Kim, Y. et al. *Tissue Engineering: Part A*, 2010; 16(9):2731-41.with permission from Mary Ann Liebert, Inc. publishers.

Chapter 2. The Design of *In Vitro* Liver Sinusoid Mimics Using Chitosan-Hyaluronic Acid Polyelectrolyte Multilayers

Y. Kim conducted the isolation of primary rat hepatocytes (Section 2.3.2), prepared 3D liver mimics as well as collagen sandwich and hepatocyte monolayer cultures (Sections 2.3.3 and 2.3.4), measured urea and albumin productions (Sections 2.3.6, 2.4.2, and 2.4.6, and Figures 2.1, 2.2, and 2.6) monitored hLSEC phenotypic functions by AcLDL uptake (Sections 2.3.9 and 2.4.5, and Figure 2.5), conducted imaging of the actin cytoskeleton, 3D liver mimics, and bile canaliculi (Sections 2.3.7, 2.3.8, 2.3.10, 2.4.3, 2.4.4, and 2.4.7, and Figures 2.3, 2.4, and 2.7) and measured cytochrome-P450 1A1/2 enzyme activity (Sections 2.3.11, 2.3.12, 2.3.13, 2.3.14, and 2.4.8, and Figure 2.8) .

A.L. Larkin conducted the measurement of the physical properties of chitosan-hyaluronic acid polyelectrolyte multilayers using quartz crystal microbalance with dissipation (Sections 2.3.5, and 2.4.1, and Table 2.1).

Reprinted from Kim, Y. et al. *Tissue Engineering: Part A*, 2010; 16(9):2731-41.with permission from Mary Ann Liebert, Inc. publishers.

Chapter 2. The Design of *In Vitro* Liver Sinusoid Mimics Using Chitosan-Hyaluronic Acid Polyelectrolyte Multilayers

2.1 Abstract

Interactions between hepatocytes and liver sinusoidal endothelial cells (LSECs) are essential for the development and maintenance of hepatic phenotypic functions. We report the assembly of 3-D liver sinusoidal mimics comprised of primary rat hepatocytes, LSECs and an intermediate chitosan-hyaluronic acid polyelectrolyte multilayer (PEM). The height of the PEMs ranged from 30-55nm and exhibited a shear modulus of ~ 100kPa. Hepatocyte-PEM cellular constructs exhibited stable urea and albumin production over a seven day period and these values were either higher or similar to cells cultured in a collagen sandwich. This is of significance, since the thickness of a collagen gel is approximately 1000-fold higher than the height of the chitosan-HA PEM. In the hepatocyte-PEM-LSEC liver mimetic cellular constructs, LSEC phenotype was maintained, and these cultures exhibited stable urea and albumin production. CYP1A1/2 activity measured over a 7-day period was significantly higher in the hepatocyte-PEM-LSEC constructs in comparison to collagen sandwich cultures. A 16-fold increase in CYP1A1/2 activity was observed for hepatocyte-PEM-10,000 LSEC samples, thereby, suggesting that interactions between hepatocytes and LSECs are critical in enhancing the detoxification capability in hepatic cultures *in vitro*.

2.2 Introduction

The liver is one of the largest organs in our bodies and performs a multitude of functions such as metabolism, detoxification, and plays a major role in the body's complex defense mechanisms. The deterioration in any one of the liver's functions can cause serious, life-threatening health problems. The liver is comprised of approximately 70% hepatocytes (parenchymal cells) and the remainder is made up of non-parenchymal (liver sinusoidal endothelial, Kupffer and hepatic stellate) cells (1). Liver sinusoids *in vivo* contain layers of hepatocytes and endothelial cells separated by the Space of Disse comprised primarily of collagen fibers (1).

The lack of organ donors, the rising cost of organ transplant surgeries, and the complications related to immune response are issues that confront patients. The use of extra-corporeal liver-assist devices also known as bio-artificial livers, have the potential to enable the recovery of patients with injured livers or function as a "bridge" to transplantation (60).

The design of extracorporeal liver assist devices can be accelerated if three-dimensional (3-D) liver mimics are available to systematically test cellular response to a variety of stimuli. In addition, the testing of drugs and pharmaceuticals are conducted on monolayers of hepatocytes or on animals. Hepatocyte monolayers do not present a physiologically relevant model and animal models can be very expensive and complex to analyze. Although two-dimensional (2-D) cell cultures and co-cultures are used extensively as model systems (17, 40, 41, 50, 53, 61-63), they do not recapitulate key spatial, geometric, and physiological characteristics of cellular architectures found *in vivo*. The complex heterotypic interactions between parenchymal (hepatocytes) and non-parenchymal (LSEC) cells in the liver are responsible for optimal hepatic function. Recent reports in the literature have shown that even at the embryonic stage, interactions between endothelial cells and hepatic progenitor cells are critical for normal liver development (64-66). Since interactions between the parenchymal and non-parenchymal cells of the liver are critical in maintaining optimal hepatic function (45, 67, 68), efforts to layer these cells to emulate liver architecture *in vivo* are ongoing. Recently, new approaches to form layered 3-D liver-like tissues have been reported (56, 58, 69-72). Temperature-responsive culture dishes, magnetic liposome technology, and organ-printing techniques have been utilized to form layered cell sheets. A temperature responsive polymer (N-isopropyl acrylamide) was used to release aortic endothelial cells as a sheet and then placed above a monolayer of hepatocytes to form a sinusoidal structure (56). In other reports, magnetic cationic liposomes were introduced into endothelial cells which were subsequently placed above hepatocytes to form a layered hepatic construct (58). Although, these methodologies offer new avenues to assemble liver mimics, issues related to long-term stability and ease in handling and assembly are of concern.

The distance of separation between hepatocytes and endothelial cells in the liver, the Space of Disse, is a critical factor in assembling liver-mimetic tissues (73). *In vitro*, the presence

of an interfacial region has been shown to play a significant role in the assembly and performance of liver mimics. In a previous report, hepatocytes and human umbilical vein endothelial cells (HUVECs) were assembled in stratified layers by incorporating a chitosan/DNA PEM between the cell layers (73). This study demonstrated the need for an interface between hepatocytes and HUVECs to obtain optimal hepatic phenotypic function and showed that PEMs could potentially mimic and function as the Space of Disse *in vitro*. Some of the drawbacks in this study were the use of DNA as the polyanion and HUVECs. DNA is susceptible to enzymatic degradation and HUVECs exhibit significantly different phenotypic characteristics in comparison to LSECs.

We report the assembly of liver mimetic architectures comprised of primary rat hepatocytes and human LSECs with an intermediate PEM comprised of chitosan and hyaluronic acid (HA). Chitosan was selected as the cationic PE due to its compatibility with hepatocytes (74-76). HA is found in the basal membranes of connective tissues is utilized to modify surfaces for the culture of endothelial cells (77, 78). We have measured the shear modulus and viscosity of the hydrated chitosan/HA PEM and have conducted studies that demonstrate that liver-specific functions such as urea and albumin secretion, as well as cytochrome P450 (CYP1A1/2) enzymatic activity are maintained and enhanced in the liver mimetic cellular architectures.

2.3 Materials and Methods

2.3.1 Materials

Dulbecco's Modified Eagle Medium (DMEM) containing 4.5 g/L glucose, phosphate-buffered saline (PBS), Earle's balanced salt solution (EBSS), Hank's buffered salt solution (HBSS), ethoxy resorufin, penicillin, streptomycin, and trypsin-EDTA was obtained from Invitrogen Life Technologies (Carlsbad, CA). Type IV collagenase, HEPES (4-(2-hydroxyethyl) piperazine-1-ethanesulfonic acid), glucagon, hydrocortisone, ammonia, dicumarol, sodium dodecyl sulfate (SDS), and hydrogen peroxide were obtained from Sigma-Aldrich (St. Louis, MO). Human LSECs and endothelial cell growth medium and supplements were obtained from ScienCell Research Laboratories (San Diego, CA). Unless noted, all other chemicals were obtained and used as received from Fisher Scientific (Pittsburgh, PA).

2.3.2 Hepatocyte Isolation and Culture

Primary rat hepatocytes were harvested from female Lewis rats (Harlan, Indianapolis, IN) that weighed between 170-200g. A two-step *in situ* collagenase perfusion method was utilized (17, 41). Briefly, animals were anesthetized with 3 L/min of a gas mixture of 3% (v/v) isofluorane/97% oxygen (Veterinary Anesthesia Systems Co., Bend, OR). The liver was perfused through the portal vein with oxygenated Krebs Ringer Buffer (KRB; 7.13 g/L sodium chloride, 2.1 g/L sodium bicarbonate, 1 g/L glucose, 4.76 g/L HEPES and 0.42 g/L potassium chloride) that contained 1mM EDTA (ethylene diamine tetra acetic acid), followed by serial perfusion with a 0.075% w/v and a 0.1% w/v collagenase (Sigma, Type IV) in KRB containing 5 mM calcium chloride. Cell suspensions were filtered through nylon meshes with porosity ranging from 250-62 μm (Small Parts, Inc., Miramar, FL). Hepatocytes were separated using a Percoll (Sigma-Aldrich) density centrifugation technique. In a typical separation procedure, 12.5 mL of cell suspension was added to 10.8 mL of Percoll and 1.2 mL of 10X HBSS and the resultant mixture was subjected to centrifugation. The cell pellet at the bottom was the hepatocyte fraction and the supernatant contained the non-parenchymal cell fraction. Hepatocyte viability was determined by trypan blue exclusion. A typical surgical excision and cell isolation typically resulted in 150-200 million hepatocytes with viability ranging from 90-97%. Hepatocytes were cultured on collagen-coated 6-well sterile tissue culture plates (Becton Dickinson Labware, Franklin Lakes, NJ) and were maintained in culture medium that consisted of DMEM supplemented with 10% heat-inactivated fetal bovine serum (Hyclone, UT), 200 U/mL penicillin, 200 μg/mL streptomycin, 20 ng/mL epidermal growth factor (BD Biosciences, San Jose, CA), 0.5 U/mL insulin (USP, Rockville MD), 14 ng/mL glucagon and 7.5 μg/mL hydrocortisone. A collagen gelling solution was prepared by mixing 9 parts of type I collagen (BD Biosciences) solution and 1 part of 10X DMEM. Sterile 6-well tissue culture plates were coated with 0.5 ml of the gelling solution and incubated at 37 ^{o}C for 1h to promote gel formation. Isolated hepatocytes were suspended in hepatocyte culture medium at a concentration of $1x10^{6}$ cells/ml and seeded on the collagen-coated wells at a density of 1 million cells/well. Collagen sandwich cultures were formed by the deposition of a second layer of collagen 24h later. Hepatocytes maintained in stable collagen sandwich and in unstable confluent monolayer cultures served as positive and negative controls, respectively. Hepatocyte cultures were

maintained at 37°C in a humidified gas mixture of 90% air/10% CO_2. The culture medium was replaced every 24h and medium samples were stored until further analysis.

2.3.3 Assembly of Polyelectrolyte Multilayers (PEMs) on Hepatocytes

Chitosan (200-300kDa M.W., Sigma-Aldrich) and hyaluronic acid (HA; > 1 million M.W., Acros Organics, Fairlawn NJ) were used as the cationic and anionic PEs, respectively. Chitosan (0.01%w/v) solutions were prepared by dissolving the polymer in a 1% v/v acetic acid solution and maintained at pH values ranging from 6.1-6.3. HA (0.01%w/v) solutions were prepared by diluting in PBS and adjusted to a pH range of 7.2-7.3. PEMs were assembled on hepatocytes by first depositing a cationic PE on the cell layer followed by the anionic PE. The exposure time for each PE solution was approximately 1-2 minutes. The desired number of bilayers was obtained through the sequential and alternate deposition of PE layers. At the end of the deposition procedure, the samples were rinsed in 1X PBS and subsequently maintained in cell-culture medium at 37^{o}C. In hepatocyte-PEM only samples, the PEM was deposited after primary hepatocytes were cultured for 24h.

2.3.4 Hepatocyte-PEM-LSEC Cellular Constructs

Human LSECs were maintained in medium supplemented with 5% (v/v) fetal bovine serum, 1% (v/v) endothelial cell growth supplement, 100 U/mL penicillin and 100 μg/mL streptomycin at 37ºC under a humidified gas mixture of 95% air/5% CO_2. Primary hepatocytes were first seeded on collagen-gel coated surfaces and allowed to spread up to 72h to form a confluent layer of cells. Thereafter, a PEM consisting of alternately charged chitosan and HA was deposited, followed immediately by seeding a layer of LSECs. LSECs were plated at a low cell density of 5,000 or 10,000 cells per sample since they proliferated over time. Non-adherent LSECs were removed 1h later. In experiments where the hepatocyte-LSEC or hepatocyte-PEM-LSEC constructs were imaged, the LSECs were tagged with a non-toxic, fluorescent, membrane-permeable dye (PKH 26 Red and Green Fluorescence Cell Linker Kit; Sigma-Aldrich) prior to seeding. Hepatocyte-LSEC cellular constructs were maintained for up to 10 days in hepatocyte culture medium. The culture medium was changed every 24h and medium samples were stored at 4^{o}C until further analysis.

2.3.5 Measurement of the Physical Properties of the PEM

The self-assembly of hydrated PEMs was monitored *in situ* using a quartz crystal microbalance with dissipation monitoring (QCM-D E4, Q-Sense, Sweden). The AT-cut quartz crystal coated (Q-Sense) with gold electrodes was cleaned with a 5:1:1 mixture of ammonia, hydrogen peroxide and 18 MΩPicoPure water (Molecular Devices, Sunnyvale CA) respectively. The quartz crystal was excited to its fundamental frequency at approximately 5MHz in the QCM-D open module chamber. The PE solution was placed directly on the crystal sensor. The deposition procedures were similar to conditions used to assemble PEMs on live hepatocytes. The change in resonant frequency and the decay time of the vibration relaxations were recorded. The PEM thickness was estimated using the Sauerbrey equation 1 (79).

$$\Delta f = -\frac{C}{n}\Delta m \qquad (1)$$

Δf = change in the resonant frequency (Hz)

Δm = change in mass per unit area (ng.cm^{-2})

C= sensitivity factor (17.7 Hz.cm^2.ng^{-1})

n = overtone number

Since HA and chitosan can also exhibit viscoelastic behavior, the Voigt model (a simple spring and dashpot in parallel operating with no-slip) was applied to the QCM-D response (80). The change in resonant frequency and change in dissipation factor for a viscoelastic film are related to changes in the resonant frequency and dissipation using equations 2-4.

$$\Delta f \approx -\frac{1}{2\pi\rho_0 h_0} h\rho\omega\left(1+\frac{2h^2\chi}{3\delta^2(1+\chi^2)}\right) \qquad (2)$$

$$\Delta D \approx \frac{2h^3\rho\omega}{3\pi f\rho_0 h_0}.\frac{1}{\delta^2(1+\chi^2)} \qquad (3)$$

where ω = angular frequency, h_0 = thickness of the quartz crystal, ρ_0 = density of the quartz crystal, δ = viscous penetration depth, χ = the viscoelastic ratio (ratio of storage to loss moduli) and h and ρ are the thickness and density of the PEM, respectively. The viscoelastic ratio is defined as:

$$\chi = \frac{\mu}{\eta\omega} \qquad (4)$$

where μ = shear modulus, and η is the film viscosity. The viscoelastic ratio and thickness were varied as the change in frequency and change in dissipation data were fitted using a mean squared error (MSE) method (81, 82). Qtools software (QSense) was used to predict the layer thickness, shear modulus, and viscosity, on the assumption that the density of a PE layer is 1.1 g cm^{-3} (73).

2.3.6 Measurement of Urea Production and Albumin Secretion

Medium samples were analyzed for rat albumin concentration by an enzyme-linked immunosorbent assay (ELISA), in triplicate, utilizing a polyclonal antibody to rat albumin (Cappel Laboratories, Aurora, OH) (73). Urea concentration was determined, via its specific reaction with diacetyl monoxime using a commercially available assay kit (BUN Assay Kit Stanbio Laboratory; Boerne TX) with volumes scaled down for use in 96-well plates. The absorbance was measured on a SpectraMax M2 microplate reader (Molecular Devices). Standard curves were generated using purified rat albumin or urea diluted in culture medium. The data reported were normalized per 1 million cells which was the initial cell count.

2.3.7 Actin Cytoskeletal Staining

Hepatocyte cultures were fixed in a 2% glutaraldehyde (Electron Microscopy Sciences, Hatfield, PA) solution in PBS at room temperature for 20 min. The cultures were exposed to a 0.1% Triton X-100 solution to render the membranes permeable and subsequently incubated with rhodamine-phalloidin (Molecular Probes) diluted in a 1% bovine serum albumin (BSA) in PBS. Actin cytoskeletal structure was imaged using an inverted Zeiss LSM510 confocal microscope (Carl Zeiss Inc.).

2.3.8 Microscopy

Cells were observed and imaged using an inverted Nikon TE-2000 (Nikon USA) microscope with 10X, and 20X objectives. Phase-contrast and fluorescent images of the cells

were collected using a Hamamatsu CCD camera (Hamamatsu City, Japan) and analyzed using Nikon's Imaging Software (NIS- Elements).

2.3.9 Uptake of Acetylated Low Density Lipoprotein (acLdL) by LSECs

Hepatocyte-LSEC cultures were incubated for 3h with 20 µg/mL of 3,3'-dioctadecylindocarbocyanine(DiI) acLdL (Invitrogen) diluted in serum-free hepatocyte culture medium. To remove non-specifically bound acLdL, the cultures were rinsed and maintained in phenol-red free DMEM. Imaging was conducted on a Nikon TE-2000 microscope.

2.3.10 Di-peptyl Peptidase IV (DPP IV) Immunostaining to Image Bile Canaliculi

Cells were fixed in a 2% glutaraldehyde/PBS solution, followed by permeabilization for in a 0.1% Triton X-100 solution. The cultures were incubated overnight at 4^{o}C in a 3% goat serum (Chemicon) solution. The samples were incubated with a mouse monoclonal antibody to rat DPP IV (Cell Sciences, Canton, MA) and a secondary FITC-conjugated rabbit anti-mouse IgG antibody (Sigma-Aldrich) and imaged using an inverted Zeiss LSM510 confocal microscope.

2.3.11 Measurement of Cytochrome P450 (CYP1A1/2) Activity

Cytochrome P450 (CYP1A1/2) activity was induced by adding 3 methyl cholanthrene (3MC, Sigma, 2µM) to the hepatocyte cultures, 48h prior to conducting measurements. Cytochrome-P450 dependent ethoxyresorufin *o*-dealkylase (EROD) detoxification was measured using ethoxyresorufin as the substrate. The incubation mixture contained the resorufin substrate (5µM) and 80µM dicumarol diluted in EBSS (Invitrogen) (83). Aliquots (100µL) were taken at 5, 15, 25, and 35 minutes after adding the resorufin mixture, transferred to a 96-well plate and the fluorescence intensity was measured using a SpectraMax M2 microplate reader (excitation wavelength = 530 nm and emission wavelength = 580 nm). Fluorescence intensity was converted to values of concentration by comparison to a standard curve for resorufin fluorescence with concentrations ranging from 0-1000 nM. The rate of resorufin formation (nM/min) was calculated from the early linear increase in the fluorescence curve, normalized to the DNA content in hepatocytes, and defined as cytochrome P450 isoenzyme activity. The absolute values obtained on day 7 for CYP1A1/2 activity were divided by the baseline activity on day 1 to obtain values of fold increase.

2.3.12 Separation of Hepatocytes and LSECs

The cultures were incubated with a 0.1% w/v collagenase solution. The cell suspensions were incubated with Dynabeads (Dynabeads® CD31 Endothelial Cell; Invitrogen) for 20 min at 4°C in an orbital shaker. Dynabead-bound cells (LSEC fractions) were collected by a magnet (DynaMag™-15; Invitrogen) and the supernatants (hepatocyte fractions) were transferred to a new tube. Purity of cell populations was observed to be > 97%. Hepatocyte fractions were centrifuged and diluted in a 0.1% sodium dodecyl sulfate (SDS) solution for measurement of DNA content.

2.3.13 Measurement of DNA Content

Cells were harvested by treatment with a 0.1% collagenase solution and subsequently lysed in a 0.1% SDS solution and stored at –20 ^{o}C until further analysis. For DNA measurements, aliquots of cell suspensions were treated with a fluorescent DNA-binding dye (Hoechst 33258, pentahydrate-bis-benzimide, Invitrogen). Fluorescence intensity was measured using a SpectraMax M2 microplate reader (excitation and emission wavelengths were 355 nm and 460 nm, respectively). Fluorescence intensity was converted to DNA concentration by comparison to a standard curve for calf thymus DNA (Sigma-Aldrich) fluorescence with concentrations ranging from 0-40 μg/ml.

2.3.14 Statistical Analysis

All data are reported as mean ± standard deviation (S.D.). t-tests were conducted to detect differences in the mean values ($\alpha = 0.05$). The Bonferroni correction was used to account for multiple hypothesis testing. The corrected p values are reported.

2.4 Results

2.4.1. Mechanical Properties of PEMs

PEMs comprised of 5 up to 30 alternating layers of chitosan and HA were assembled above a confluent layer of primary hepatocytes. The height of the hydrated PEM as well as its modulus and viscosity were determined by QCM-D measurements (79, 81, 82). The film thickness, shear modulus and visocosity of each layer were modeled by following an iterative method using the Voigt model approximation (80), Table 1. The thickness was found to be

approximately 6 nm/PE layer for a PEM consisting of 5 layers. The thickness per PE layer reached a maximum value of 5.2 nm/layer for a PEM of 10 layers. While the reason for the sub-linear growth of film thickness with layer number in the present case is not completely clear, it may be due to the fact that the chitosan was not highly charged at the pH at which it was deposited. The values for shear modulus were initially high due to substrate effects (95.7 ± 66.3 kPa for 5 layers) but decreased as more layers were deposited before increasing again to reach a maximum value (104.5 ± 13.6 kPa) for a PEM comprised of 15 bilayers. The PEM exhibited viscoelastic characteristics and was found to be less rigid as more layers were deposited. The PEM film viscosity values were found to be similar to that of water (1.01cP) indicating a high degree of hydration (84).

Table 2.1 Thickness, shear modulus and viscosity values for hydrated chitosan/HA PEMs.

Layer	**Thickness (nm)**	**Shear Modulus (kPa)**	**Film Viscosity (mPas)**
5	30.82 ± 6.71	95.7 ± 66.3	1.69±0.18
10	52.27 ± 5.25	56.6 ±17.8	1.78±0.09
15	55.50 ± 4.18	104.5 ± 13.6	2.12±0.09

2.4.2 Urea Production and Albumin Secretion of Hepaptocyte-PEM Cultures

In the first step towards assembling 3D liver mimics, hepatocyte-PEM cultures were investigated. Urea production and albumin secretion were measured to evaluate the phenotypic function and the results were compared to collagen sandwich cultures (positive control) and hepatocyte monolayers (negative control) (**Figure 2.1**). Over a 7 day period, urea production decreased by 64% and 33% for hepatocyte monolayer and collagen sandwich cultures respectively. Urea production was observed to be lower in cultures with PEMs in comparision to HM or CS samples on day 1. This was attributed to the fact that hepatocytes that undergo PEM deposition take approximately 2 days to stabilize from the deposition procedure, however, these cells exhibited increased urea production over the culture period. The increase in urea production was found to be 12% and 48% for hepatocyte cultures that had either 5 or 15 PE

layers respectively. The values for urea production on day 7 were higher and statistically significant ($p<0.05$) in hepatocyte cultures with 5 (49.1±4.4 μg/10^6 hepatocytes, $p=0.0016$) or 15 (45.7±3.3 μg/10^6 hepatocytes, $p=0.008$) PE layers in comparison to hepatocyte monolayer (36.8±4.6 μg/10^6 hepatocytes) and were similar and statistically insignificant ($p>0.05$) in comparison to values measured for collagen sandwich (46.7±9.1μg/10^6 hepatocytes) cultures. In stable hepatocyte cultures, albumin secretion has been shown to increase with time (17, 41). Over a 7-day period, albumin secretion increase by 71% in collagen sandwich cultures and decreased by 50% in monolayer cultures (**Figure 2.2**). Albumin secretion in hepatocyte-PE cultures increased over the 7 day observation period. In hepatocyte cultures with 5 or 15 PE layers, albumin secretion increased by approximately 36% or 7% respectively. Cultures with PEM consisting of 30 or 45 PE layers did not exhibit satisfactory urea or albumin production and were not included in further analyses. The values for albumin secretion on day 7 were higher and statistically significant ($p<0.05$) in hepatocyte cultures with 5 (5.2±1.6 μg/10^6 hepatocytes, $p=0.003$) or 15 PE layers (2.8±0.3 μg/10^6 hepatocytes, $p=0.0024$) in comparison to hepatocyte monolayers (1.8±0.7 μg/10^6 hepatocytes) and were similar and statistically insignificant ($p>0.05$) in comparison to values measured for collagen sandwich (6.1±0.9 μg/10^6 hepatocytes) culture.

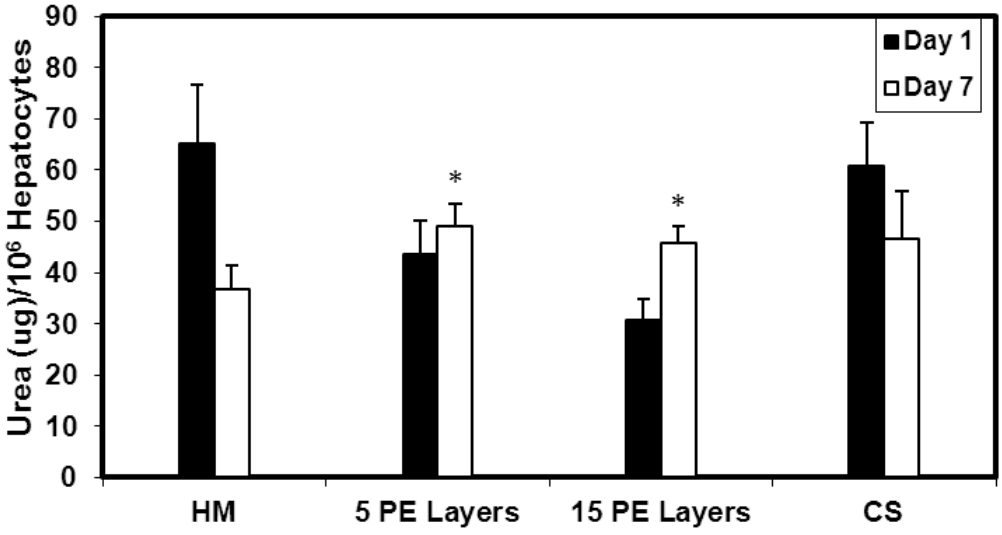

Figure 2.1 Urea production measured over a 7-day period for HM (n=6), with 5 PE layers (5 PE layers, n=6), with 15 PE layers (15 PE layers, n=6), and in a CS (n=6). *$p<0.05$ when compared

to hepatocyte monolayers on day 7. CS, collagen sandwich; HM, hepatocytes cultured as a monolayer.

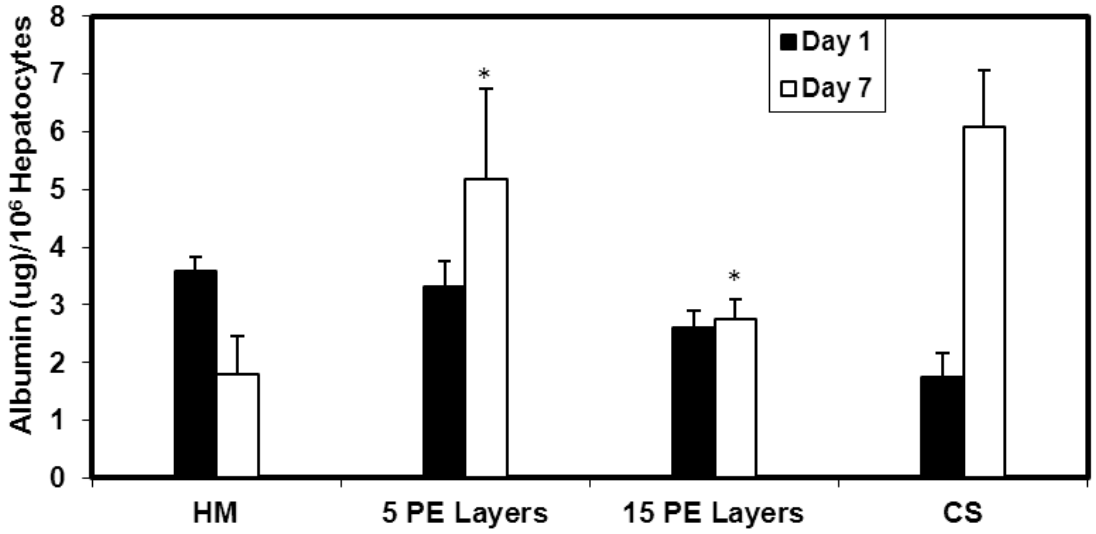

Figure 2.2 Albumin secretion measured over a 7-day period for HM (n=6), with 5 PE layers (5 PE layers, n=6), with 15 PE layers (15 PE layers, n=6), and in a CS (n=6). *$p<0.05$ when compared to hepatocyte monolayers on day 7. CS, collagen sandwich; HM, hepatocytes cultured as a monolayer.

2.4.3 Cytoskeletal Organization in Hepatocyte-PEM Cultures

The actin cytoskeletal organization revealed significant differences between hepatocyte monolayers and hepatocyte-PEM cultures. In the absence of rhodamine phalloidin, fluorescence was not observed in hepatocytes, and, this was defined as the negative control (**Figure 2.3A**). Hepatocyte monolayer cultures exhibited a mesh-like network of f-actin through the entire cross-section of the cell (**Figure 2.3A**). The cytoskeletal organization in hepatocytes-PEM samples (**Figures 2.3C and D)** was observed to be very similar to hepatocytes cultured in a collagen sandwich culture (**Figure 2.3B**). In these cells, f-actin was observed to be localized only along the peripheral regions of the cell similar to hepatocytes cultured in a collagen sandwich.

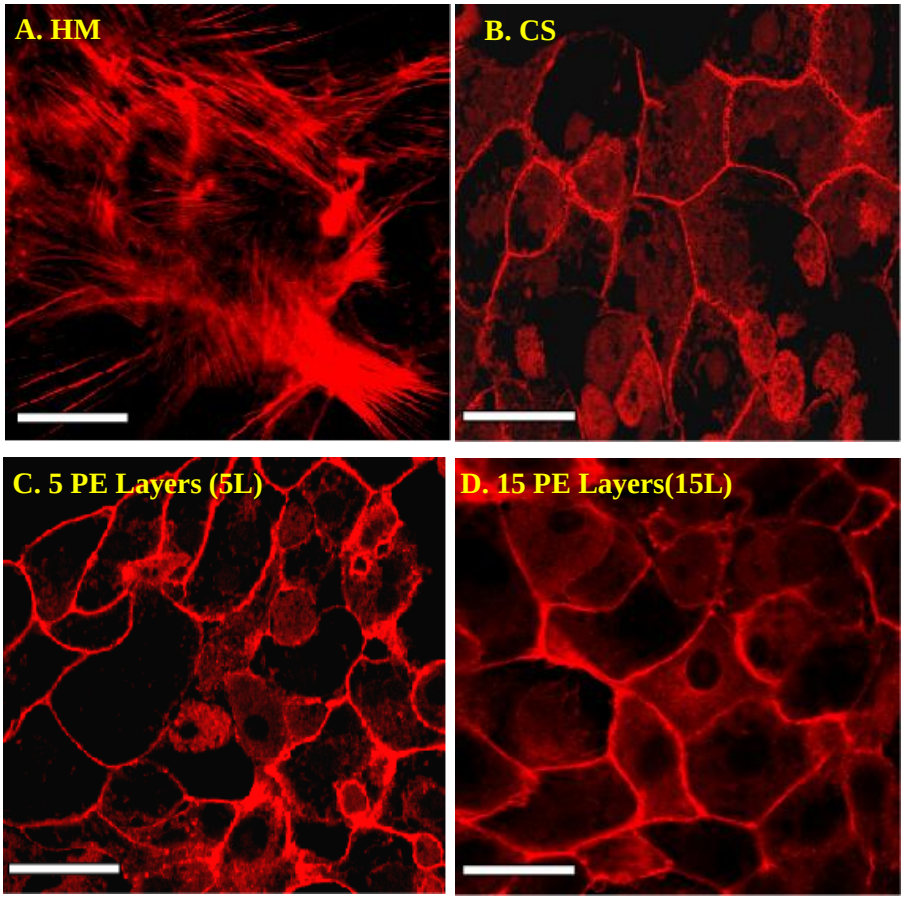

Figure 2.3 Actin cytoskeletal organization in (A) Hepatocyte monolayer, (B) CS culture, (C) Hepatocytes–5PE Layers, and (D) Hepatocytes–15 PE Layers. Scale bar=50 mm.

2.4.4 Cellular Structure of Hepatocyte-PEM-LSEC Constructs

A second layer of LSECs was deposited on hepatocyte-PEM cultures as well as on hepatocyte monolayers (**Figure 2.4**). Images taken 2h post-LSEC seeding indicated that in the absence of an intermediate PE scaffold, LSECs were non-adherent (**Figure 2.4A**). However, in the presence of the chitosan/HA PEM, LSECs were adherent (**Figure 2.4B**). These trends prevailed over longer culture periods as well suggesting that the PEM provides a biocompatible surface for LSECs to adhere and proliferate. On day 7, in the absence of the chitosan/HA scaffold, LSECs were not observed above hepatocytes (**Figure 2.4C**), whereas high concentrations of LSECs were observed on hepatocyte/PE/LSEC constructs (**Figure 2.4D-F**). It is significant to note that LSECs appeared to be adherent only above hepatocytes and were not found in regions between adjacent hepatocyte aggregates (**Figures 2.4D-F).**

Reprinted from Kim, Y. et al. *Tissue Engineering: Part A*, 2010; 16(9):2731-41.with permission from Mary Ann Liebert, Inc. publishers.

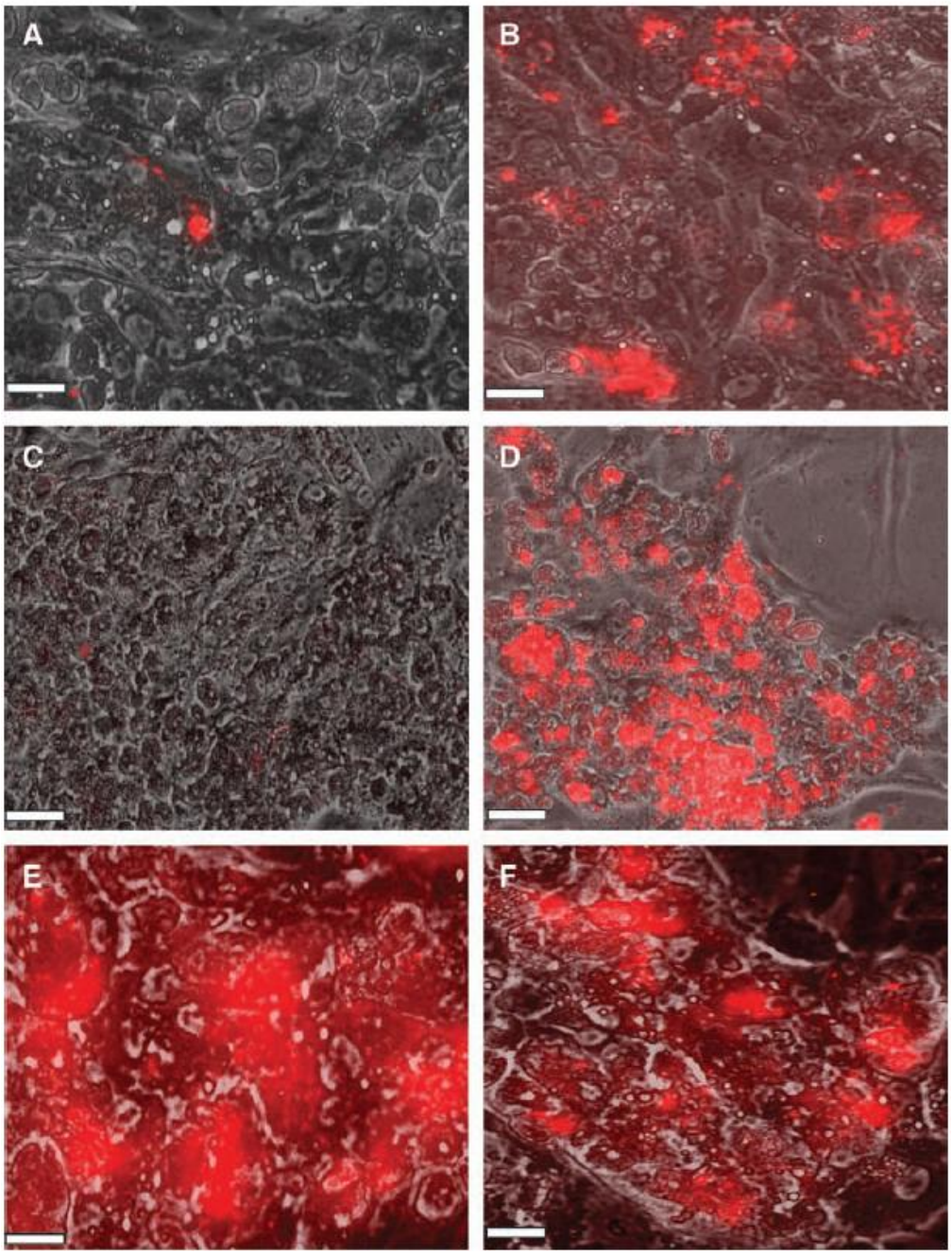

Figure 2.4 Merged phase-contrast (hepatocytes) and red-fluorescent LSECs. Images taken 2 h post-LSEC seeding. (A)Hepatocytes–LSECs and (B) Hepatocytes-5 PE Layers–5000 LSECs. Merged phase-contrast (hepatocytes) and fluorescent (LSECs) images taken 7 days post-LSEC seeding. (C) Hepatocytes–LSECs, (D) Hepatocytes–5 PE Layers–5000 LSECs, (E) Hepatocytes–5 PE Layers–10,000 LSECs, and (F) Hepatocytes–15 PE Layers–5000 LSECs. Scale bar=100 μm LSEC, liver sinusoidal endothelial cell.

2.4.5 Receptor-Mediated Endocytosis of Ac-LdL by LSECs

The maintenance of LSEC phenotype was assessed by fluorescent imaging of the receptor-mediated uptake of ac-LdL. In the absence of ac-LdL, no fluorescence was observed in LSECs or hepatocytes (**Figures 2.5A and B**). Since hepatocytes do not have this receptor, these cells did not exhibit any fluorescence (**Figures 2.5C and D)** as well as LSECs cultured on hepatocytes in the absence of a PEM (**Figures 2.5E and F**). However, LSECs adherent on hepatocyte-PEM samples exhibited fluorescence thereby, indicating the endocytosis of the low density lipoprotein (**Figures 2.5G - J**). These results indicate that LSEC phenotype is maintained in the 3-D constructs.

2.4.6 Albumin Secretion and Urea Production in Hepatocyte-PEM-LSEC Cultures

On day 7, (**Figure 2.6A**), albumin secretion in hepatocyte-PEM-LSEC cultures was statistically higher ($p<0.05$) in comparison to hepatocyte monolayers. The p values for hepatocyte-5L-5000 LSECs, hepatocyte-5L-10000 LSECs and hepatocyte-15L-5000 LSECs were found to be 0.04, 0.006, and 0.015 respectively. Samples containing LSECs in the presence of a PE interface exhibited statistically higher albumin secretion in comparison to hepatocyte-LSEC cultures. The p values for hepatocyte-5L-10000 LSECs and hepatocyte-15L-5000 LSECs were found to be 0.039 and 0.03 respectively when compared to albumin production in the absence of a PE multilayer. However, the albumin secretion for all 3D liver mimics was found to be similar to collagen sandwich cultures and the values were statistically insignificant. Urea production decreased over the 7-day period for all samples. HM samples exhibited approximately 70% decrease in urea production over a 7-day period (**Figure 2.6B**). The decrease for the heaptocyte-PEM-LSEC samples was approximately 40-45% and similar to the decrease observed in CS cultures.

Reprinted from Kim, Y. et al. *Tissue Engineering: Part A*, 2010; 16(9):2731-41.with permission from Mary Ann Liebert, Inc. publishers.

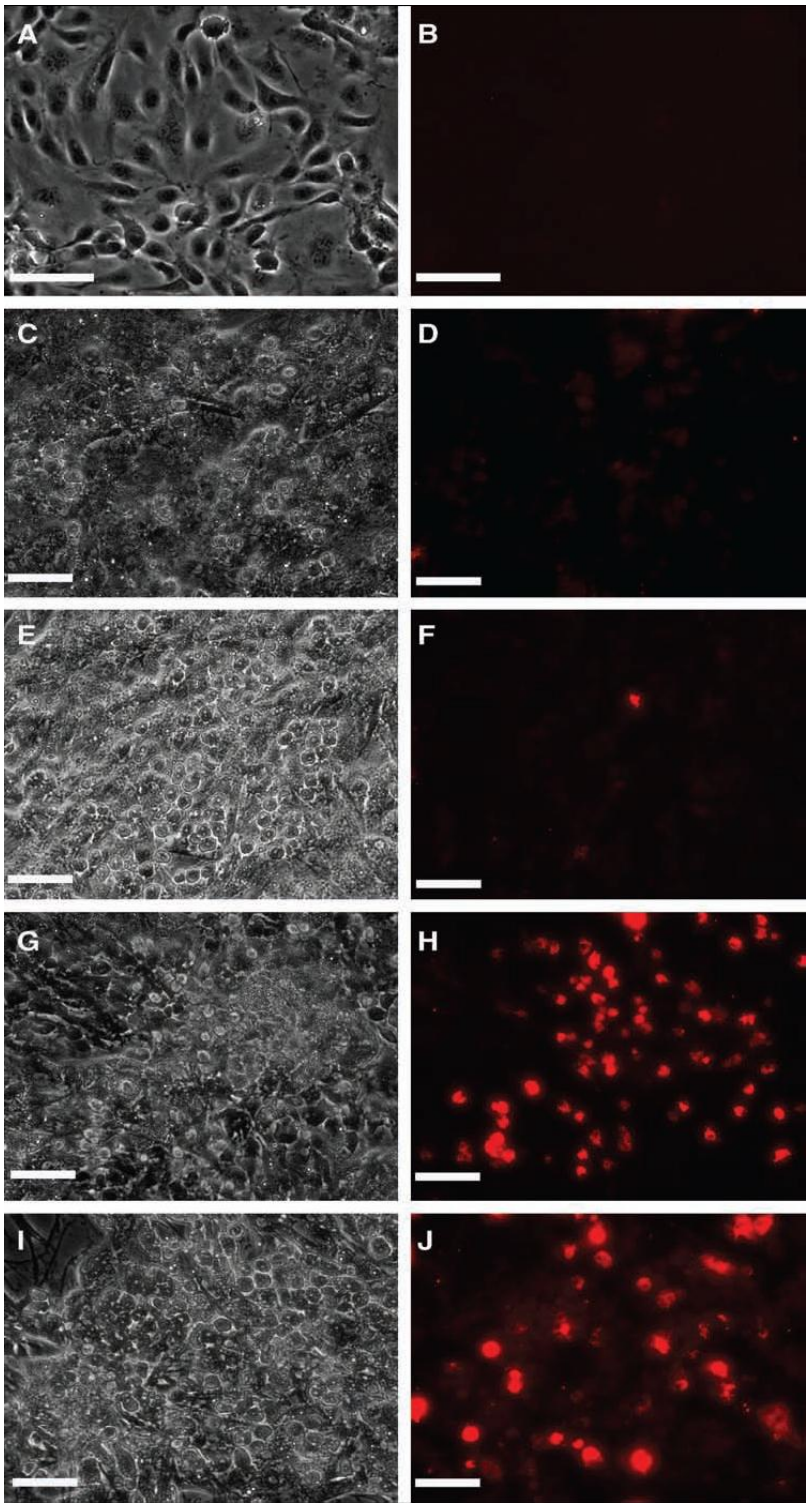

Figure 2.5 Phase-contrast images of (A) LSECs, (C) Hepatocytes, (E) Hepatocyte–LSECs, (G) Hepatocytes–5 PE Layers–5000 LSECs, and (I) Hepatocytes–15 PE Layers–5000 LSECs. Fluorescent images of acetylated low-density lipoprotein uptake for (B) LSECs (negative control, in the absence of acetylated low density lipoprotein), (D) Hepatocytes, (F) Hepatocytes–LSECs,

Reprinted from Kim, Y. et al. *Tissue Engineering: Part A*, 2010; 16(9):2731-41.with permission from Mary Ann Liebert, Inc. publishers.

(H) Hepatocytes–5 PE Layers–5000 LSECs, and (J) Hepatocytes–15 PE Layers–5000 LSECs. Scale bar=100 μm.

(A)

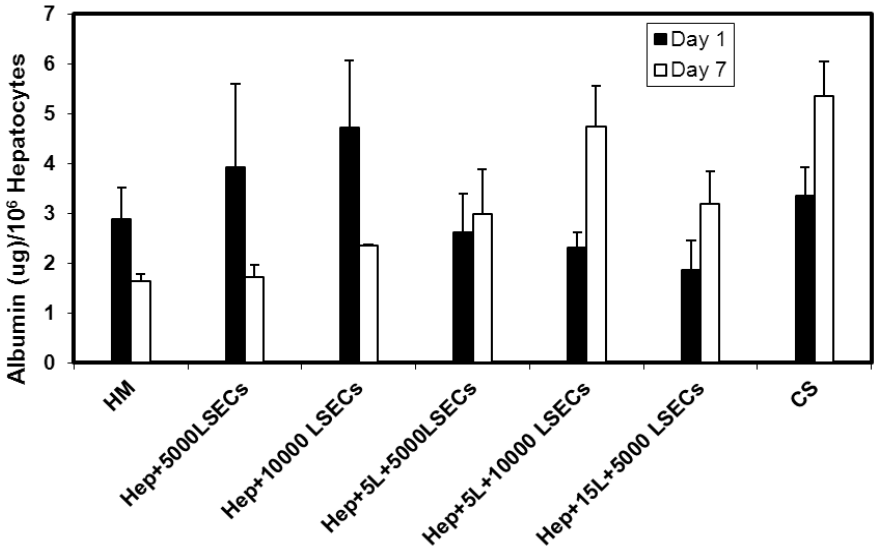

(B)

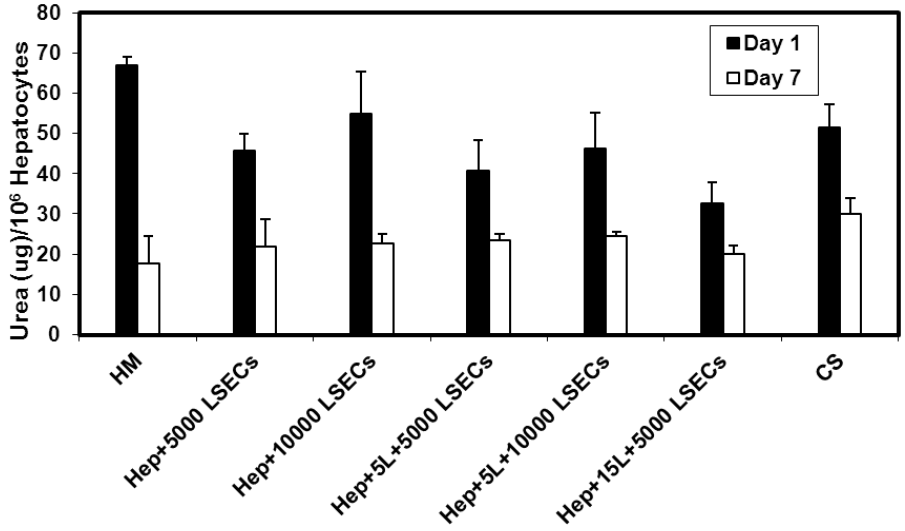

Figure 2.6 Albumin secretion (A) and urea production (B) measured over a 7-day period for HM, with LSECs in the absence of a PEM (Hep-5000 LSECs and Hep-10,000 LSECs), with LSECs in the presence of a PEM (Hep-5L-5000 LSECs, Hep-5L-10,000 LSECs, and Hep-15L-5000 LSECs) and in a CS (n=3 for all conditions). PEM, polyelectrolyte multilayer.

Reprinted from Kim, Y. et al. *Tissue Engineering: Part A*, 2010; 16(9):2731-41.with permission from Mary Ann Liebert, Inc. publishers.

2.4.7 Presence of Bile Canaliculi

An important differentiated function of hepatocytes is the presence of bile canaliculi, the channels through which bile acids are transported from the liver (85, 86). The presence of canaliculi was determined through the localization of a fluorescent DPP IV enzyme. Very diffuse fluorescence was observed in hepatocyte monolayers and hepatocyte-LSEC cultures (**Figures 2.7C and D**) indicating that well-defined canaliculi were not formed. These structures were better defined in hepatocyte-PEM cultures (**Figure 2.7E**). However, well defined bile canaliculi were observed in hepatocyte-PEM-LSEC (**Figures 2.7F and G**) and collagen sandwich cultures (**Figure 2.7B**). These results suggest that the PEM plays an important role in maintaining cellular polarity and in modulating the heterotypic interactions between hepatocytes and LSECs.

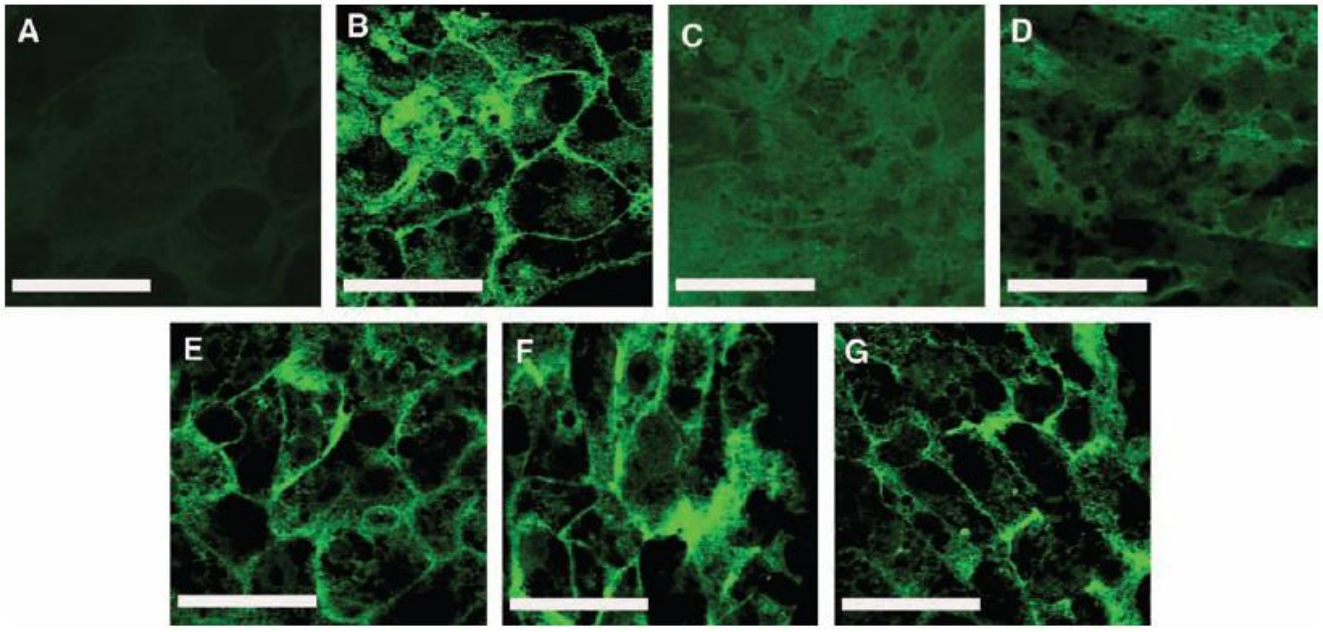

Figure 2.7 Di-peptyl-peptidase IV immunostaining for bile canaliculi measured 3 days post-LSEC seeding. (A) Negative control (CS culture in the absence of antibodies), (B) CS culture, (C) Hepatocyte Monolayer, (D) Hepatocytes-5000 LSECs, (E) Hepatocytes-15 PE layers, (F) Hepatocytes-15 PE-5000 LSECs, and (G) Hepatocytes-15 PE-10,000 LSECs. Scale Bar=50 μm.

2.4.8 CYP1A1/2 Enzyme Activity

CYP1A1/2 isoenzyme activity was monitored over a 7-day period since the metabolism of toxins, an important phenotypic function of hepatocytes, is mediated through the CYP class of microsomal enzymes. Control measurements conducted on LSEC cultures revealed that LSECs exhibited extremely low enzymatic activity. For example on Day 1, the CYP1A1/2 activity for LSECs was found to be 0.12±0.03 nM/min/μg DNA in comparison to the activity in a CS culture (4.14±0.4 nM/min/μg DNA). On Day 7, the values were found to be 0.06 ± 0.02 and 8.45 ± 1.6 nM/min/μg DNA for LSECs and CS cultures respectively. Since the enzymatic activity on Day 7 exhibited by hepatocytes alone is approximately 140 times higher than that observed for LSECs alone we concluded that the CYP enzyme activity observed in the 3D constructs is primarily due to hepatocytes. The CYP1A1/2 activity remained stable in hepatocyte-PEM samples and exhibited a 2-fold increase in collagen sandwich cultures. A significant increase was observed only in hepatocyte-PEM-LSEC constructs where the fold increase over the observation period ranged from 4-fold up to 16-fold (**Figure 2.8**). 3-D liver mimics that contained 10,000 of LSECs exhibited either 7.5-fold (hepatocyte-5 PE Layers-10000 LSECs) or a 16-fold increase (hepatocyte-15 PE Layers-10000 LSECs). These trends suggest that the communications and interactions between these two cells types are critical for enhancing the detoxification capability of hepatocytes *in vitro*.

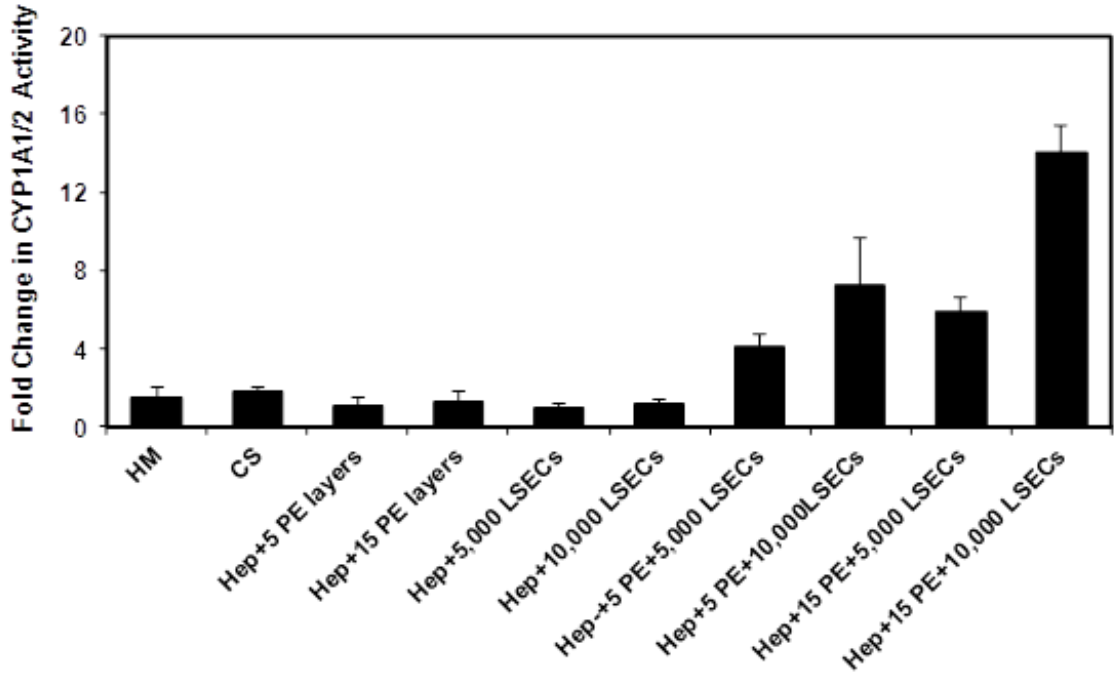

Figure 2.8 Fold change in CYP1A1/2 enzyme activity for HM and CS, with PEMs only, with LSECs only, and in three dimensional liver mimics (n=3 for all conditions).

2.5 Discussion and Conclusions

The design of 3-D structures of hepatic parenchymal and non-parenchymal cells using PE scaffolds is an innovative approach to mimic liver sinusoidal structure found *in vivo*. Although hepatocytes cultured in a collagen sandwich configuration are stable over extended periods of time, they do not resemble liver architecture *in vivo*. Additionally, the presence of thick collagen gels prevents the assembly of 3-D stratified cellular constructs. LSECs have been shown to function as a scavenger system *in vivo*, by playing a vital role in the balance of lipids, cholesterol and vitamins (20, 87-90). Through blood clearance LSECs can remove waste macromolecules that are either soluble or colloidal in nature. Several components of connective tissue are eliminated rapidly from the blood through receptor-mediated endocytosis in LSECs.

Chitosan-HA PEMs exhibited shear modulus values that are in the range reported for the bulk modulus values of the liver (91, 92). PEMs exhibiting elastic moduli in the 100kPa range have been shown to maintain and modulate hepatic phenotype suggesting that the shear modulus

values reported in this study are suitable for the assembly of liver sinusoidal mimics (93). The films are well hydrated, thereby, promoting the diffusion of small molecules such as cytokine and other signaling molecules. Hepatocyte-PEM cultures with either 5 or 15 PE layers were found to exhibit urea and albumin production similar to collagen sandwich cultures. This is of importance, since the height of the PEM ranges from 30-55nm, which is significantly lower than the thickness of a collagen gel (in the mm range). It is hypothesized that that height of the PEM decreases slightly due to the formation of chitosan aggregates (94, 95). These data suggest that cellular polarization, an important feature of hepatocytes cultured in collagen sandwich cultures, occurs even in the presence of a nano-scale PEM. Furthermore, the nano-scale dimensions of the PEM offer the potential to promote and control homotypic and heterotypic cellular interactions.

The chitosan-HA PEM provides a surface for LSECs to adhere and proliferate. LSECs were found to adhere only on hepatocytes in the presence of a PEM and were non-adherent in the absence of PEMs or in regions adjacent to hepatocyte aggregates. Hepatic phenotypic features such as bile canaliculi were well defined in hepatocyte-PEM-LSEC samples in comparison to hepatocyte monolayers or hepatocyte-LSEC cultures, thereby suggesting enhanced autocrine/paracrine signaling through the PEM. Cytochrome P450, CYP1A1/2 activity was enhanced up to 16-fold over a 7 day period in hepatocyte-PEM-LSEC cultures. These observations suggest that the hepatocyte-PEM-LSEC constructs could provide a more physiologically relevant model system to study the metabolism of drugs and toxins. In the future, our goal is to investigate the enzyme kinetics of CYP3A which accounts for the metabolism of approximately 50% of pharmaceuticals available today (96, 97) as well as the CYP2B and CYP2C family of enzymes, implicated in the metabolism of amphetamines and anti-inflammatory agents (98, 99). The modes through which hepatic parenchymal and non-parenchymal cells communicate remain cryptic. Through detailed studies on profiling cytokine levels as well through gene expression studies, our future goals are to unearth molecular signatures and the key signaling molecules that enhance cell-cell communications in hepatic architectures.

Some alternate approaches to design hepatic structures are the use of a temperature-responsive polymer such as N-isopropyl acrylamide (56, 69, 70), the use of cationic magnetic

liposome (58) and the use of laser guided writing techniques (100, 101). In the first two approaches, issues related to working with cell sheets and the long-term effects of magnetic liposomes pose problems. Although laser guided writing techniques are a promising approach, the design of large 3D liver models could potentially be time-consuming. More recently, studies on perfused co-cultures of primary hepatocytes and LSECs reveal that such systems can maintain LSEC phenotype (87). Our approach to design 3D liver mimics through the incorporation of PEMs and hepatic cells is a simple and effective methodology. The PEMs used in this study are biocompatible and biodegradable and do not affect hepatic phenotype. In the future, the PEMs can be modified with hepatocyte-specific adhesive ligands to promote receptor-mediated adhesion. Cellular constructs that mimic liver sinusoidal structure *in vivo* could aid in the design of liver-assist devices and provide accurate models for applications in toxicity and drug testing. Since LSECs are the first barrier to blood-borne pathogens in the liver, tissue mimics that incorporate these cells could play a vital role in advancing our knowledge on the communications and signaling between hepatic parenchymal and non-parenchymal cells.

2.6 Acknowledgment

We gratefully acknowledge financial support from the National Institutes of Health (NIDDK-1R21DK077802, P.R.) the National Science Foundation (DMR-090750, P.R. and R.M.D), Thomas F. and Kate Miller Jeffress Foundation (P.R.), the Institute for Critical Technology and Applied Sciences (P.R.) and the MILES-NSF IGERT program at Virginia Polytechnic Institute and State University (P.R.).

Reprinted from Kim, Y. et al. Tissue Engineering Part C. Methods. 2010 Jun 7. [Epub ahead of print] with permission from Mary Ann Liebert, Inc. (doi:10.1089/ten.tec.2010.0012.)

Chapter 3. A Comparative Study of Genome Wide Transcriptional Profiles of Primary Hepatocytes in Collagen Sandwich and Monolayer Cultures

This study was done by collaboration with Christopher D. Lasher, a graduate student in Genetics, Bioinformatics, and Computational Biology program at Virginia Tech.

Y. Kim was responsible for isolation of primary rat hepatocytes (Sections 3.3.1 and 3.3.2), preparation of collagen sandwich and hepatocyte monolayer cultures (Section 3.3.2), extraction of total RNA (Section 3.3.3), analysis of gene set data (Sections 3.4.3, 3.4.4, and 3.5, Table 3.1, and Figure 3.8), and making correlation of the gene sets of interest with the pre-established metabolic pathways (Figures 3.3, 3.4, and 3.6)

C. D. Lasher was responsible for analysis of DNA microarray data *via* Gene Set Enrichment Analysis (GSEA) (Sections 3.3.4, 3.3.5, 3.4.1, and 3.4.2, Table 3.2, and Figures 3.1, 3.2, 3.5, and 3.7) and construction of gene set level network (Figure 3.9).

Reprinted from Kim, Y. et al. Tissue Engineering Part C. Methods. 2010 Jun 7. [Epub ahead of print] with permission from Mary Ann Liebert, Inc. (doi:10.1089/ten.tec.2010.0012.)

Chapter 3. A Comparative Study of Genome Wide Transcriptional Profiles of Primary Hepatocytes in Collagen Sandwich and Monolayer Cultures

3.1 Abstract

Two commonly used culture systems in hepatic tissue engineering are the collagen sandwich and monolayers of cells. In this study, genome-wide gene expression profiles of primary hepatocytes were measured over an 8-day period for each cell culture system using Affymetrix GeneChips and compared via Gene Set Enrichment Analysis (GSEA) in order to elicit biologically meaningful information at the level of gene sets. Our results demonstrate that the gene expression in hepatocytes in collagen sandwich cultures steadily and comprehensively diverges from that in monolayer cultures. Gene sets up-regulated in collagen sandwich cultures include several associated with liver metabolic and synthesis functions, such as metabolism of lipids, amino acids, carbohydrates, and alcohol and synthesis of bile acids. Monooxygenases such as Cytochrome-P450 enzymes do not show any change between the culture systems after one day, but exhibit significant up-regulation in collagen sandwich cultures after three days in comparison to hepatocyte monolayers. These data provide insights into the up- and down-regulation of several liver-critical gene sets and their subsequent effects on liver-specific functions. These results provide a baseline for further explorations into the systems biology of engineered liver mimics.

3.2 Introduction

As one of the important organs in our bodies, the liver performs many essential functions such as metabolism, synthesis, secretion, and, detoxification (102). Hepatocytes are the principal cells in the liver, comprising over 80% of its mass. Hepatocytes perform several characteristic functions of the liver, such as lipid metabolism, glucose homeostasis, regulation of urea, production of plasma proteins, alcohol clearance, and biotransformation of xenobiotics (102). In hepatic tissue engineering, two widely used culture systems are hepatocyte monolayers (HMs) and the collagen sandwich (CS) (17, 41). In HMs, hepatocytes are cultured on a single collagen gel. Such cells progressively lose their phenotypic characteristics over time. In CS cultures, hepatocytes are maintained between two collagen gels and remain stable over extended periods

of time (16, 103). Studies have indicated that CS cultures exhibit the preservation of differentiated functions including secretion of urea, expression of plasma proteins such as albumin and fibrinogen, polygonal morphology, the presence of bile canaliculi, as well as the synthesis of gap junction and tight junction proteins (16, 103). Although morphological and physiological characteristics of hepatocytes in CS cultures have been studied extensively, comprehensive evaluations of temporal genome-wide gene expression programs in these culture systems have not been reported. The global gene expression of human hepatocellular carcinoma cells (HepG2) in monolayer and spheroidal cultures revealed up-regulated metabolic functions in spheroids but not in monolayer cultures (104). Since these data were taken at a single time point, they did not reveal temporal variations. Another study that monitored temporal gene expression in hepatocyte monolayers cultured over a three day time period revealed the down-regulation of cytochrome-P450 expression (105). However, neither did this study investigate longer time points nor did it compare monolayers to other, more stable culture conditions. DNA microarray measurements have also been used to study specific pathways through which toxicity was conferred in human hepatoblastoma cells (106) and to understand the effects of non-parenchymal cells in 2D co-cultures of hepatocytes with fibroblasts or sinusoidal endothelial cells (62, 85).

We hypothesized that the enhanced *in vivo* liver-like phenotypes in CS cultures were a result of the underlying differences in the transcriptional program between hepatocytes cultured in CS and HMs. Accordingly, genome-wide gene expression profiles of primary hepatocytes were measured at four different time points over an 8-day period for each cell culture system using Affymetrix GeneChips. Among the wide range of techniques that are available to analyze DNA microarray data, a method was desired that would summarize, at the level of pre-defined biological pathways, the differences between the culture conditions at each time point. Gene Set Enrichment Analysis (GSEA) (107) was selected since it satisfies this criterion. GSEA is one among a family of techniques that can summarize differential expression at the level of gene sets (108). GSEA is widely used, generates detailed information on the results, and has shown very good performance in a comparison of methods that compute enrichment at the level of gene sets (109). Furthermore, GSEA has been used to identify pathways involved in liver toxicity in human hepatoblastoma cells (106). GSEA is designed to identify pre-defined gene sets that are differentially expressed in a treatment and a control. All the genes expressed on each gene chip

are ranked based upon their differential expression in CS and HM cultures. Therefore, a gene set could be important if its members are clustered within the ranked gene list. GSEA measures the statistical significance of the distribution of ranks within the gene set against the background of the ranks of all the genes.

Over the 8 day culture period, the gene expression program of hepatocytes in CS cultures monotonically diverged from cells cultured as a monolayer. Gene sets that were up-regulated to a statistically-significant extent in CS cultures included those associated with liver-specific functions such as bile acid synthesis and lipid, amino acid, carbohydrate, and alcohol metabolism. Nuclear receptors, which play a key role in controlling the transcriptional activation of target proteins, were up-regulated in CS cultures on day 1 in culture. Sets containing genes whose expression is mediated by nuclear receptors were up-regulated in collagen sandwich systems after one day. Gene sets related to xenobiotic metabolism and monoxygenase activity were not differentially expressed after one or two days, but showed highly-significant up-regulation after three days, suggesting a recovery in the expression of the genes in these sets. Numerous gene sets related to the cell cycle were down-regulated, suggesting that the cell cycle was arrested in hepatocytes maintained in CS culture systems in comparison to HMs. These findings recapitulated well-known aspects of liver function, thereby suggesting that DNA microarrays are a powerful tool for shedding light on the transcriptional signatures that underlie differences between these two culture systems. The DNA microarray data generated in this study are available at NCBI's Gene Expression Omnibus under accession number GSE20659 at http://www.ncbi.nlm.nih.gov/geo/query/acc.cgi?token=vbuzfygaacacoho&acc=GSE20659. All our results are available at the following supplementary website: http://bioinformatics.cs.vt.edu/~murali/supplements/2010-kim-tissue-engineering.

3.3 Materials and Methods

3.3.1 Materials

Dulbecco's Modified Eagle Medium (DMEM) containing 4.5 g/L glucose, phosphate-buffered saline (PBS), penicillin, streptomycin, and trypsin-EDTA were obtained from Invitrogen Life Technologies (Carlsbad, CA). Type IV collagenase, HEPES (4-(2-hydroxyethyl) piperazine-1-ethanesulfonic acid), glucagon, and hydrocortisone were obtained from Sigma-

Aldrich (St. Louis, MO). Unless otherwise noted, all chemicals were used as received from Fisher Scientific (Pittsburgh, PA).

3.3.2 Hepatocyte Isolation and Culture

Primary rat hepatocytes were harvested from female Lewis rats (Harlan, Indianapolis, IN) that weighed between 170-200g. Animal care and surgical procedures were conducted as per procedures approved by Virginia Polytechnic Institute and State University's Institutional Animal Care and Use Committee. A two-step *in situ* collagenase perfusion method was utilized to excise the liver (16, 103). Briefly, animals were anesthetized with 3 L/min of a gas mixture of 3% (v/v) isofluorane/97% oxygen (Veterinary Anesthesia Systems Co., Bend, OR). The liver was perfused through the portal vein with oxygenated Krebs Ringer Buffer (KRB; 7.13 g/L sodium chloride, 2.1 g/L sodium bicarbonate, 1 g/L glucose, 4.76 g/L HEPES and 0.42 g/L potassium chloride) that contained 1mM EDTA (ethylene diamine tetra acetic acid), followed by serial perfusion with a 0.075% w/v and a 0.1% w/v collagenase (Sigma-Aldrich, Type IV) in KRB containing 5 mM calcium chloride. Cell suspensions were filtered through nylon meshes with porosity ranging from 250-62 μm (Small Parts, Inc., Miramar, FL). Hepatocytes were separated using a Percoll (Sigma-Aldrich) density centrifugation technique. Cell viability was determined by trypan blue exclusion. Hepatocytes were cultured on collagen-coated 6-well sterile tissue culture plates (Becton Dickinson Labware, Franklin Lakes, NJ) and were maintained in culture medium that consisted of DMEM supplemented with 10% heat-inactivated fetal bovine serum (Hyclone, UT) 200 U/mL penicillin, 200 μg/mL streptomycin, 20 ng/mL epidermal growth factor (BD Biosciences, San Jose, CA) 0.5 U/mL insulin (USP, Rockville MD) , 14 ng/mL glucagon and 7.5 μg/mL hydrocortisone. A collagen gelling solution was prepared by mixing 9 parts of type I collagen (BD Biosciences) solution and 1 part of 10X DMEM. Sterile 6-well tissue culture plates were coated with 0.5 ml of the gelling solution and incubated at 37^{o}C for 1h to promote gel formation. Isolated hepatocytes were suspended in hepatocyte culture medium at a concentration of $1x10^{6}$ cells/ml and seeded on the collagen-coated wells at a density of 1 million cells/well. CS cultures were formed by the deposition of a second layer of collagen one day after the hepatocytes were seeded (16, 103). Hepatocytes maintained in stable CS and in unstable confluent HM cultures served as positive and negative

controls, respectively. Hepatocyte cultures were maintained at 37°C in a humidified gas mixture of 90% air/10% CO_2. The culture medium was replaced every 24 hours.

3.3.3 RNA Extraction and Gene Chip Hybridization

Primary rat hepatocytes cultured in CS and HM cultures were maintained for an eight-day culture period. The samples were analyzed at four time points: days 1, 2, 3 and 8 after deposition of the second layer of collagen gel on hepatocytes. Total RNA was extracted and purified from cells for each culture system using an RNeasy mini kit (QIAGEN, Valencia, CA) following the manufacturer's protocol. Isolated RNA samples in triplicate at each time point were labeled according to the Affymetrix Standard Target labeling process, hybridized to the GeneChip Rat Genome 230 2.0 array (Affymetrix, Santa Clara, CA), and scanned as described by the manufacturer. Complementary RNA (cRNA) synthesis, hybridization and scanning were performed at the Virginia Bioinformatics Institute Core Laboratory facility as follows. Briefly, total RNA was converted into double-stranded complementary DNA using a T7- oligo (dT) primer (5' – GGCCAGTGAATTGTAATACGACTCACTATAGGGAGGCGG–(dT)24 –3') and reverse transcription. Synthesized cDNA was converted into biotinylated cRNA by transcription using T7 RNA polymerase. Randomly fragmented cRNA was hybridized to GeneChip and the arrays were washed and stained according to Affymetrix's protocols. The arrays were scanned using an Affymetrix 7G scanner.

3.3.4 Microarray Data Analysis

The BioConductor package (110) was used to perform initial statistical analysis of the DNA microarray data. The data from 24 chips (2 culture conditions x 4 time points x 3 replicates) were normalized using the Robust Multichip Average method for further analysis. The affylmGUI interface to Linear Models for Microarray Data (LIMMA) (111) was used to perform differential gene expression analysis for the contrasts shown in **Table 3.1**. Specifically, for each contrast, LIMMA was used to compute a *p*-value for each probe set that indicated the statistical significance of the difference of the expression levels of that probe set between the two conditions in the contrast.

Reprinted from Kim, Y. et al. Tissue Engineering Part C. Methods. 2010 Jun 7. [Epub ahead of print] with permission from Mary Ann Liebert, Inc. (doi:10.1089/ten.tec.2010.0012.)

Table 3.1 Contrasts analyzed using GSEA

Contrast name	**Treatment**	**Control**
Collagen sandwich vs. Monolayer cultures		
CS vs HM 1d	Collagen sandwich 1 day	Hepatocyte monolayer 1 day
CS vs. HM 2d	Collagen sandwich 2 days	Hepatocyte monolayer 2 days
CS vs. HM 3d	Collagen sandwich 3 days	Hepatocyte monolayer 3 days
CS vs. HM 8d	Collagen sandwich 8 days	Hepatocyte monolayer 8 days
Within Collagen sandwich		
CS 8d vs. 1d	Collagen sandwich 8 days	Collagen sandwich 1 day
CS 8d vs. 2d	Collagen sandwich 8 days	Collagen sandwich 2 days
CS 8d vs. 3d	Collagen sandwich 8 days	Collagen sandwich 3 days

3.3.5 Gene Set Enrichment Analysis

The normalized gene expression data were analyzed using Gene Set Enrichment Analysis (GSEA) (107). Given replicate gene expression measurements for a control phenotype (e.g., HM at 1 day) and for a treatment phenotype (e.g., CS at 1 day), GSEA starts by ranking all genes by the extent of their differential expression in the two phenotypes. Thus, the lower the rank of a gene, the more up-regulated it is in the treatment, when compared to the control. Next, given a gene set of interest (e.g., the genes involved in metabolism of xenobiotics), GSEA uses a modified Kolmogorov-Smirnov test (112) to determine if the genes in this set have surprisingly high or low ranks in the list of differentially-expressed genes. GSEA computes an enrichment score that summarizes the ranks of genes in the gene set. This score has the following

interpretation: the more positive the score, the more up-regulated the genes in the gene set are in the treatment (compared to the control), and the more negative the score, the more down-regulated the genes in that gene set are. Since the size of a gene set may influence its enrichment score, GSEA controls this bias by performing a permutation test and calculating a *p*-value that represents the statistical significance of the enrichment score. Finally, GSEA converts the *p*-value into a *q*-value that measures the false discovery rate, after adjusting for multiple hypothesis testing. Note that the *q*-value is unsigned but the enrichment score is signed (positive for overall up regulation and negative for overall down regulation). We applied GSEA using the following criteria:

1.Sort genes in decreasing order of the signal-to-noise measure.

2. Compute *p*-values using 10,000 permutations of the sample-to-phenotype associations.

3. Report all gene sets with *q*-value (false discovery rate) at most 0.2. Note that with this cut-off, we expect one out of five gene sets to be a false discovery.

3.4 Results

LIMMA and GSEA were applied to compare the two culture conditions, as shown in Table 1. The first set of four contrasts compared the hepatocyte transcriptional program in CS cultures to that in HMs, at each of the four time-points analyzed. These contrasts were expected to reveal time-dependent differences between these two culture conditions. The second set of three contrasts compared CS samples to each other: 8 days to 1 day, 8 days to 2 days, and 8 days to 3 days. Such contrasts were expected to provide information on how transcriptional programs may vary within CS cultures condition over time.

3.4.1 The transcriptional program in CS cultures steadily and comprehensively diverges from that in HMs

For each of the first four contrasts in **Table 3.1**, the number of differentially-expressed probe sets was counted after applying different cutoffs on the *p*-values computed by LIMMA. The first column in **Table 3.2** indicates the *p*-value cutoff, while each of the other four columns show the number of probe sets whose *p*-value meets the cutoff specified in each row. An important feature revealed by these data is the monotonic divergence between the transcriptional programs of CS and HM samples over the 8-day culture period. For each cutoff, the number of

differentially-expressed probe sets increased steadily from day 1 to day 8. Furthermore, this trend was maintained even over a variation of four orders of magnitude in the *p*-value cutoff. On day 8, as many as 6,185 probe sets had a *p*-value of at most 0.01 (2,242 had a *p*-value of at most 10^{-5}). Since, the Affymetrix Rat230_2 GeneChip has 31,099 probe sets, these results suggest widespread transcriptional perturbation in CS cultures compared to HM cultures.

Table 3.2 The number of differentially-expressed genes in the each of the four CS vs. HM contrasts at different p-value cutoffs.

***p*-value cut-off**	**CS vs. HM 1d**	**CS vs. HM 2d**	**CS vs. HM 3d**	**CS vs. HM 8d**
1e-05	31	224	1046	2242
0.0001	61	362	1535	3092
0.001	118	569	2277	4287
0.01	276	1095	3497	6185
0.05	552	1812	5134	8551

Upon the identification of the global trends, GSEA was employed to study patterns of differential expression in specific gene sets. GSEA was applied to the gene expression data obtained through our experiments and to the following gene sets in the Molecular Signature DataBase (MSigDB): 1892 curated gene sets from various sources such as online pathway databases, publications in PubMed, and knowledge of domain experts, 837 motif gene sets containing genes that share a cis-regulatory motif that is conserved across the human, mouse, rat, and dog genomes, and 1454 gene sets corresponding to genes annotated by different Gene Ontology (GO) terms. For each contrast in Table 1 and for each of these gene sets, GSEA was used to compute a *q*-value.

Gene sets were filtered to those that exhibited a monotonic up-regulation in the CS-HM comparison. Specifically, gene sets were restricted to those whose *q*-values decreased monotonically from 1 day to 8 days and whose enrichment scores were positive in all four CS-HM contrasts (the first four contrasts in Table 1). Gene sets that were monotonically down-regulated in collagen sandwiches over the 8 day period were also identified (*q*-values decreasing monotonically and negative enrichment scores in all four CS-HM contrasts). Since MSigDB

collates data from several sources, many gene sets in it have high degrees of overlap. When an overlapping group of gene sets is up-regulated or down-regulated in our data, only one gene set per group is discussed below. The complete sets of results are available on our supplementary web page.

3.4.2 Liver-specific gene sets are up-regulated at day 1 or day 2 in CS cultures

Hsiao *et al* (113) created a compendium of gene expression in normal human tissues with the goal of defining a reference for basic organ systems biology. They identified 251 genes expressed selectively in the liver, which are included in MSigDB in the HSIAO_ LIVER_SPECIFIC_GENES gene set. In a similar study, Su *et al.* (114) profiled gene expression from 91 human and mouse samples across a diverse array of tissues, organs and cell lines. They identified 37 genes that were expressed specifically in human liver tissue samples; these genes belong to the HUMAN_TISSUE_LIVER gene set. The gene sets HSIAO_LIVER_SPECIFIC_GENES and LIVER_SPECIFIC_GENES were up-regulated significantly at day 1 and day 2, respectively. They were monotonically up-regulated on subsequent days. Both these gene sets had insignificant *q*-values in the CS-CS contrasts, suggesting that liver-specific genes are up-regulated on day 1 in CS cultures, and that they continue to be monotonically up-regulated on subsequent days (**Figure 3.1**). The presence and concentration of albumin is often used as a marker of phenotypic function of *in vitro* hepatic models (16, 103). The Albumin gene (*ALB*) was expressed in several gene sets such as HSIAO_LIVER_SPECIFIC_GENES and V$HNF1_Q6 that were up-regulated over the 8 day culture period (Figure 1). The promoter regions of genes in the set V$HNF1_Q6 contain binding sites for hepatic nuclear factor (HNF1), a transcription factor that activates gene expression of albumin (115, 116). This gene set has an overlap of 25 genes with the gene set HSIAO_ LIVER_ SPECIFIC_ GENES, indicating that HNF1 monotonically up-regulates the expression of ALB and other liver-specific genes in CS cultures but not in HMs. These observations support the conclusion that transcriptional programs that have been identified in other datasets to be liver-specific are active through the 8-day period in CS cultures but are not active in HMs.

Reprinted from Kim, Y. et al. Tissue Engineering Part C. Methods. 2010 Jun 7. [Epub ahead of print] with permission from Mary Ann Liebert, Inc. (doi:10.1089/ten.tec.2010.0012.)

CS vs. HM				Set Name	Description
1d	2d	3d	8d		
Liver-specific					
				HSIAO_LIVER_SPECIFIC_GENES	liver tissue genes
				HUMAN_TISSUE_LIVER	genes specifically expressed in human liver tissue
				V$HNF1_Q6	promoter motif for hepatic nuclear factor

Color legend for up-regulated *q*-values						
q-value	1	0.2	0.05	0.01	0.001	0.0001
Color						

Figure 3.1 Liver-specific up-regulated gene sets. The legend below shows the q-value ranges for each color. The color scheme used in these figures is RdYlGn from Color Brewer (http://colorbrewer2.org).

3.4.3 Gene sets involved in cholesterol, fatty-acid, alcohol, and carbohydrate metabolism are significantly up-regulated starting on day 1 or day 2 in CS cultures

3.4.3.1 Cholesterol Metabolism

Cholesterol metabolism is an important component of hepatic phenotypic function (102). The trends exhibited by gene sets linked to cholesterol metabolism in our data were investigated. Multiple gene sets involved in cholesterol metabolism were up-regulated in CS cultures compared to HMs. These gene sets include HSA00120_BILE_ACID_BIOSYNTHESIS, MONOOXYGENASE_ACTIVITY, CELLULAR_LIPID_METABOLIC_PROCESS, NUCLEAR_RECEPTORS, and CARBOXYLIC_ACID_TRANSMEMBRANE_TRANSPORTER_ACTIVITY (**Figure 3.2**). Bile acids mediate cholesterol metabolism and the synthesis of bile acids is initiated through the activity of CYP7A1, CYP8B1 and CYP27A1 enzymes (117-119) (**Figure 3.3**). In CS samples, the three CYP enzymes mentioned above are present either in the gene set HSA00120_BILE_ACID_ BIOSYNTHESIS or in the gene set MONOOXYGENASE_ACTIVITY, both of which are up-regulated in CS cultures. The gene expression of CYP enzymes is activated by nuclear receptors, specifically, the retinoid X receptor (RXR) and the liver X receptor (LXR) (120-123). The gene set NUCLEAR_RECEPTORS, which contains nuclear receptors involved in the activation of hepatic functions, behaved similarly to the liver-specific gene sets discussed earlier: it had

insignificant *q*-values in the CS-CS contrasts, suggesting that nuclear receptors were up regulated on day 1 in CS cultures and remained up-regulated on subsequent days. The nuclear receptor Farnesoid X receptor (FXR) plays a critical role in liver functioning. FXR is responsible for regulating the concentration of bile acids (117-121, 124, 125). Bile acid-mediated activation of FXR leads to the transcriptional activation of the ATP-binding cassette transporter B11 (ABCB11, also known as bile salt export pump), a process that is crucial for cholesterol secretion into the bile canaliculi (123, 124). In CS samples, the transcription of ABCB11, present in gene set CARBOXYLIC_ACID_TRANSMEMBRANE_TRANSPORTER_ACTIVITY, was shown to be up-regulated over the culture period in comparison to HMs. This gene set contains genes annotated with the Gene Ontology molecular function that involves the catalysis of the transfer of carboxylic acids from one side of the membrane to the other. These trends and data indicate that genes responsible for the formation, transformation, and transport of bile acids are up-regulated in CS cultures, thereby promoting cholesterol metabolism.

3.4.3.2 Fatty Acid Metabolism (PPAR-mediated metabolism)

Peroxisome proliferator-activated receptor alpha (PPARα) is a nuclear receptor that activates gene expression of enzymes linked to fatty acid metabolism (126-129). PPARα-mediated fatty acid metabolism initiates transcriptional activation of liver fatty acid-binding protein (*L-FABP* or *FABP1*), which deliver fatty acids to its cognitive nuclear receptor, PPARα, and promote expression of two transporters, *ABCD2* and *ABCD3*, which are necessary to transport fatty acids into peroxisomes, where target enzymes catalyze the clearance of fatty acids (117, 126, 128, 129). PPARα, being dependent on intracellular FABP concentrations, regulates expression of Acyl-CoA oxidases (*ACOXs*), short/branched-, long- and very long-chain Acyl-CoA dehydrogenase (*ACADs*), and mitochondrial enzymes involved in β-oxidation (130-134). In our data, the gene sets involved in PPARα-mediated fatty acid metabolism are HSA00071_FATTY_ACID_METABOLISM, PEROXISOME, HSA03320_PPAR_ SIGNALING_PATHWAY, and MITOCHONDRIAL_FATTY_ACID_BETAOXIDATION (**Figure 3.2**). All these gene sets were monotonically up-regulated in CS samples over the 8-day period in contrast to HMs. The gene *FABP1*, which belongs to the gene set HSA03320 _PPAR_SIGNALING_PATHWAY, was up-regulated in CS cultures and its expression increased over time. In response to the expression of *FABP1*, the gene *PPARα* is expressed

(126). The PPARα signaling pathway promotes the transcriptional activation of fatty acid metabolic enzymes (*ACOX* (acyl-CoA oxidase), *ACAD* (acyl-CoA dehydrogenase), *CAT* (carnitine palmitoyltransferase), *LPL* (lipoprotein lipase) and *ACAT* (acetyl-CoA acetyltransferease) (126, 130-132). These genes are members of the HSA00071_FATTY_ACID_METABOLISM, PEROXISOME, and MITOCHONDRIAL_ FATTY_ ACID_ BETAOXIDATION gene sets. The combination of the expression of key enzymes responsible for fatty acid metabolism as well as the expression of two members of the ABC transporter family (*ABCD2* and *ABCD3*) indicates that PPARα-mediated metabolism was up-regulated in CS samples.

CS vs. HM				Set Name	Description
1d	2d	3d	8d		
Cholesterol metabolism					
				HSA00120_BILE_ACID_BIOSYNTHESIS	KEGG bile acid synthesis genes
				MONOOXYGENASE_ACTIVITY	(GO MF) integration of one oxygen atom into a compound
				CELLULAR_LIPID_METABOLIC_PROCESS	(GO BP) lipid reactions and pathways
				CARBOXYLIC_ACID_TRANSM_TRANSP	(GO MF) transfer of carboxylic acid across a membrane
				NUCLEAR_RECEPTORS	GenMAPP nuclear receptor genes
Fatty-Acid Metabolism					
				HSA00071_FATTY_ACID_METABOLISM	KEGG fatty acid metabolism pathways
				MITOCHONDRIAL_FATTY_ACID_BETA	GenMAPP fatty acid oxidation in mitochondria
				PEROXISOME	(GO CC) associated with peroxisome
				HSA03320_PPAR_SIGNALING_PATHWAY	KEGG PPAR signaling pathway
Alcohol Metabolism					
				ALCOHOL_METABOLIC_PROCESS	(GO BP) reactions and pathways involving alcohols
				HSA00071_FATTY_ACID_METABOLISM	KEGG fatty acid metabolism pathways
				HSA00980_METABOLISM_OF_XENOBIOTICS	metabolism of xenobiotics by cytochrome P450
Carbohydrate Metabolism					
				GLUCOSE_METABOLIC_PROCESS	(GO BP) pathways involving glucose
				HSA00010_GLYCOLYSIS_AND_GLUCON	KEGG glycolysis and gluconeogenesis pathways

Color legend for up-regulated *q*-values						
q-value	1	0.2	0.05	0.01	0.001	0.0001
Color						

Figure 3.2 Up-regulated gene sets involved in cholesterol, fatty-acid, alcohol, and carbohydrate metabolism. The legend below shows the *q*-value ranges for each color.
Abbreviations:
CARBOXYLIC_ACID_TRANSM_TRANSP for
CARBOXYLIC_ACID_TRANSMEMBRANE_TRANSPORTER_ACTIVITY

MITOCHONDRIAL_FATTY_ACID_BETA for
MITOCHONDRIAL_FATTY_ACID_BETAOXIDATION

HSA00980_METABOLISM_OF_XENOBIOTICS for
HSA00980_METABOLISM_OF_XENOBIOTICS_BY_CYTOCHROME_P450,

HSA00010_GLYCOLYSIS_AND_GLUCON for
HSA00010_GLYCOLYSIS_AND_GLUCONEOGENESIS,
GO for Gene Ontology, BP for Biological Process, CC for Cellular Component, and MF for Molecular Function.

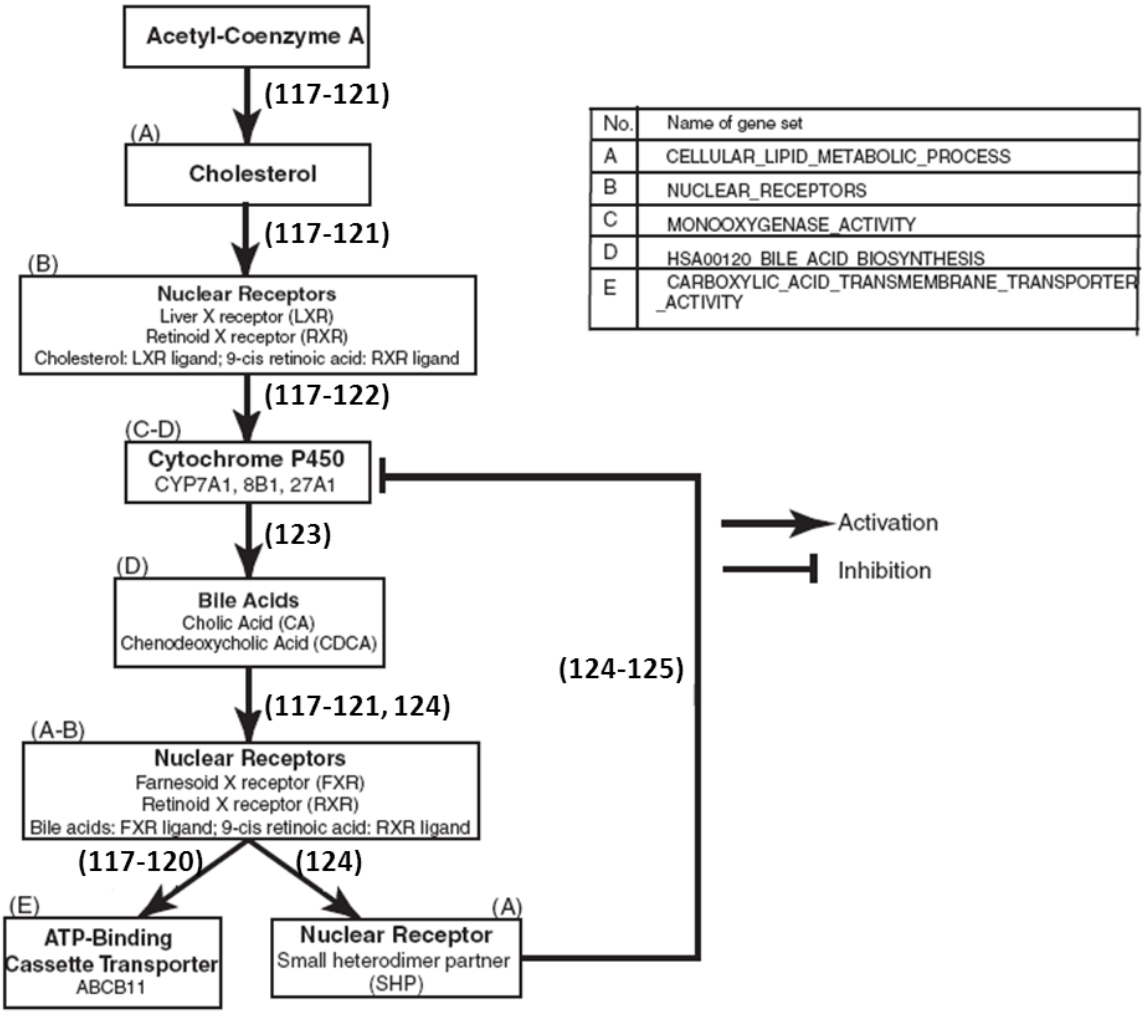

Figure 3.3 Pathway for cholesterol metabolism that shows gene sets involved in this process.

3.4.3.3 Alcohol Metabolism

Alcohol, specifically ethanol, is metabolized in the liver by several enzymes present in the subcellular compartments of hepatocytes. Alcohol dehydrogenase (ADH), a key cytoplasmic enzyme plays an important role in converting ethanol to acetaldehyde (135-137). Acetaldehyde,

a toxic molecule, is subsequently converted to non-toxic acetates by mitochondrial acetaldehyde dehydrogenase (ALDH) (135, 137). Additionally, CYP2E1 enables the clearance of ethanol through an oxidative reaction (137-139) (**Figure 3.4**). The gene sets ALCOHOL_METABOLIC_PROCESS, HSA00980_METABOLISM_OF_XENOBIOTICS_BY_CYTOCHROME_P450, and HSA00071_FATTY_ACID_METABOLISM were up-regulated over time in CS cultures in comparison to HMs (**Figure 3.2**). These gene sets include three alcohol dehydrogenase genes ADH, ADH1A, and ADH7 that mediate the transformation of alcohol.

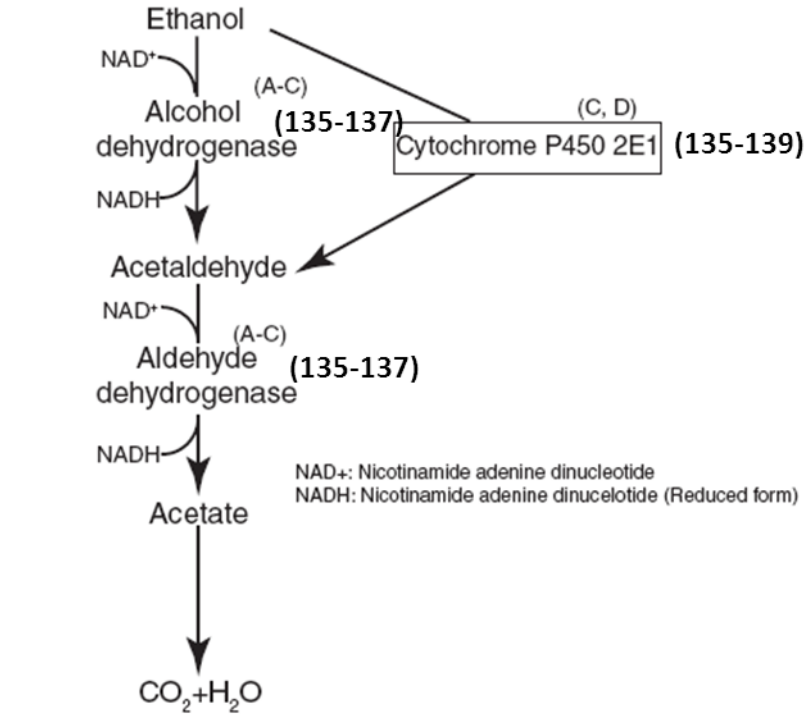

No.	Name of gene set
A	ALCOHOL_METABOLIC_PROCESS
B	HSA00071_FATTY_ACID_METABOLISM
C	HSA00980_METABOLISM_OF_XENOBIOTICS_BY_CYTOCHROME_P450
D	HSIAO_LIVER_SPECIFIC_GENES

Figure 3.4 Pathway for alcohol metabolism that shows gene sets involved in this process.

3.4.3.4 Carbohydrate Metabolism

Gluconeogenesis and glycolysis are essential to maintain glucose homeostasis (139-143). The maintenance of a healthy glucose level is dependent upon the presence and concentration of insulin and glucagon (140-142). In our gene expression data, genes for key enzymes involved in

the formation and metabolism of glucose are up-regulated in CS cultures in contrast to HMs. The relevant gene sets include HSA00010_GLYCOLYSIS_AND_GLUCONEOGENESIS and GLUCOSE_METABOLIC_ PROCESS (**Figure 3.2**). Specifically, genes corresponding to enzymes implicated in glycolysis are hexokinase (*HK*) , glucose phosphate isomerase (or phosphoglucose isomerase, *GPI* or *PGI*), phophofructokinase (*PFK*), aldolase (*ALDOB* and *ALDOC*), triosephosphate isomerase (*TPI1*), phosphoglycerate kinase 1 (*PGK1*), phosphoglycerate mutase (*PGAM*), pyruvate kinase (*PKLR*), and lactate dehydrogenase C (*LDH*) (terminal) (143). PKLR catalyzes the transphosphorylation of phosphoenolpyruvate into pyruvate and ATP, which is the rate-limiting step of glycolysis. LDH catalyzes the terminal step in glycolysis. Genes that code for enzymes involved in gluconeogenesis are phosphoenolpyruvate carboxykinase 1 (*PCK* or *PEPCK*), glucose-6-phosphatase (*G6PC*), pyruvate carboxylase (*PC*) and fructose-1, 6-bisphophatase 1 (*FBP1*) (142-144). In the gene sets related to carbohydrate metabolism, genes such as *ALDOB, ALDOC, PKLR, PFK, PGK1, GPI,* and *PFK* that are involved in glycolysis and genes such as *G6PC, FBP1, PCK1,* and *PC* that are involved in gluconeogenesis were up-regulated in CS samples.

3.4.3.5 Urea Production

In the liver, the formation of urea is a critical step in ammonia clearance. The metabolism of amino acids results in the formation of urea through the conversion of glutamate, an intermediate metabolite (102). Gene sets involved in glutamate metabolism such as HSA00251_GLUTAMATE_METABOLISM are gradually up-regulated over time in CS cultures (**Figure 3.5**). Urea is formed as a result of the action of five enzymes: carbamoyl phosphate synthetase 1 (CPS-1), ornithine transcarbamylase (OTC), argininosuccinate synthase (ASS), argininosuccinate lyase (ASL), and arginase (ARG) (145-150) (**Figure 3.6**). These five genes are present in the gene set HSA00220_UREA_CYCLE_AND_ METABOLISM_OF_AMINO_ GROUPS. This gene set is up-regulated in CS cultures over the 8-day period. In addition, the gene sets NITROGEN_COMPOUND_ CATABOLIC_ PROCESS and NITROGEN_COMPOUND_ METABOLIC_PROCESS include genes such as *ASL, ARG* and *ASS.* Both gene sets are also monotonically up-regulated in CS cultures. The nuclear receptor HNF-4α (a member of the up-regulated gene set NUCLEAR_RECEPTORS) plays an important role in triggering the transcription of key enzymes for urea production (145).

Together, these data provide information on why urea production is stable in CS cultures but not in HMs.

CS vs. HM				Set Name	Description
1d	2d	3d	8d		
				Urea Production	
				HSA00251_GLUTAMATE_METABOLISM	KEGG glutamate metabolism pathways
				HSA00220_UREA_CYCLE	KEGG pathways of urea cycle and metabolism and amino groups
				NITROGEN_COMPOUND_CATABOLIC_PROCESS	(GO BP) pathways for breakdown of nitrogenous compounds
				NITROGEN_COMPOUND_METABOLIC_PROCESS	(GO BP) pathways for synthesis and breakdown of nitrogenous compounds
				NUCLEAR_RECEPTORS	GenMAPP nuclear receptor genes

Color legend for up-regulated *q*-values						
q-value	1	0.2	0.05	0.01	0.001	0.0001
Color						

Figure 3.5 Up-regulated gene sets involved in urea production. The legend below shows the q-value ranges for each color. Abbreviations: HSA00220_UREA_CYCLE for HSA00220_UREA_CYCLE_AND_METABOLISM_OF_AMINO_GROUPS.

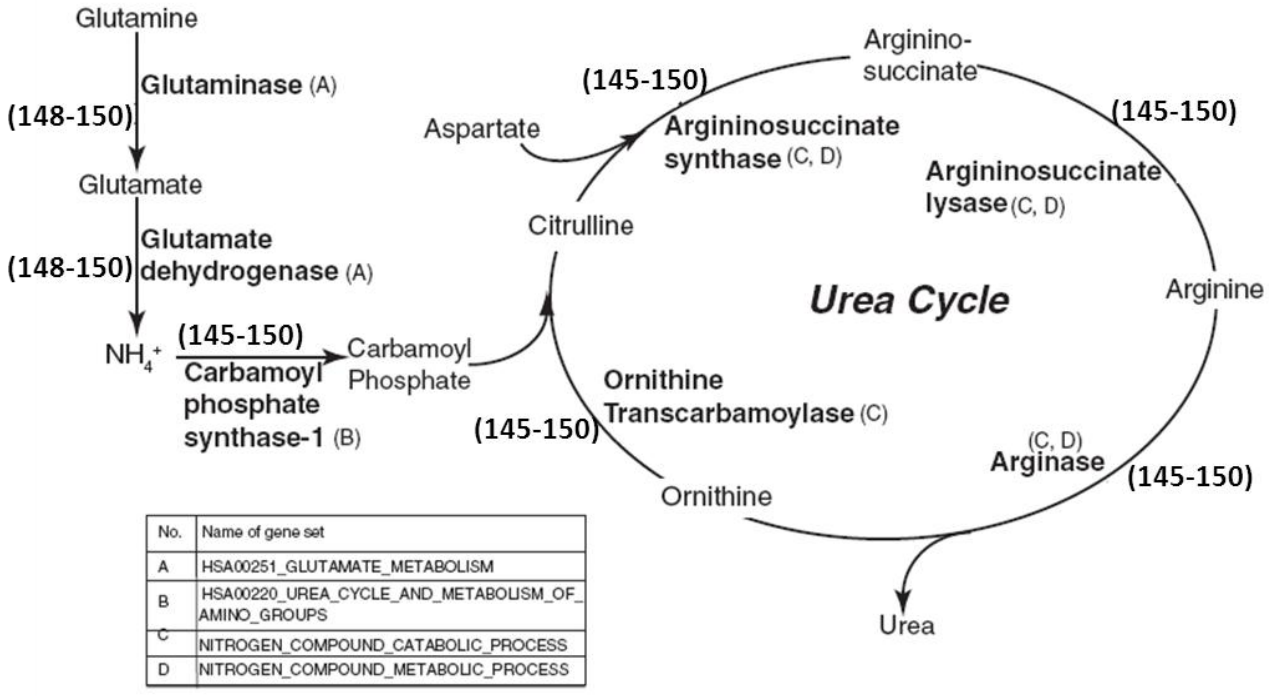

Figure 3.6 Pathway for urea production that shows gene sets involved in this process.

3.4.4 Mono-oxygenases are initially not differentially expressed but recover after day 3 in CS cultures

Xenobiotic metabolism in the liver is mediated through cytochrome P450 enzymes (151-154). The expression of these enzymes has been shown to decrease upon the isolation of hepatocytes from the liver (153, 154). The gene set MONOOXYGENASE_ACTIVITY contains several cytochrome P450 genes and flavin containing monooxygenase. This gene set had *q*-values of 0.03, 0.01, 6×10^{-3}, and 7×10^{-5} at days 1, 2, 3, and 8, respectively (**Figure 3.7**). The *q*-values at day 1 and day 2 were nearly identical but decreased by an order of magnitude at day 3 and by another order of magnitude at day 8. These trends were examined further by computing the *q*-values for this gene set in the CS-CS contrasts. This gene set was up-regulated with *q*-value 0.13 for the day 8-day 1 contrast, 0.11 for the day 8-day 2 contrast, and 1.00 for the day 8-day 7 contrast. The statistical significance values for corresponding contrasts among the HM samples were also computed. This gene set was down-regulated in all three contrasts. The *q*-values were 0.13, 0.06, and 0.13, respectively. Thus, the variation in expression of this gene set arises from a combination of up-regulation in CS cultures and down-regulation in HM cultures. Taken together, these trends indicate that the genes in this set "recovered" or became up-regulated at day 3 and later within CS cultures, in comparison to HM cultures. This trend is of significance since genes in this set include those that encode for CYP3A, CYP4A, CYP1A and CYP2C enzymes. CYP3A and 4A enzymes metabolize a wide range of pharmaceuticals and drugs and the CYP2C and CYP1A enzymes break down toxins and xenobiotics. The gene set HSA00980_ METABOLISM_ OF_XENOBIOTICS_BY_ CYTOCHROME_P450, which contains cytochrome P450s, phase II metabolizing enzymes such as UDP-glucuronosyl-transferase (U*DP-GT*) isoforms, and glutathione S-transferase (*GST*), also exhibited a similar trend. It showed no significant regulation at day 1, had a *q*-value of 0.20 at day 2, but had *q*-values an order of magnitude less at days 3 and 8 (2×10^{-3} and 10^{-3}, respectively). In the three CS-CS contrasts, the *q*-values for this gene set were 0.12, 0.05, and 0.13 (all for up regulation), while they were 0.1, 0.12, and 1 in the HM-HM contrasts (all for down regulation). In a previous study, the expression of a single CYP enzyme, specifically, CYP1A1 was monitored and was shown to "recover" on day 3 (155). However, additional time points or CYP enzymes were not investigated. The results in this work point to a more widespread recovery phenomenon among the CYP gene family.

CS vs. HM				Set Name	Description
1d	2d	3d	8d		
0.03	0.01	6e-03	7e-05	MONOOXYGENASE_ACTIVITY	(GO MF) integration of one oxygen atom into a compound
1.00	0.20	2e-03	1e-03	HSA00980_METABOLISM_OF_XENOBIOTICS	metabolism of xenobiotics by cytochrome P450

Color legend for up-regulated *q*-values						
q-value	1	0.2	0.05	0.01	0.001	0.0001
Color						

Figure 3.7 Gene sets that show recovery after day 3. We show the *q*-values to underscore the recovery.

3.4.5 Cell-cycle activity decreases significantly in CS cultures

Analysis of the down regulated gene sets presented interesting insights into cellular response within CS and HM systems. Our results suggested a significant difference in cell cycle activity between the HM and CS samples over the 8 day culture period. The monotonic down regulation of the gene sets MITOTIC_CELL_CYCLE and CELL_CYCLE_KEGG coupled with insignificant *q*-values in the CS-versus-CS comparisons (data not shown) suggested decreasing cell cycle activity within the CS cultures (**Figure 3.8**). Nuclear transport and import functions show decreased activity within CS samples as indicated by the monotonically down regulated gene sets NUCLEOCYTOPLASMIC_TRANSPORT and PROTEIN_IMPORT_INTO_NUCLEUS. In addition, the down regulation of processes involved in microtubule organization (gene sets such as MICROTUBULE_CYTOSKELETON, MICROTUBULE_ ORGANIZING_CENTER, SPINDLE and CENTROSOME) were also observed. Our results are similar to a previous study in which the cell cycle and cell proliferation were found to be up-regulated in HMs in comparison to hepatoma cells cultured in a 3D spheroid culture (104). Although hepatocytes cultured in spheroids experience an environment that differs from CS configurations, they have been shown to exhibit metabolic and synthesis profiles similar to CS cultures (104).

CS vs. HM				Set Name	Description
24h	48h	72h	8d		
Cell Cycle					
				MITOTIC_CELL_CYCLE	(GO BP) participation in eukaryotic cell cycle events
				CELL_CYCLE_KEGG	KEGG cell cycle pathway
Nuclear Transport					
				NUCLEOCYTOPLASMIC_TRANSPORT	(GO BP) movement of molecules between nucleus and cytoplasm
				PROTEIN_IMPORT_INTO_NUCLEUS	(GO BP) protein transport into nucleus
Cell Replication					
				MICROTUBULE_CYTOSKELETON	(GO CC) microtubules of the cytoskeleton
				MICROTUBULE_ORGANIZING_CENTER	(GO CC) region of microtubule growth
				SPINDLE	(GO CC) microtubule array for segregating duplicated chromosomes
				CENTROSOME	(GO CC) centriole and spindles

Color legend for down-regulated q-values						
q-value	1	0.2	0.05	0.01	0.001	0.0001
Color						

Figure 3.8 Down-regulated gene sets. The legend below the table shows the *q*-value ranges for each color.

3.5 Discussion

In vitro hepatic cultures play an increasingly important role in the design and development of pharmaceutics, toxicity testing, and the design of bio-artificial liver devices. Therefore, obtaining a comprehensive understanding of the global trends in transcription over time is critical to the advancement of each of these applications. A common problem associated with *in vitro* cultures of primary hepatocytes is the onset of de-differentiation soon after the cells are removed from the tissue. The temporal genome-wide transcriptional studies reported in this study provide insights into the up- and down-regulation of various liver-critical gene sets and their subsequent effects on various metabolic activities, synthesis of proteins, and detoxification. A gene set level network was constructed in order to obtain a systems level perspective of the current results (**Figure 3.9**). Each node in this network is an up-regulated gene set and two gene sets are connected by an edge if they share a statistically significant number of genes. Only those connections between gene sets are included that are significant after correcting for testing multiple hypotheses using the method of Benjamini and Hochberg (156), at an alpha of 0.05. This correction resulted in the omission of several insignificant connections. A gene set was

placed at the first time point at which it was significantly up-regulated (i.e., had a *q*-value reported by GSEA of at most 0.2). Although this network does not reveal the multiple signaling pathways involved in liver-related processes in their entirety, it presents a preliminary high-level view of the temporal cascade of transcriptional activation in CS cultures. For instance, nuclear receptors, liver-specific genes, and the PPAR-alpha pathway are up-regulated significantly on day 1. Processes related to alcohol metabolism, bile acid biosynthesis and urea production are up-regulated significantly on day 2. Lipid metabolism and transport are activated at later time points. Although monooxygenase activity and xenobiotic metabolism appear on days 1 and 2 respectively in this network, these gene sets show much more statistical significance at days 3 and 8, as noted earlier. Nuclear receptors are known to trigger the gene expression of CYP 450 enzymes (which are monoxygenases and involved in metabolism of xenobiotics). It is intriguing that nuclear receptors are up-regulated at day 1 but with a *q*-value of 0.1. At later time points, this gene set becomes more statistically significant (*q*-values of 0.01 at days 2 and 3 and a *q*-value of 3×10^{-3} at day 8), mirroring the trend observed for monooxygenase activity and xenobiotic metabolism. These observations will direct future experimental studies.

The time-dependent overview of the transcriptional changes that occur in HM and CS cultures illustrated in Figure 9 enables the investigation of liver phenotypic functions at appropriate time points. For example, in the absence of inducers, measuring the enzymatic activity and kinetics of CYP enzymes would be appropriate after hepatocytes are maintained in CS cultures for 3 days or more. In contrast, investigating metabolic activity could reveal important information when conducted on hepatocytes maintained in CS cultures for a minimum of 2 days. *In vitro* hepatic cultures can never replace or truly replicate animal models. However, their significance lies in their ability to serve as models to explore a wide range of physiological phenomena. Therefore, obtaining a comprehensive view of the numerous transcriptional changes that occur over a period of time and characterizing these changes in terms of succinct gene-set-level signatures will be valuable in guiding further investigations of cell signaling, metabolism, and protein synthesis functions in engineered livers.

In summary, the genome-wide gene expression profiles in two major hepatocyte culture systems have been analyzed, the first such dataset to our knowledge. The comparative analysis

of transcriptional data obtained from the two culture systems reveals numerous liver-specific transcriptional programs that are up-regulated in collagen sandwich cultures but not in monolayers. These processes span a wide range of biological processes important to liver function. Taken together, these trends and results provide a baseline for further systems-level modeling of engineered liver tissues.

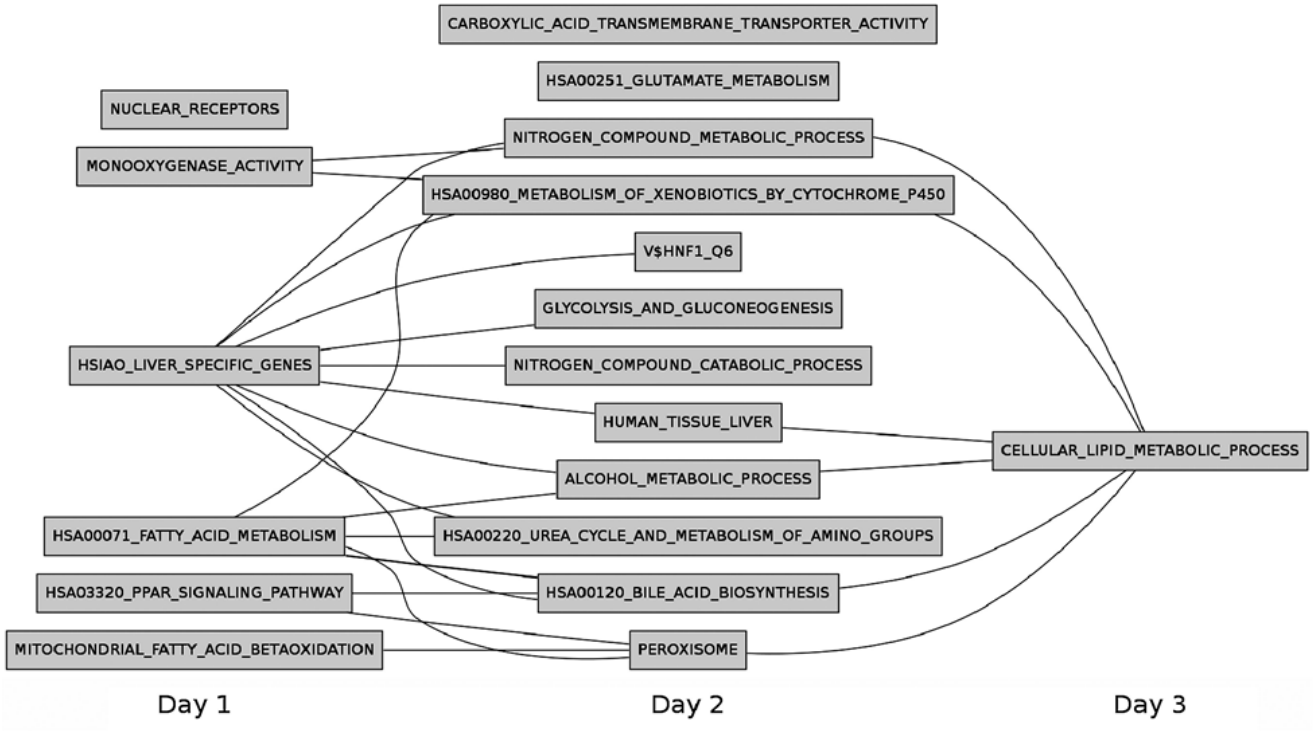

Figure 3.9 Gene set level network of up-regulated processes in CS cultures.

3.6 Acknowledgements

We gratefully acknowledge financial support from the National Science Foundation (CBET-0933225, P.R. and T.M.M.), the National Institutes of Health (NIDDK-1R21DK077802, P.R.) and the Institute for Critical Technology and Applied Sciences (P.R. and T.M.M.) at Virginia Polytechnic Institute and State University. We thank the staff at the Virginia Bioinformatics Institute Core Laboratory facility for their assistance with this project.

Chapter 4. 3D Hepatic Cultures Simultaneously Maintain Primary Hepatocyte and Liver Sinusoidal Endothelial Cell Phenotypes

4.1 Abstract

Developing *in vitro* engineered hepatic tissues that exhibit stable phenotype is a major challenge in the field of hepatic tissue engineering. However, the rapid dedifferentiation of hepatic parenchymal (hepatocytes) and non-parenchymal (liver sinusoidal endothelial, LSEC) cell types when removed from their natural environment *in vivo* remains a major obstacle. The primary goal of this study was to demonstrate that hepatic cells cultured in layered architectures could preserve or potentially enhance liver-specific behavior of both cell types. Primary rat hepatocytes and rat LSECs (rLSECs) were cultured in a layered three-dimensional (3D) configuration. The cell layers were separated by a chitosan-hyaluronic acid polyelectrolyte multilayer (PEM), which served to mimic the Space of Disse. Hepatocytes and rLSECs exhibited several key phenotypic characteristics over a twelve day culture period. Immunostaining for the sinusoidal endothelial 1 antibody (SE-1) demonstrated that rLSECs cultured in the 3D hepatic model maintained this unique feature over twelve days. In contrast, rLSECs cultured in monolayers lost their phenotype within three days. The unique stratified structure of the 3D culture resulted in enhanced heterotypic cell-cell interactions, which led to improvements in hepatocyte functions. Albumin production increased three to six fold in the rLSEC-PEM-Hepatocyte cultures. Only rLSEC-PEM-Hepatocyte cultures exhibited increasing CYP1A1/2 and CYP3A activity. Well-defined bile canaliculi were observed only in the rLSEC-PEM-Hepatocyte cultures. Together, these data suggest that rLSEC-PEM-Hepatocyte cultures are highly suitable models to monitor the transformation of toxins in the liver and their transport out of this organ. In summary, these results indicate that the layered rLSEC-PEM-hepatocyte model, which recapitulates key features of hepatic sinusoids, is a potentially powerful medium for obtaining comprehensive knowledge on liver metabolism, detoxification and signaling pathways *in vitro*.

4.2 Introduction

Two of the most commonly observed cell types in the liver are hepatocytes and liver sinusoidal endothelial cells (LSECs). Together, they account for more than 80% of the liver's mass. Hepatocytes are responsible for several metabolic and detoxification functions that are unique to the liver (1). LSECs exhibit characteristics that are distinct from endothelial cells that line other blood vessels. They participate in metabolic activities, exhibit fenestrae(1, 157) and are often the initial target of hepatic toxicants (158). LSECs also function as a scavenger system in the liver by removing waste macromolecules and play a vital role in the balance of lipids, cholesterol and vitamins (20, 88, 90, 159-162).

These primary hepatic cell types are well known to exhibit a dramatic loss in their phenotypic characteristics when removed from the organ (1). Specifically, hepatocytes and LSECs dedifferentiate within 72h when cultured as monolayers *in vitro* (17, 40, 41, 154). Various approaches have been utilized to design *in vitro* hepatocyte cultures in order to maintain their phenotype. For instance, hepatocytes cultured in a collagen sandwich or in 2D co-cultures with non-parenchymal cells remain stable over two an extended period of time (17, 40, 41, 45, 47, 48, 50, 53, 61, 62). More recently, hepatocytes sandwiched between two Matrigel layers were reported to exhibit stable function (163). Despite their advantages, collagen or Matrigel sandwich cultures do not provide the complex multi-cellular environment found *in vivo,* whereas 2D co-cultures do not mimic the layered liver architecture. Maintaining the phenotype of LSECs has proven to be equally difficult. Recently, studies have demonstrated that modulating the microenvironment in LSEC cultures can delay the dedifferentiation of LSECs (164-166). For example, LSECs cultured on extra-cellular matrices derived from the liver, bladder or intestine maintained liver-specific characteristics up to 3 days when cultured individually or up to 7 days when co-cultured with primary hepatocytes (165). Varying the cellular microenvironment in combination with culturing LSECs with fibroblasts and hepatocytes delayed the dedifferentiation of LSECs up to 14 days (166). The addition of growth factors such as vascular endothelial cell growth factor (VEGF), hepatocyte growth factor (HGF), and platelet derived growth factor (PDGF) can also prolong the loss of LSEC-specific characteristics (30, 87, 167). In spite of these advances, it has proven extremely difficult to simultaneously maintain the phenotypes of hepatocytes and LSECs *in vitro*. Consequently, the multitude of critical hepatic functions that

hepatocytes and LSECs perform cannot be studied adequately or monitored for long periods *in vitro*.

In vivo, hepatocytes and LSECs are separated by a protein-based interface called the Space of Disse (1). We hypothesized that constructing an *in vitro* model that mimicked the Space of Disse might assist in delaying the de-differentiation of hepatic cells. In previous attempts to test this hypothesis, we have reported the assembly of 3D hepatic cellular constructs assembled from primary hepatocytes, human umbilical vein endothelial cells (HUVECs)/human LSECs (hLSECs) and a polyelectrolyte-derived interfacial region that mimics the Space of Disse (73, 168). The polyelectrolyte multilayer (PEM) was deposited above a layer of hepatocytes and was comprised of cationic (chitosan) and anionic (hyaluronic acid) polyelectrolytes. The height of the PEM was determined to be approximately 30nm and 55nm for five and fifteen layers respectively. The PEM exhibited a high degree of hydration (1.01 mPas) and shear modulus values of approximately 100kPa, similar to those observed within the liver *in vivo* (168). When human LSECs (hLSECs) were cultured on the PEM-coated hepatocyte layer, the resulting construct exhibited significantly enhanced hepatic properties in comparison to hepatocyte monolayers or collagen sandwich cultures. However, we did not monitor the phenotypes of the LSECs in these earlier studies.

In this study, our goal was to incorporate primary rat LSECs (rLSECs) into the 3D hepatic model to determine if such an arrangement of hepatic cells would prevent or delay the dedifferentiation of both hepatocytes and rLSECs. In the 3D model reported herein, hepatocytes and rLSECs were separated by a nanoscale PEM that could potentially mediate intercellular signaling and ultimately promote heterotypic interactions. The phenotypic characteristics of primary rat hepatocytes and rLSECs were monitored through a combination of hepatocellular-specific assays and immunostaining. Hepatocyte function was monitored through urea and albumin production, cytochrome P450 enzyme kinetics, and by immunostaining for bile canaliculi. For rLSECs, immunostaining for the sinusoidal endothelial marker (SE-1) provided a convenient method to verify their differentiated state.

4.3 Materials and Methods

4.3.1 Materials

Dulbecco's modified eagle medium (DMEM) containing 4.5 g/L glucose, phosphate-buffered saline (PBS), Earle's balanced salt solution (EBSS), Hank's buffered salt solution (HBSS), ethoxy resorufin, benzyloxy resorufin, resorufin, penicillin, streptomycin, and trypsin-ethylenediaminetetraacetic acid were obtained from Invitrogen Life Technologies (Carlsbad, CA). Type IV collagenase, HEPES (4-[2-hydroxyethyl] piperazine-1-ethanesulfonic acid), glucagon, hydrocortisone, dicumarol, sodium dodecyl sulfate (SDS), hydrogen peroxide, pronase, and glutaraldehye were obtained from Sigma-Aldrich (St. Louis, MO). Endothelial cell growth medium and supplements were obtained from ScienCell Research Laboratories (San Diego, CA). Unless noted otherwise, all other chemicals were obtained and used as received from Fisher Scientific (Pittsburgh, PA).

4.3.2 Hepatocyte Isolation and Culture

Primary rat hepatocytes were harvested from female Lewis rats (Harlan, Indianapolis, IN) that weighed between 170-200g. Animal care and surgical procedures were conducted in accordance with procedures approved by Virginia Polytechnic Institute and State University's Institutional Animal Care and Use Committee. A two-step *in situ* collagenase perfusion method was utilized to excise the liver (17, 41, 73, 168). Briefly, rats were anesthetized with 3 L/min of a gas mixture of 3% (v/v) isofluorane/97% oxygen (Veterinary Anesthesia Systems Co., Bend, OR). The liver was perfused with oxygenated Krebs Ringer Buffer (KRB; 7.13 g/L sodium chloride, 2.1 g/L sodium bicarbonate, 1 g/L glucose, 4.76 g/L HEPES and 0.42 g/L potassium chloride) that contained 1mM EDTA (ethylene diamine tetra acetic acid), followed by perfusion with a 0.1% w/v collagenase (Sigma, Type IV). Cell suspensions were filtered through nylon meshes with porosity ranging from 250 to 62 μm (Small Parts, Inc., Miramar, FL). Hepatocytes were separated using a Percoll (Sigma-Aldrich) density centrifugation technique. Hepatocyte viability was determined by trypan blue exclusion. Hepatocytes were cultured on collagen-coated 6-well sterile tissue culture plates (Becton Dickinson Labware, Franklin Lakes, NJ) and were maintained in culture medium that consisted of DMEM supplemented with 10% heat-inactivated fetal bovine serum (Hyclone, UT), 200 U/mL penicillin, 200 μg/mL streptomycin, 20 ng/mL epidermal growth factor (BD Biosciences, San Jose, CA), 0.5 U/mL insulin (USP,

Rockville, MD), 14 ng/mL glucagon and 7.5 μg/mL hydrocortisone. A collagen gelling solution was prepared by mixing 9 parts of Type I collagen (BD Biosciences) solution and 1 part of 10X DMEM. Sterile 6-well tissue culture plates were coated with 0.5 ml of the gelling solution and incubated at 37 ^{o}C for 1h to promote gel formation. Hepatocytes were seeded at a density of 1 million cells/well. Hepatocyte cultures were maintained at 37°C in a humidified gas mixture of 90% air/10% CO_2. The culture medium was replaced every 24h and medium samples were stored at -20^{o}C for further analysis.

4.3.3 Isolation and Culture of Primary Rat LSECs

Primary rat LSECs (rLSECs) were isolated from the supernatant taken from the centrifugation steps for hepatocyte isolation as well as from hepatic tissue fragments treated with pronase (0.02% (w/v)). The resulting cell fraction was added to 25%/50% Percoll/PBS gradients. Cells located at the interface between 25 and 50% Percoll/PBS were collected for further separation. rLSECs were separated from other non-parenchymal hepatic cells through a differential adhesion step involving incubation on a tissue culture plastic surface at 37°C for 30 min. The non-adherent rLSECs were maintained in medium supplemented with 5% (v/v) fetal bovine serum, 1% (v/v) endothelial cell growth supplement, 100 U/mL penicillin, and 100 μg/mL streptomycin at 37ºC under a humidified gas mixture of 95% air/5% CO_2.

4.3.4 Assembly of 3D Constructs of Primary Rat Hepatic Cells

Primary rat hepatocytes were cultured on collagen-gel coated substrates and allowed to spread up to 72 h to form a confluent monolayer (168). Upon obtaining a confluent cell layer, a polyelectrolyte multilayer (PEM) was deposited. The PEM was comprised of alternating layers of chitosan (200-300kDa, 0.01% (w/v)) and hyaluronic acid (> 1x10^{6} kDa, 0.01% (w/v)). PEMs were deposited on hepatocytes by first layering chitosan as a cationic PE on the cells followed by hyaluronic acid as an anionic PE. The exposure time for each PE layer was approximately 1-2 minutes. The desired number of layers was assembled through sequential and alternate deposition of PEs on hepatocytes. At the end of the deposition procedure, the samples were rinsed in 1X PBS and subsequently maintained in cell-culture medium at 37 °C. Thereafter, a layer of primary rat LSECs was seeded. Typically, 25,000 (denoted as 25K) or 50,000 (denoted as 50K) rLSECs were added to each sample and non-adherent cells were removed after 2 h. In

order to visually observe the 3D primary hepatic cell constructs, LSECs were labeled with a fluorescent, membrane permeable dye (PKH26 Red Fluorescent Cell Linker Kit; Sigma-Aldrich) prior to seeding. The culture medium was replaced every 24hr and medium samples were collected and stored -20°C until further analysis. Cells were observed and imaged under an inverted Nikon TE-2000 (Nikon) microscope coupled with a Hamamatsu CCD camera.

4.3.5 Immunostaining for Sinusoidal Endothelial -1 (SE-1) LSEC Marker

LSECs were fixed in a 2% glutaraldehyde/PBS v/v solution for 30 min at room temperature and subsequently incubated with a 0.1% Triton X-100 solution to permeabilize their membrane. The LSEC samples were placed overnight in a blocking solution (1% BSA/PBS w/v) solution at 4^{o}C. The samples were first exposed to a primary antibody (SE-1, Immuno-Biological Laboratories, Minneapolis, MN) for 2h at 37 ^{o}C and followed by exposure to a FITC-conjugated secondary antibody (Sigma-Aldrich) for 1 hr at room temperature. Images were acquired on a Zeiss LSM confocal microscope.

4.3.6 Urea and Albumin Production by Primary Rat Hepatocytes

Urea concentration of medium samples was determined via its specific colorimetric reaction with diacetyl monoxime using a commercially available assay kit (BUN Assay kit; Stanbio Laboratory, Boerne, TX) (73, 168). Albumin concentration of medium samples was analyzed by an enzyme-linked immunosorbent assay (ELISA), in triplicate, utilizing a polyclonal antibody to rat albumin (Cappel Laboratories, Aurora, OH). The absorbance was measured on a SpectraMax M2 microplate reader (Molecular Devices, Sunnyvale, CA). Standard curves were generated using purified rat albumin or urea diluted in culture medium. The data reported were normalized to the DNA content of hepatocytes.

4.3.7 Preparation of SE-1 Antibody-Conjugated Dynabeads®

In order to efficiently separate rLSECs and hepatocytes in the 3D hepatic cell cultures, SE-1 antibody conjugated Dynabeads® (Invitrogen) were utilized. SE-1 antibody-coated Dynabeads® were obtained by incubating human anti-mouse IgG-tagged Dynabeads® (CELLection™ Pan Mouse IgG Kit; Invitrogen) with mouse anti-rat SE-l antibody (Immuno-Biological Laboratories, Minneapolis, MN)) at room temperature for 30 min (30). The optimal

amount of antibody per Dynabeads® was chosen as 2 µg of antibody for labeling $4x10^7$ beads (100 µL of original bead suspension supplied by the company). The SE-1 antibody coated Dynabeads® was stored on ice until used.

4.3.8 Determination of Separation Efficiency of SE-1 Antibody-Conjugated Dynabeads®

The separation efficiency of SE-1 antibody-tagged Dynabeads® was determined in 50K rLSECs-5 PE layers-Hepatocytes and 100K rLSECs-5 PE layers-Hepatocytes as representative 3D hepatic models. On day 7, post-LSEC seeding, a 0.1% (w/v) collagenase solution was added to the hepatic cultures. After collagenase treatment, the cell suspensions were centrifuged and resuspended in 1 mL of 1% (w/v) BSA/PBS solution. The cell suspensions that contained two different liver cell populations (hepatocytes and rLSECs) were incubated with 25µL of SE-1 antibody-coated Dynabeads® for 20 min at 4°C. Dynabeads®-bound rLSEC fraction was separated from the mixed cell suspension using a magnet (DynaMag™-15; Invitrogen) and the unbound hepatocyte fraction (supernatant) was collected and transferred to a new tube. After separation, the LSEC and hepatocyte fractions were seeded on fibronectin-coated or collagen-gel coated substrates respectively, to quantify the degree of purity for each sample. The number of cells for each fraction was counted using a non-destructive imaging method. Approximately fifty images were taken per sample to determine purity. Analysis of the images based upon the distinctive polygonal or elongated morphology for hepatocytes and rLSECs respectively. These studies revealed the purity of cell populations to be greater than 95%. The percent recovery for each cell type was found to be equal to or greater than 90% by quantifying using hemotocymeter.

4.3.9 Measurement of DNA Content

Hepatocytes were lysed in a 0.1% (w/v) SDS solution and stored at –20 ^oC until further analysis. For DNA measurements, aliquots of cell suspensions were treated with a fluorescent DNA-binding dye (Hoechst 33258, pentahydrate-bis-benzimide; Invitrogen). The fluorescence intensity was measured using a SpectraMax M2 microplate reader (excitation and emission wavelengths were set at 355 nm and 460 nm respectively) and converted to DNA concentration by comparison to a standard curve for calf thymus DNA (Sigma-Aldrich) with concentrations ranging from 0 to 40 µg/ml.

4.3.10 Cytochrome P450 Enzyme Activity (CYP1A1/2 and CYP3A)

Cytochrome P450-dependent ethoxyresorufin *o*-dealkylase (EROD) or benzyloxyresorufin *o*-dealkylase (BROD) activity was induced by adding 3-methylcholanthrene (3MC, Sigma-Aldrich, 2 μM) or dexamethasone (Sigma-Aldrich, 37.5 μM), respectively, to the hepatocyte cultures 48h prior to conducting measurements. Cytochrome-P450 dependent EROD or BROD detoxification activity was measured using ethoxyresorufin or benzyloxyresorufin as substrate. The incubation mixture contained the appropriate resorufin substrate (5 μM) and 80 μM dicumarol diluted in EBSS (Invitrogen) (73, 83, 168). Aliquots (100 μL) were taken at 5, 15, 25, and 35 minutes after adding the resorufin mixture, transferred to a 96-well plate and the fluorescence intensity was measured using a SpectraMax M2 microplate reader (excitation and emission wavelengths were set to 530 nm and 580 nm respectively). Fluorescence intensity was converted to values of concentration by comparison to a standard curve for resorufin fluorescence with concentrations ranging from 0 to 1000 nM. The rate of resorufin formation (nM/min) was calculated from the early linear increase in the fluorescence curve, normalized to the DNA content in hepatocytes, and defined as cytochrome P450 isoenzyme activity. The absolute values obtained on day 12 for EROD or BROD activity were divided by the baseline activity on day 4 to obtain values of fold change.

4.3.11 Di-peptyl Peptidase IV (DPP IV) Immunostaining to Image Bile Canaliculi

Hepatocyte monolayers as well as rLSEC-Hepatocyte and rLSEC-PEM-Hepatocyte cultures were fixed in a 2% glutaraldehyde/PBS solution, followed by permeabilization for in a 0.1% Triton X-100 solution. The cultures were incubated overnight at 4^{o}C in a 1% BSA/PBS solution. The samples were incubated with a mouse monoclonal antibody to rat DPP IV (Cell Sciences, Canton, MA) and a secondary FITC-conjugated rabbit anti-mouse IgG antibody (Sigma-Aldrich) and imaged using an inverted Zeiss LSM510 confocal microscope (16, 169).

4.3.12 Statistical Analysis

All data are reported as mean ± standard deviation (S.D.). *t*-tests were conducted to detect differences in the mean values between day 4 and day 12 for each culture. *p*-values were adjusted for multiple hypothesis testing using the Bonferroni correction. Statistically significant samples at an alpha of 0.05 are denoted with an asterisk (*).

4.4 Results

4.4.1 Urea and Albumin Production in 5K rLSECs-PEM-Hepatocyte and 10K rLSECs-PEM-Hepatocyte Constructs

rLSECs were seeded at concentrations of either 5K, 10K, 25K or 50K above PEM-coated primary hepatocytes. In addition, the number of polyelectrolyte layers within the PEM was varied from 5 to 30. Preliminary studies indicated that using 5K and 10K LSECs or PEMs comprised of greater than 15 layers did not maintain or enhance hepatocellular phenotypic functions.

Urea production in rLSEC-PEM-Hepatocyte cultures at initial concentrations of either 5K or 10K LSECs was measured over a twelve day culture period (**Figure 4.1**). Urea production in HM, 5K rLSECs-Hep, and 10K rLSECs-Hep decreased by 60%, 25%, and 20% over the culture period, respectively (**Figure 4.1A**). Although urea production in 5K rLSECs-PEM-Hep and 10K-PEM-Hep remained stable, the values on day 12 were not statistically significant in comparison to that in HMs as well as rLSEC-Hep samples. On the other hand, 5K rLSECs-PEM-Hep and 10K rLSECs-PEM-Hep exhibited increasing albumin secretion over the 12 day period (**Figure 4.1B**). On day 12, rLSECs-30 PE layers-Hepatocyte constructs exhibited the lowest albumin secretion among the rLSEC-PEM-Hepatocyte samples.

Although 25K rLSECs-30L-Hepatocyte and 50K rLSECs-30L-Hepatocyte cultures exhibited stable urea production over a 12 day culture period, the values were similar to that observed in HMs as well as rLSECs-Hepatocyte samples (**Figure 4.2A**). Albumin secretion in rLSECs-PEM-Hepatocyte samples increased over the culture time whereas HM and rLSECs-Hepatocyte cultures decreased (**Figure 4.2B**). However, the values were lower than that in rLSECs-5L-Hep and rLSEC-15L-Hep cultures at initial concentrations of 25K or 50K LSECs (to be reported in Chapter 4.4.5).

(A)

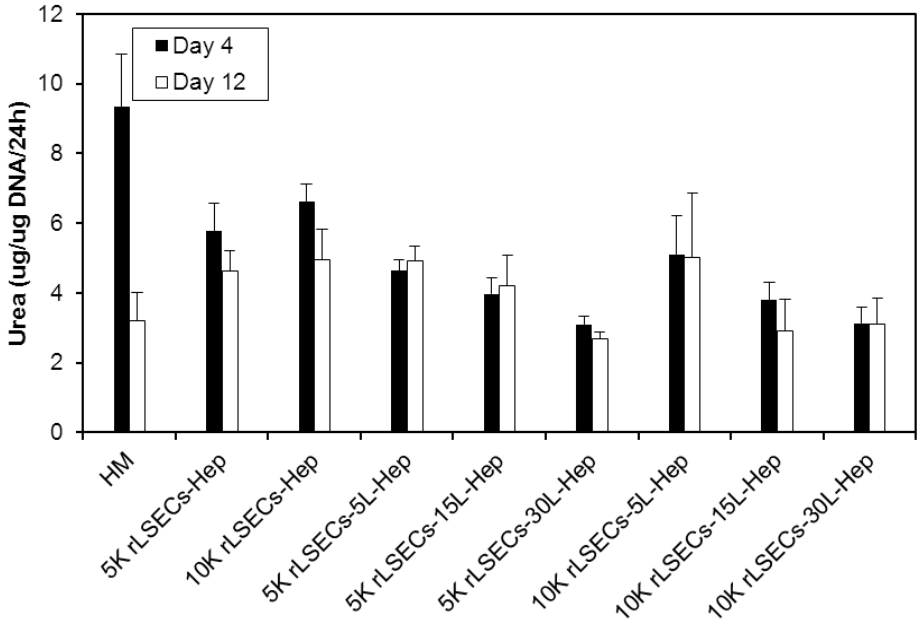

(B)

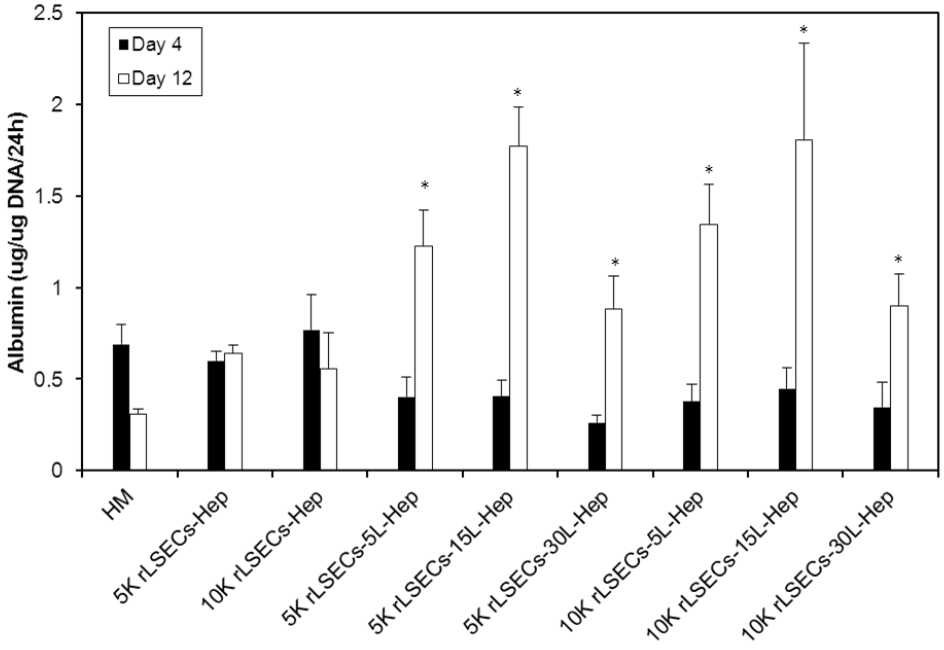

Figure 4.1 Urea production (A) and albumin secretion (B) in HM, rLSECs-Hep, rLSECs-5L-Hep, rLSECs-15L-Hep, and rLSECs-30L-Hep at initial concentrations of either 5K or 10K LSECs over a 12 day culture period. An asterisk (*) indicates a statistically significant increase (*$p < 0.05$) on day 12 in comparison to HMs. Hep = hepatocytes.

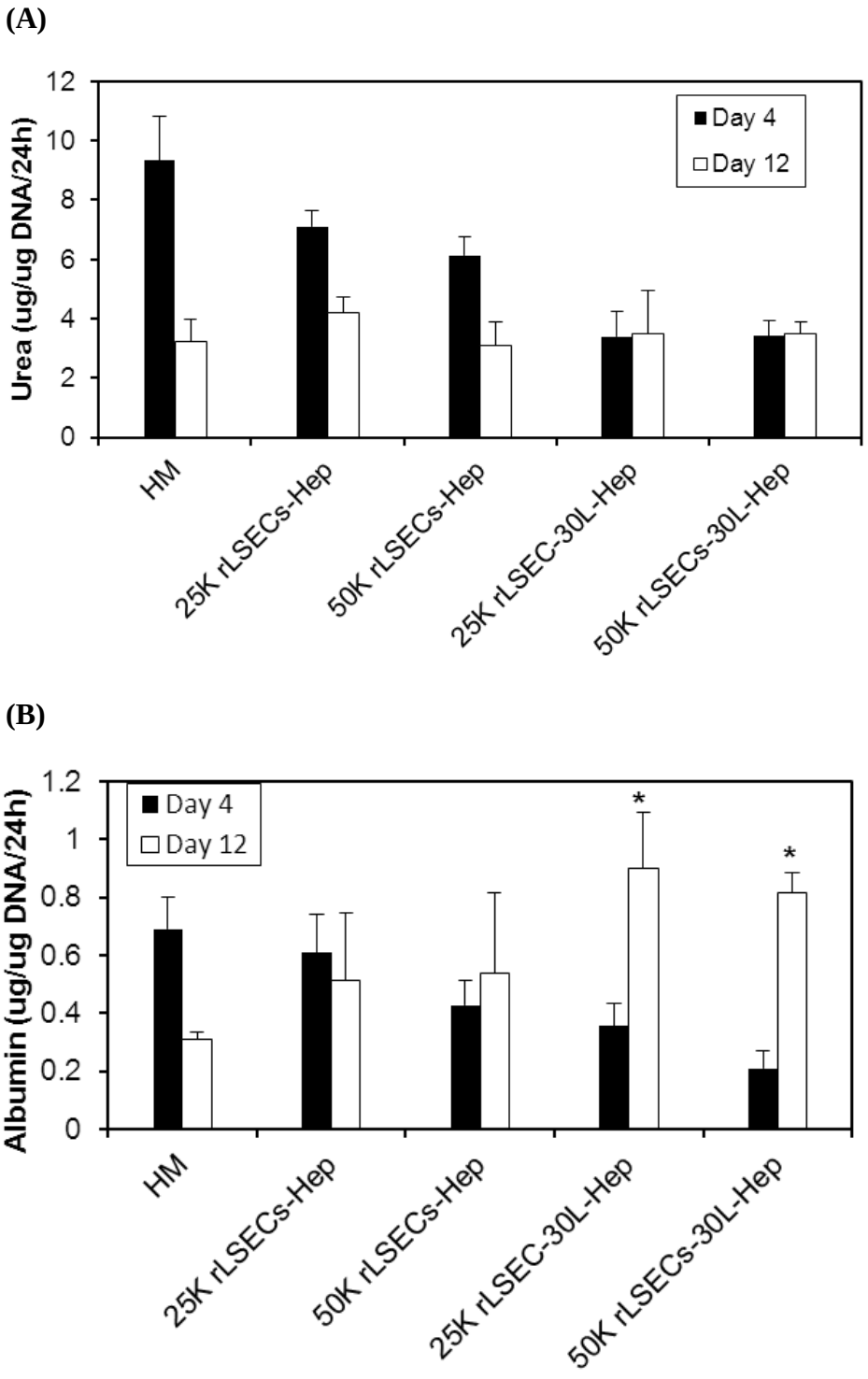

Figure 4.2 Urea production (A) and albumin secretion (B) in 25K rLSECs-30L-Hep and 50K rLSECs-30L-Hep in comparison to 25K rLSECs-Hep and 50K rLSECs as well as HM over a 12 day culture period. An asterisk (*) indicates a statistically significant increase (*$p < 0.05$) on day 12 in comparison to HMs. Hep = hepatocytes.

4.4.2 Cellular Structure of rLSECs-PEM-Hepatocyte Constructs

We focused our attention on 25K or 50K rLSECs and PEMs comprised of either 5 or 15 layers. In order to determine whether rLSECs would adhere to the underlying PEM, they were incubated with a red-fluorescent non-toxic membrane permeable dye prior to seeding. Images taken over a period of twelve days demonstrated that rLSECs where only adherent when a chitosan-HA PEM was present (**Figure 4.3**). In the absence of the PEM (denoted as rLSEC-Hepatocyte), rLSECs were not observed 24h post-seeding. Over the culture period, rLSECS proliferated only above the PEM-coated hepatocytes (denoted as rLSEC-PEM-Hepatocyte), indicated by an increase in the area occupied by these cells. These trends prevailed when the PEM was comprised of either 5 or 15 PE layers and at an initial LSEC seeding density of either 25K or 50K (denoted as 25K rLSEC-5L-Hepatocytes, 25K rLSEC-15L-Hepatocytes, 50K rLSEC-5L-Hepatocytes, and 50K rLSEC-15L-Hepatocytes).

4.4.3 Expression of SE-1 by rLSECs

In LSECs, a cell-surface marker, recently identified as Cd32b, binds to the SE-1 antibody providing a convenient method to validate their phenotype (30, 166, 170). Immunostaining for the SE-1 antibody was conducted on days 3 and 12 for LSECs cultured as a monolayer, with hepatocytes (rLSEC-Hepatocyte) and with PEM-coated hepatocytes (rLSEC-PEM-Hepatocyte). Three days after the isolation of rLSECs from the liver, rLSEC monolayers only exhibited weak fluorescence (**Figure 4.4A**) and rLSECs cultured with hepatocytes in the absence of a PEM appeared to have dedifferentiated (**Figure 4.4B**). However, 50K LSEC-5L-Hepatocyte and 50K LSEC-15L-Hepatocyte cultures maintained their phenotype, as indicated by green fluorescence (**Figures 4.4C and 4.4D**). By day 12, rLSEC monolayers did not exhibit any fluorescence. In contrast, rLSEC-PEM-Hepatocyte cultures exhibited bright green fluorescence (**Figure 4.5**). These results indicated that rLSECs maintained their phenotype in the 3D hepatic models.

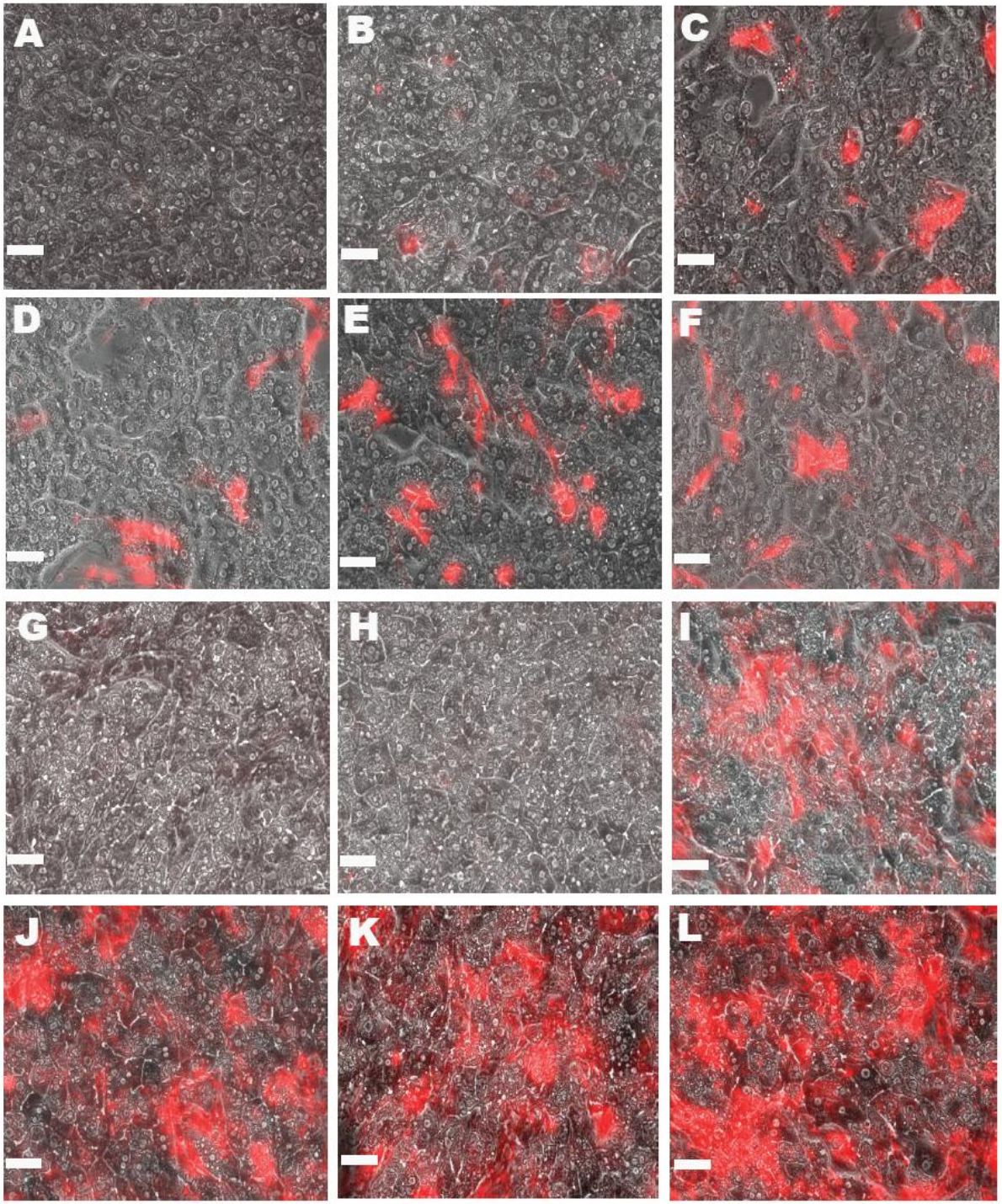

Figure 4.3 Merged phase-contrast (hepatocytes) and fluorescent images of red-fluorescent rLSECs obtained one day (**A-F**) and eight days (**G-L**) after seeding rLSECs. **A.** 25K rLSEC-Hepatocyte, **B.** 50K rLSEC-Hepatocyte, **C.** 25K rLSEC-5L-Hepatocyte, **D.** 50K rLSEC-5L-Hepatocyte, **E.** 25K rLSEC-15L-Hepatocyte, **F.** 50K rLSEC-15L-Hepatocyte. Figures G-L represents the same conditions as in A-F. Scale bar = 50 microns.

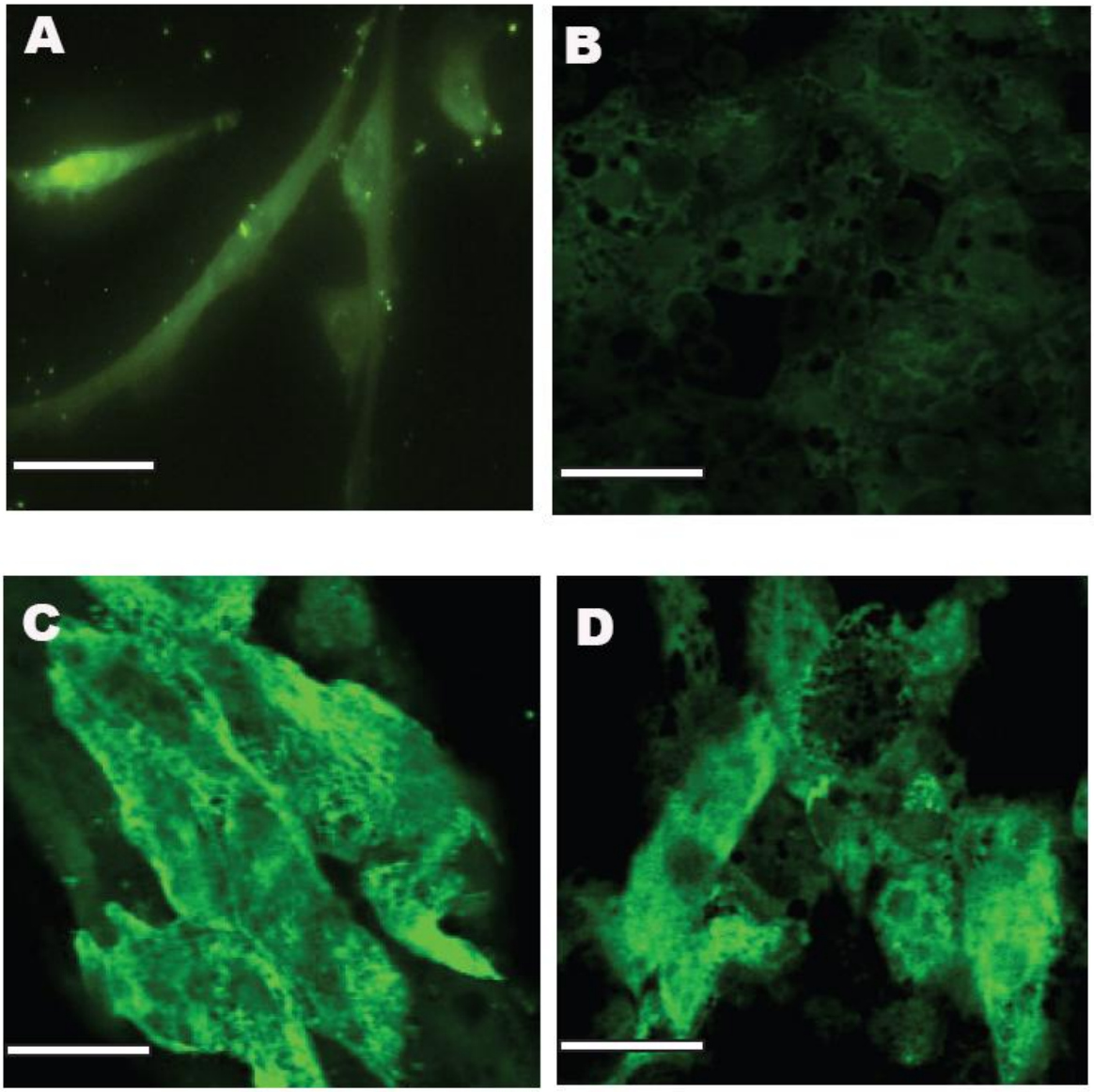

Figure 4.4 SE-1 immunostaining to monitor rLSEC phenotype, images taken on day 3 in culture. **A.** rLSEC monolayer, **B.** 50K rLSEC-Hepatocyte, **C.** 50K rLSEC-5L-Hepatocyte, and **D.** 50K rLSEC-15L- Hepatocyte. Scale bar = 50 microns.

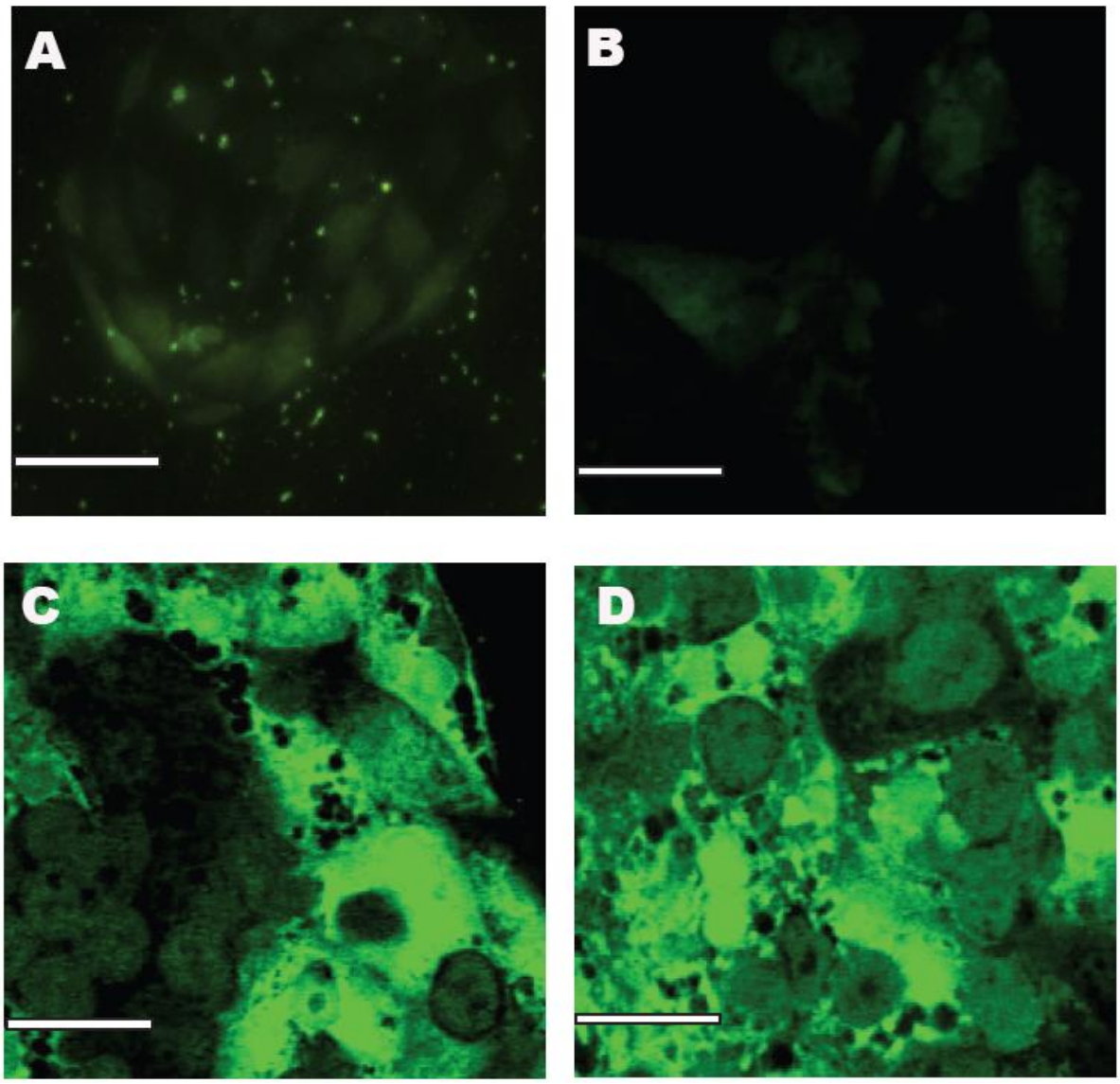

Figure 4.5 SE-1 immunostaining to monitor rLSEC phenotype, images taken on day 12 in culture. **A.** rLSEC monolayer, **B.** 50K rLSEC-Hepatocyte, **C.** 50K rLSEC-5L-Hepatocyte, and **D.** 50K rLSEC-15L- Hepatocyte. Scale bar = 50 microns.

4.4.4 Separation of rLSECs and Hepatocytes Using SE-1 Antibody-Tagged Dyanbeads®

The ability to separate and obtain single cell samples of high purity is a critical step in obtaining information on hepatocyte performance. This enables the normalization of hepatocyte function to the actual number of hepatocytes present in each sample. Since the SE-1 antigen is considered to be one the most reliable makers for rLSECs, the antibody to this antigen was conjugated to Dynabeads®. 50K rLSECs-5L-Hepatocytes and 100K rLSECs-5L-Hepatocytes were used to evaluate the separation efficiency.

In the hepatocyte fraction, the mean values for cell purity were 95.13 ± 1.65 (%) and 93.84 ± 1.02 (%) for 50K r LSECs-5 PE layers-Hepatocytes and 100K rLSECs-5 PE layers-Hepatocytes, respectively (**Table 4.1**). The purity of LSEC fractions was > 99%. **Figure 4.6** showed that the cell morphology of each fraction was distinctive and each fraction contained very little contamination of the other cell type. These results indicate that the SE-1 antibody-tagged Dynabeads® is a suitable method to efficiently separate rLSECs and hepatocytes in the 3D constructs. The purified cell fractions can be used for further analyses such as measurement of DNA content or gene expression profiles in 3D hepatic models.

Table 4.1 Separation efficiency using SE-1 antibody-conjugated Dynabeads® in 3D liver mimetic constructs

Samples	50K rLSECs-5 PE layers-Hepatocytes		100K rLSECs-5 PE layers-Hepatocytes	
Fraction after separation	Hepatocyte Fraction (n=50)	rLSEC Fraction (n=50)	Hepatocyte Fraction (n=50)	rLSEC Fraction (n=50)
Purity (%)	95.13 ± 1.65	99.78 ± 0.08	93.84 ± 1.02	99.74 ± 0.10
Recovery (%)	89.2 ± 1.2	98.2 ± 0.1	91.6 ± 2.1	97.6 ± 1.3

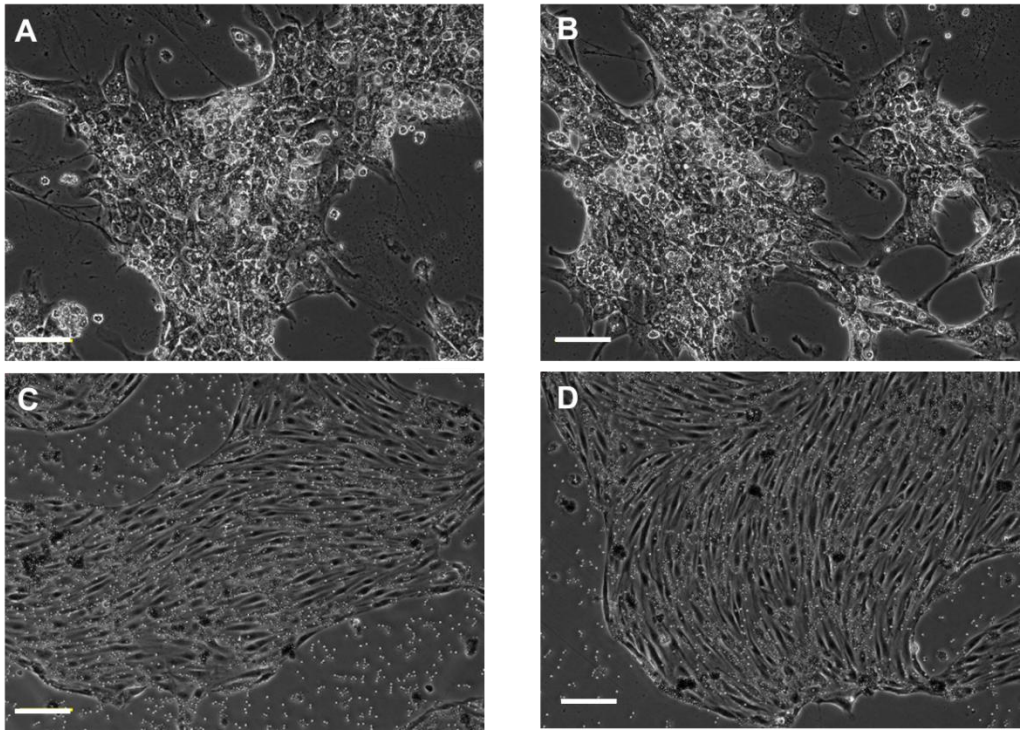

Figure 4.6 Representative images of hepatocyte (A and B) and rLSEC (C and D) fractions after separation using SE-1 antibody-tagged Dynabeads®. Images were taken after separation in 50K rLSECs-5L-Hepatocytes (A and C) and 100K rLSECs-5L-Hepatocytes (B and D) cultured for 7 days. Scale bar = 100 microns.

4.4.5 Maintenance of Hepatocyte Phenotypic Functions

Urea and albumin production were monitored to determine whether the presence of rLSECs would stabilize or enhance hepatocyte function. These are two reliable markers of hepatocellular performance (17, 41). Urea production monitored over a 12 day period indicated a decrease of 60%, 48% and 50% in HMs, 25K rLSEC-Hepatocyte and 50K rLSEC-Hepatocyte cultures respectively between day 4 and day 12 (**Figure 4.7A**) . In contrast, urea production either remained stable or increased in the rLSEC-PEM-Hepatocyte samples. For example, urea production increased approximately 18%, 10% and 20% in the 25K rLSEC-5L-Hepatocytes, 50K rLSEC-5L-Hepatocytes, and 50K rLSEC-15L-Hepatocytes, respectively.

HMs exhibited a decrease in albumin production by approximately 65% over the 12 day observation period (**Figure 4.7B**). 25K rLSEC-Hepatocyte samples exhibited a decrease of approximately 16% and 50K rLSEC-Hepatocyte cultured exhibited an increase of 28%. In contrast, all the 3D hepatic cultures exhibited a significant 3~6 fold elevation in albumin

production. Specifically, the fold increases were 3.4, 5.7, 3.3, and 4.5 for 25K rLSEC-5L-Hepatocytes, 25K rLSEC-15L-Hepatocytes, 50K rLSEC-5L-Hepatocytes and 50K rLSEC-15L-Hepatocytes samples respectively. The increase in albumin secretion was statistically significant in each rLSEC-PEM-Hepatocyte cultures in comparison to HMs with *p*-values lower than 0.05.

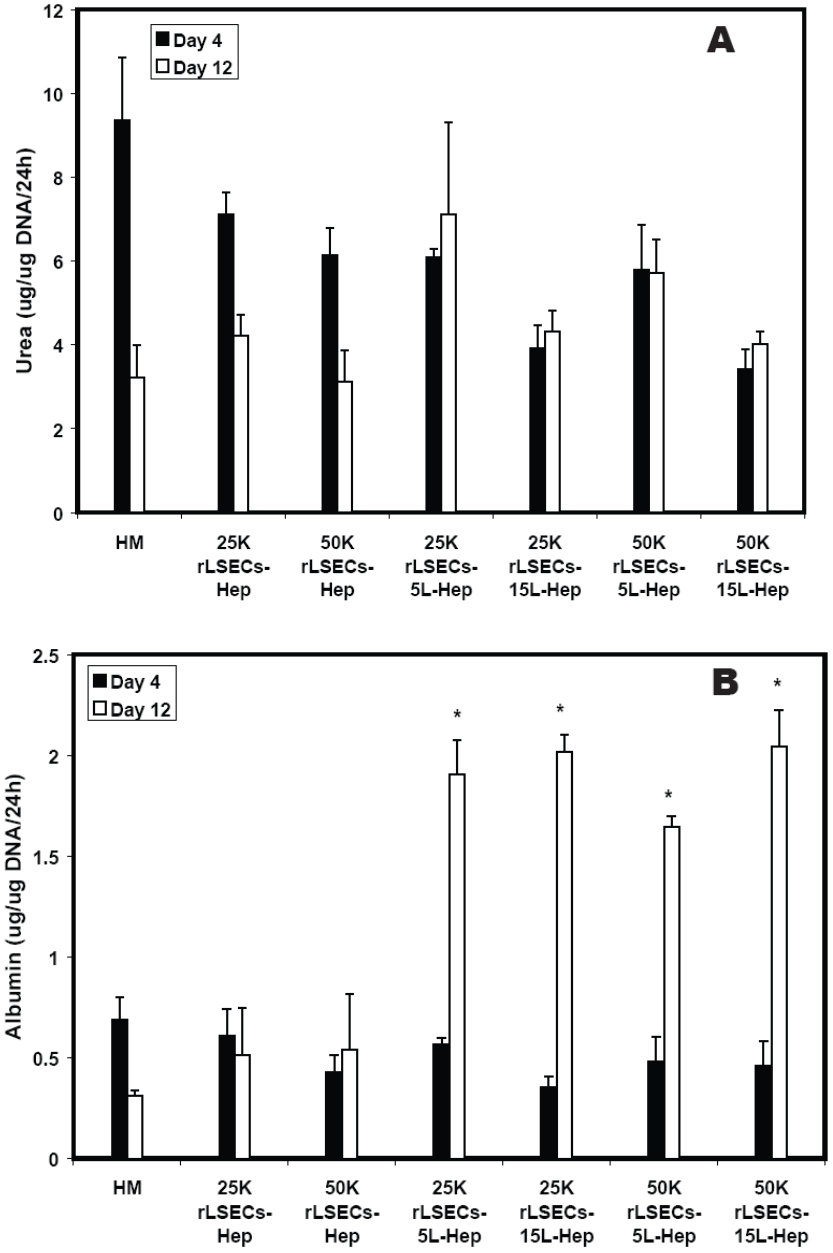

Figure 4.7 (A) Urea production monitored over a 12 day culture period. **Figure 4.10 (B)** Albumin secretion monitored over a 12 day culture period. An asterisk (*) indicates a statistically significant increase (*p< 0.05) on day 12 in comparison to HMs. Hep = hepatocytes.

Urea and albumin production were monitored over 24-day culture time in 50K rLSECs-5L-Hepatocyte and 50K rLSECs-15L-Hepatocyte cultures (**Figure 4.8**). Urea production decreased by 86%, 59%, 46%, and 45% for HM, 50K rLSECs-5L-rHep, 50K rLSECs-15L-rHep, and CS over 24-day culture period. The extent of decrease in 3D liver mimics was similar to that in CS. Albumin production in 50K rLSECs-5L-rHep and 50K rLSECs-15L-rHep exhibited 6-fold increase over culture period as compared to 4-fold increase in CS culture. Likewise, the hepatocyte phenotypes were maintained in 3D liver mimics over 24-day culture period.

(A)

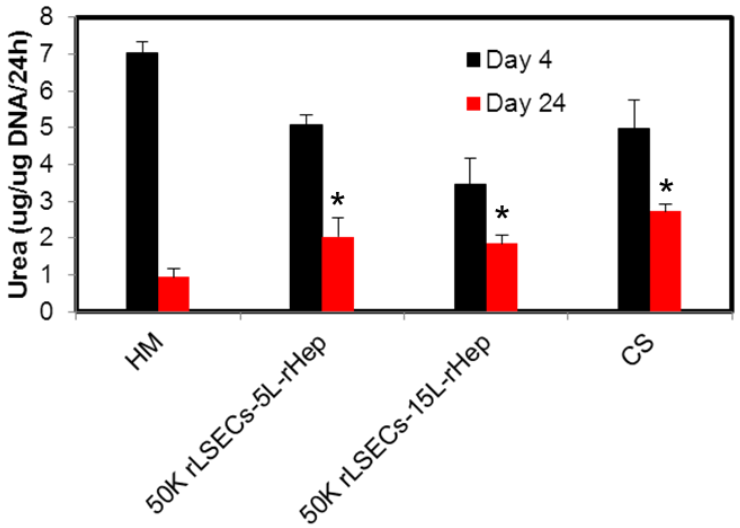

(B)

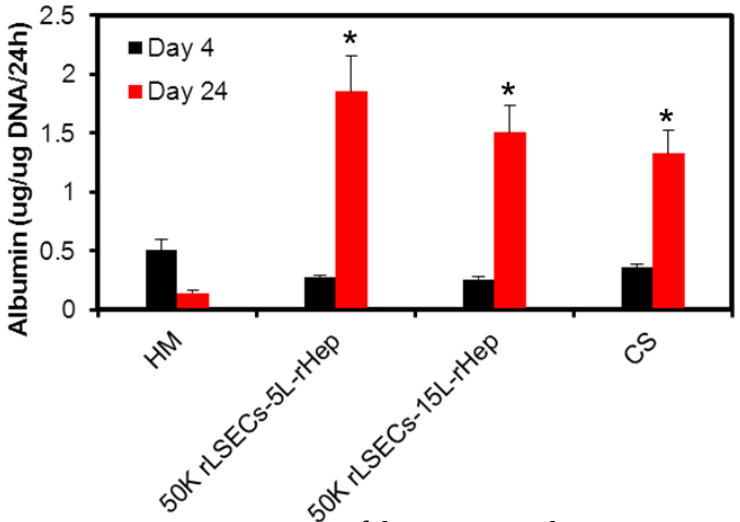

Figure 4.8 Long-term maintenance of hepatocyte phenotypes in rLSECs-PEM-Hepatocyte as compared to that in HM and CS. An asterisk (*) indicates a statistically significant increase (*$p < 0.05$) on day 12 in comparison to HMs. Hep = hepatocytes.

4.4.6 CYP1A1/2 and CYP3A Enzyme Activity

Cytochrome P450 enzymatic activity is another critical function of hepatocytes. This class of enzymes mediates the metabolism of multiple toxins, xenobiotics and pharmaceuticals (85, 96, 97, 171). Cytochrome P4501A1/2 (CYP1A1/2) and CYP3A activities were monitored in all cultures on days 4 and 12. Our goal was to determine if the enzymatic kinetics increased or decreased over the observation period, since decreasing enzymatic activity is usually exhibited due to deteriorating phenotype. Thus, we report the difference in CYP enzyme activity as a fold change between day 4 and day 12. CYP1A1/2 activity was decreased by approximately 44% in HMs and up to 67% in rLSEC-Hepatocyte cultures (**Figure 4.9**). All rLSEC-PEM-Hepatocyte samples exhibited an increased CYP1A1/2 activity, with the fold increase ranging from 2.6 to 4.6. The greatest increase was observed in 50K rLSEC-15L-Hepatocyte samples. The increase in enzymatic activity in each rLSEC-PEM-Hepatocyte cultures was found to be statistically higher (p-value <0.05) in comparison to HMs. A similar trend was observed for CYP3A enzymatic activity (**Figure 4.10**). CYP3A enzymatic activity decreased by approximately 27%, 87%, and 87% in HMs, 25K rLSEC-Hepatocyte and 50K rLSEC-Hepatocyte cultures, respectively. In contrast, CYP3A enzymatic activity increased in all rLSEC-PEM-Hepatocyte samples. The increase was 3-6 fold and was statistically significant in comparison to HMs (p-value <0.05). Once again, the greatest increase was observed in 50K rLSEC-15L-Hepatocyte samples.

CYP1A1/2 and CYP3A enzymatic activity in 5K rLSECs-PEM-Hepatocyte and 10K rLSECs-PEM-Hepatocyte cultures was monitored over the 12 day culture period (**Figures 4.11 and 4.12**). When 5K and 10K LSECs were seeded on PEM-coated hepatocytes, the enzyme activity in the 3D hepatic cultures was similar or inferior to that in HMs.

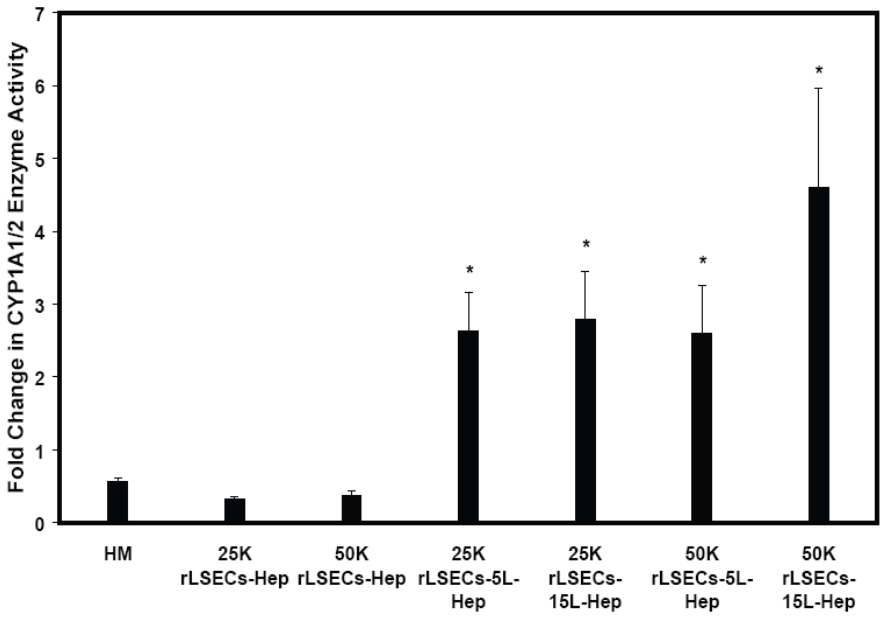

Figure 4.9 Fold change in CYP1A1/2 activity to monitor changes in enzymatic kinetics over a 12 day period. An asterisk (*) indicates a statistically significant increase on day 12 in comparison to HMs. Hep = hepatocytes.

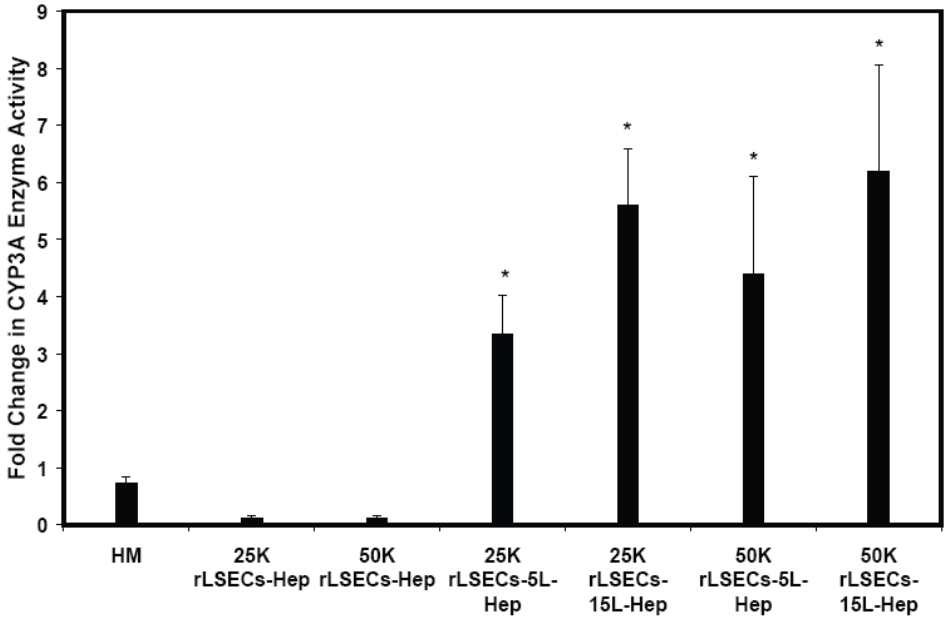

Figure 4.10 Fold change in CYP3A activity to monitor changes in enzymatic kinetics over a 12 day period. An asterisk (*) indicates a statistically significant increase on day 12 in comparison to HMs. Hep = hepatocytes.

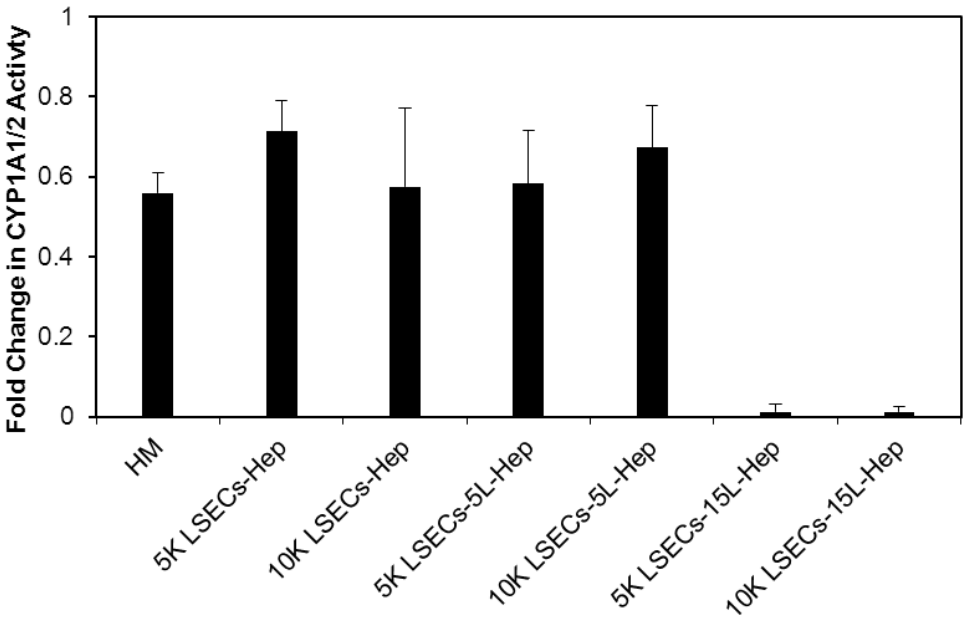

Figure 4.11 Fold change in CYP1A1/2 enzymatic activity over a 12 day period in HM as well as rLSECs-Hep, rLSECs-5L-Hep, and rLSECs-15L-Hep at initial concentration of 5K and 10K LSECs.

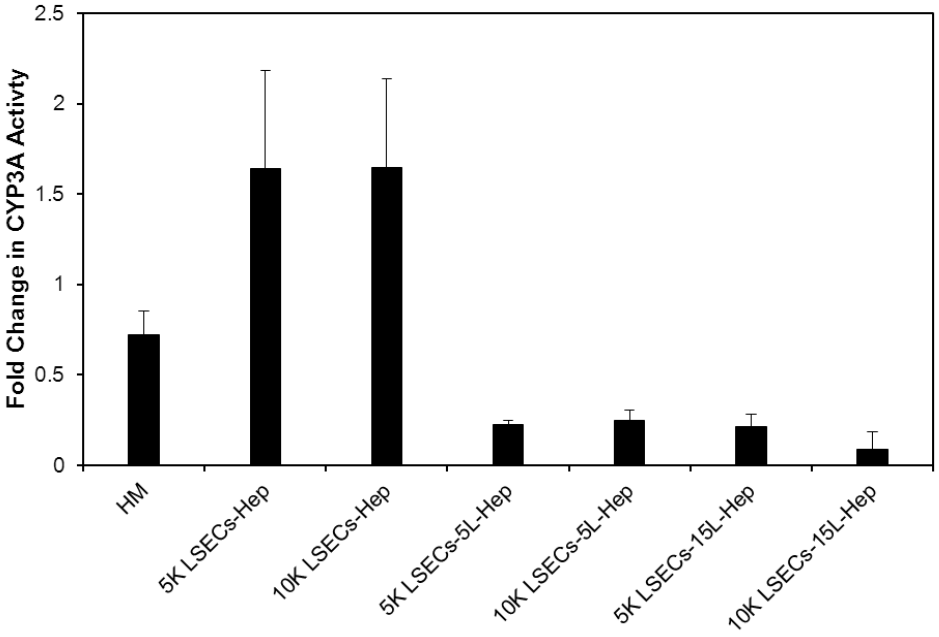

Figure 4.12 Fold change in CYP3A enzymatic activity over a 12 day period in HM as well as rLSECs-Hep, rLSECs-5L-Hep, and rLSECs-15L-Hep at initial concentration of 5K and 10K LSECs.

4.4.7 Bile Canaliculi in the 3D Hepatic Constructs

Immunostaining was conducted to determine the presence of bile canaliculi in the 3D hepatic constructs. These are intercellular minute channels through which bile acids are shuttled between the liver and intestines. Their presence indicates the polarization of hepatocytes which plays a key role in maintenance of hepatic phenotypes such as lipid metabolism and biotransformation of xenobiotics and drugs (172, 173). HMs and rLSEC-Hepatocyte cultures did not exhibit these channels (**Figure 4.13**). In contrast, all four rLSEC-PEM-Hepatocyte samples exhibited well-defined bile canaliculi. These structures prevailed only in rLSEC-PEM-Hepatocytes cultures over the 12-day culture period (**Figure 4.14**). These results indicate that cellular polarity can be maintained in the 3D hepatic constructs.

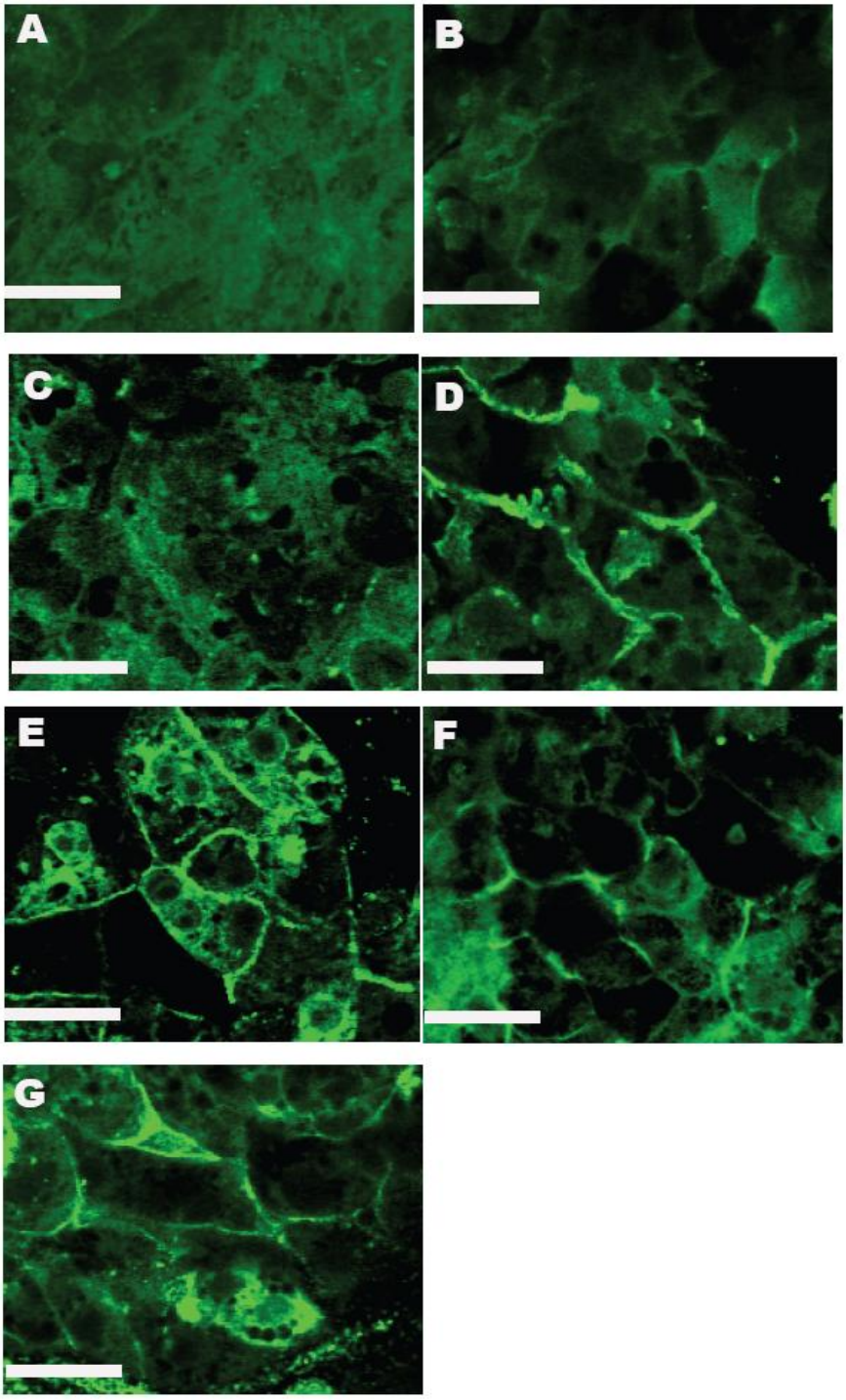

Figure 4.13 Dipeptidyl peptidase IV (DPP IV) immunostaining for bile canaliculi obtained on day 6 in culture. **A.** HM, **B.** 25K rLSECs-Hepatocyte, **C.** 50K rLSECs-Hepatocyte, **D.** 25K rLSECs-5L-Hepatocyte, **E.** 25K rLSECs-15L-Hepatocyte, **F.** 50K rLSECs-5L-Hepatocyte, **G.** 50K rLSECs-15L-Hepatocyte. Scale bar = 50 microns.

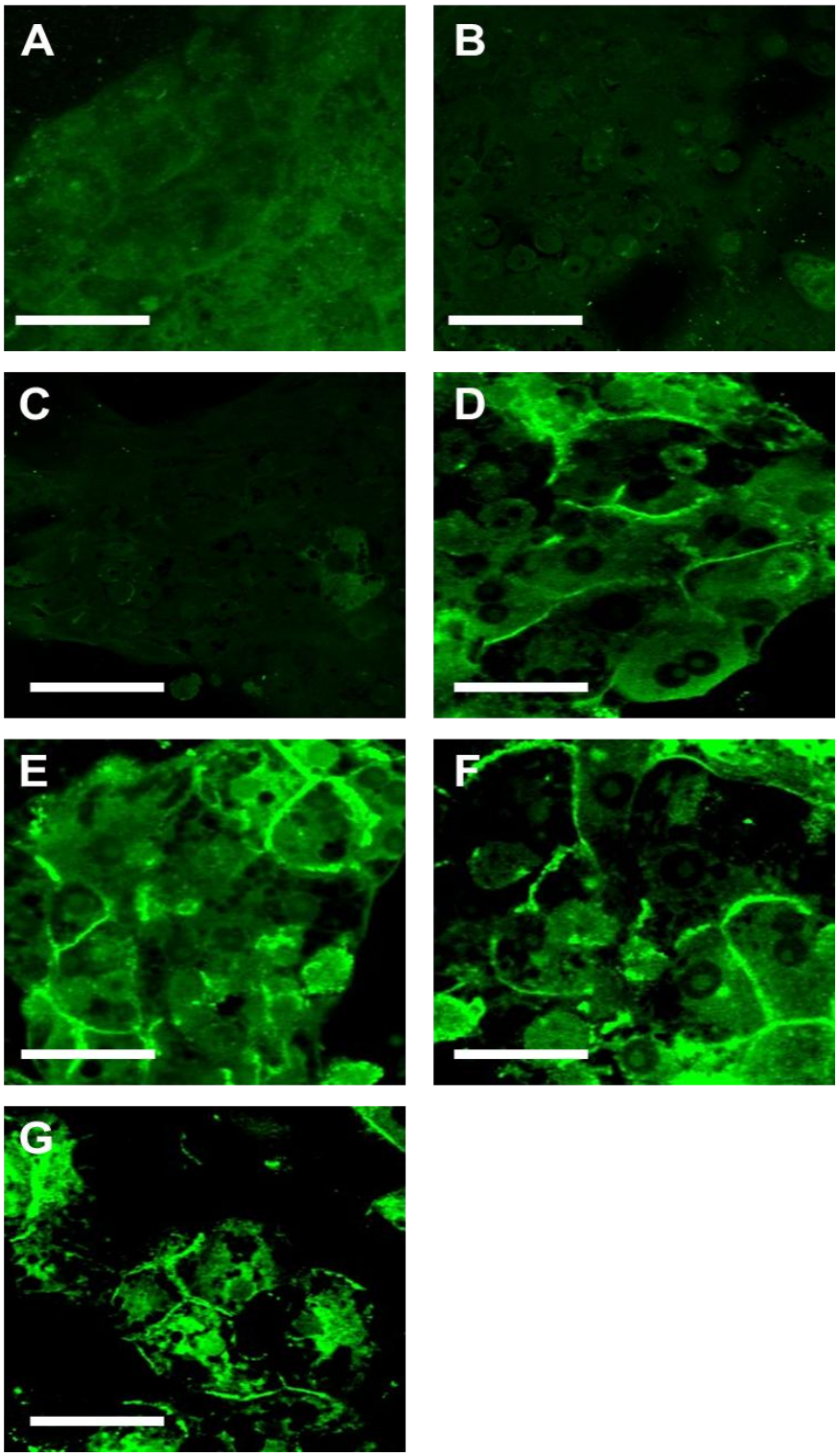

Figure 4.14 Dipeptidyl peptidase IV (DPP IV) immunostaining for bile canaliculi obtained on day 12 in culture. **A.** HM, **B.** 25K rLSECs-Hepatocyte, **C.** 50K rLSECs-Hepatocyte, **D.** 25K rLSECs-5L-Hepatocyte, **E.** 25K rLSECs-15L-Hepatocyte, **F.** 50K rLSECs-5L-Hepatocyte, **G.** 50K rLSECs-15L-Hepatocyte. Scale bar = 50 microns.

4.5 Discussion

The liver is one of the largest organs in our bodies. It performs a multitude of functions such as metabolism, detoxification, and mediation of the body's complex defense mechanisms. Due to the rapid dedifferentiation of hepatic parenchymal and non-parenchymal cells after they are isolated from the liver, the development of *in vitro* liver-like tissues has been non trivial. A liver model that recapitulates key features of hepatic sinusoids is a potentially powerful medium for obtaining comprehensive knowledge on metabolism, detoxification and signaling pathways. A critical component in the development of such a model is maintaining the phenotype of hepatic cells *in vitro.* As a first step towards establishing such a liver model, we have assembled 3D hepatic architectures comprised of primary hepatocytes, rLSECs and a polyelectrolyte-derived interface that acts as the Space of Disse. This model mimics the stratified structure of the liver *in vivo* and incorporates the two major cell types found in this organ.

Recent reports have emphasized the difficulty in maintaining LSEC phenotype beyond a few days in monolayer or co-cultures (87, 165, 166). In the hepatic model reported herein, only rLSECs cultured in an rLSEC-PEM-Hepatocyte construct exhibited binding to the SE-1 antibody twelve days after isolation from the liver. Both monolayers of LSECs and hepatocyte cultures that did not contain a PEM exhibited a loss in phenotype after three days, a result that is in agreement with other studies (165, 166). The physical properties of the PEM, specifically the modulus that closely mirrors bulk liver modulus, may have played a critical role in rLSEC adhesion. In addition, the high degree of hydration of the PEM may have potentially modulated inter-cellular signaling (168). We hypothesize that cultures with lower concentrations of rLSECs (5,000 or 10,000) did not maintain hepatocellular functions due to lower heterotypic cell-cell interactions. PEMs with greater than 15 layers also did not exhibit optimal function. One potential reason could be that the longer deposition process as well as the higher concentration of the polyelectrolytes could have resulted in imparting stress to hepatocytes.

A significant finding of our study was the three- to six-fold increase in albumin production in rLSEC-PEM-Hepatocyte cultures. These trends clearly indicate that hepatocellular functions are maintained as well, since albumin is one of the key markers of hepatic function. In contrast, previous reports on 2D co-cultures of rLSECs and hepatocytes, show that albumin

secretion decreased as a function of time (166). We hypothesize that that higher albumin secretion in our 3D models is due to significantly higher hepatocyte-rLSEC heterotypic interaction in comparison to conventional 2D co-cultures. These data further underscore the need for tissue engineered liver models that recapitulate the layered hepatic architecture found *in vivo*.

Optimal CYP enzymatic activity in hepatocytes is critical for the liver to conduct detoxification of a wide range of toxins, drugs and xenobiotics. Since LSECs are often the first cell type that comes in contact with a drug or toxin, models that do not include these cells will not provide relevant information required for therapeutic strategies of the future. A recent study showed that when a combination of alcohol and acetoaminophen was administered to the liver, significant rLSEC death and loss of actin cytoskeletal organization occurred (158). A more significant outcome of this report was that LSECs were affected a few hours prior to any effect on hepatocytes. Thus, *in vitro* cultures that do not include LSECs cannot capture the unique inter-cellular mechanisms that govern detoxification and the subsequent effect on other liver metabolites.

We focused our attention on two major classes of CYP enzymes, CYP1A1/2 and CYP3A, since these enzymes typically mediate the metabolism of polyaromatic compounds and pharmaceuticals. Once again, the rLSEC-PEM-Hepatocyte cultures exhibited increasing enzymatic activity over the twelve day observation period. These trends were mirrored in the immunostaining experiments for bile canaliculi. Multiple cytochrome P450 enzymes are often involved in the biotransformation of bile acids (174, 175). Furthermore, bile canaliculi are the channels through which metabolites of the detoxification processes are transported away from the liver. Therefore, together these data suggest that rLSEC-PEM-Hepatocyte cultures are highly suitable models to monitor the effects of drugs and toxins on the liver.

Complications arising from drug-drug and drug-toxin interactions are becoming an increasing concern for human health. There is a need to develop liver-like tissue models that can serve as accurate models for drug and toxicity testing. Such models cannot rely on the use of a single hepatic cell type. Instead, the inclusion of multiple cell types found in the liver is a pre-requisite to obtaining a comprehensive overview on all perturbed liver functions. In the current

study, the inclusion of hepatocytes and rLSECs in a layered 3D model resulted not only in the simultaneous maintenance of their individual phenotype but also in increased hepatocellular functions. The intricate inter-cellular signaling pathways through which these cells communicate within the 3D liver model will be the focus of future studies.

Chapter 5. Conclusions and Future Work

5.1 Conclusions

The primary focus of this research project was to assemble *in vitro* three-dimensional (3D) liver-mimetic models comprised of primary rat hepatocytes, liver sinusoidal endothelial cells (LSECs), and a nano-scale polyelectrolyte multilayer (PEM) as an interface between these two cell types. Upon assembling the tissue-engineered hepatic models, detailed studies were conducted to monitor the phenotypic properties and functions. Towards these goals, three complimentary tasks were performed: (1) the design and assembly of 3D liver mimics comprised of primary rat hepatocytes, a PEM, and human LSECs, (2) genome-wide transcriptional profiles of primary hepatocytes cultured in a collagen sandwich configuration (CS) and hepatocyte monolayers (HM), and (3) the construction of *in vitro* 3D liver-mimetic models comprised of primary hepatocytes, a chitosan-hyaluronic acid PEM, and primary rat LSECs.

In Chapter 2, we reported the assembly of 3D liver mimics comprised of primary rat hepatocytes, a nano-scale chitosan-hyaluronic acid PEM, and hLSECs. Prior to assembling the 3D liver mimics, four different numbers of PE layers (5, 15, 30, and 45) were deposited to determine the number of PEs that would result in optimal hepatic function. Hepatocytes coated with either 5 or 15 PE layers exhibited stable urea production and albumin production over a 7 day culture period. The physical properties of PEM were measured using a quartz crystal microbalance with dissipation (QCM-D). The height of the PEMs ranged from 30-55nm and exhibited a shear modulus of ~ 100kPa. The PEMs were found to be highly hydrated suggesting that the PEM can promote the diffusion of signaling molecules. Hepatocyte-PEM-hLSEC constructs exhibited liver-specific functions that were comparable or superior to HM, hepatocyte-hLSEC, and CS cultures. The 3D liver mimics exhibited stable albumin and urea production and maintenance of LSEC phenotype over the 8-day culture period. A four- to sixteen-fold increase in CYP1A1/2 enzyme activity was observed in hepatocyte-PEM-hLSEC samples. These results demonstrate that the 3D hepatic constructs described herein can function as relevant models of the liver.

In Chapter 3, we investigated genome-wide transcriptional profiles of primary rat hepatocytes cultured in two widely used systems, collagen sandwich (CS) and hepatocyte monolayer (HM). Although the morphological and physiological characteristics of hepatocytes in these cultures have been studied extensively, a comprehensive evaluation of temporal genome-wide gene expression had not been reported. Hepatocytes cultured in CS and HM cultures were maintained for an 8-day culture period and total RNA extracted from the cells was used to conduct DNA microarray analyses. Through gene set enrichment analysis (GSEA), the gene expression profiles were summarized at the level of gene sets. Over the 8-day culture period, the transcriptional program in CS samples monotonically diverged from HMs. The gene sets that were up-regulated in the CS cultures included those related to liver-specific functions such as cholesterol, fatty-acid, alcohol, and carbohydrate metabolism. The gene sets linked to those hepatic functions were shown to be steadily up-regulated starting on day 1 or 2 in CS cultures. For example the gene sets related urea production in CS cultures was gradually up-regulated as a function of time. These results suggest that the enhanced hepatic phenotypes in the CS cultures primarily rely on the fluctuation in transcriptional changes between hepatocytes in CS and HMs. Also, the gene sets analyzed were in accord with the metabolic pathways that have been previously identified. Gene sets related to xenobiotic metabolism were not statistically significant on days 1 and 2 but were differentially expressed starting on day 3 in CS cultures. The gene sets related to biotransformation of xenobiotics included several cytochrome P450s enzymes. The gene sets linked to cell cycle were down-regulated in CS cultures. Such temporal and comprehensive information can provide a baseline for further investigation into genome-wide transcriptional profiles of engineered liver models.

In Chapter 4, 3D hepatic models comprised of primary rat hepatocytes and rLSECs, and a chitosan-hyaluronic acid PEM were assembled to examine the preservation and enhancement of hepatocyte and LSEC phenotypes. Primary rat hepatocytes and rLSECs were cultured in the layered 3D configuration. Hepatocytes and rLSECs exhibited key liver-specific phenotypes in the stratified hepatocellular constructs over a twelve day culture period. Immuno-staining for the sinusoidal endothelial 1 (SE-1) marker revealed that rLSEC phenotype could be maintained only in the 3D hepatic cultures over a 12 day culture period while rLSEC-hepatocyte cultures did not maintain their phenotype. rLSECs cultured in monolayers lost their phenotype within three days.

In order to precisely quantify hepatocyte-specific functions, the separation of rLSECs and hepatocytes was conducted. The use of the SE-1 antibody-conjugated Dynabeads® enabled the efficient separation of rLSECs from the hepatic cultures. The purity of each fraction after separation was higher than 95%. Only rLSEC-PEM-Hepatocyte cultures exhibited a four-fold increase in albumin secretion and three to six-fold increase in CYP1A1/2 and CYP3A enzymatic activities. Bile canaliculi were well defined in the 3D hepatic cultures, indicating that the cellular polarity was maintained in rLSEC-PEM-Hepatocyte samples in comparison to rLSEC-Hepatocytes. Taken together, these results demonstrated that the rLSEC-PEM-Hepatocytes cultured in the stratified configuration can serve as hepatic models for future studies.

5.2 Significance

5.2.1 The Design of 3D Liver Mimics

This research project has the potential to have an impact on hepatic tissue engineering by assembling 3D liver mimics that recapitulate key geometric, spatial and physiological features of liver found *in vivo*. To the best of our knowledge, this is the first assembly of 3D liver mimics comprised of hepatocytes and liver sinusoidal endothelial cells. The detailed phenotypic measurements clearly demonstrate the importance of developing such liver mimetic tissues. As demonstrated in Chapters 2 and 4, the results suggested that the 3D liver mimetic cellular architecture can serve as a powerful medium for obtaining comprehensive knowledge on liver physiology.

Unlike other hepatic models such as the collagen sandwich (17, 41, 103), hepatocyte monolayers (103), 2D co-cultures of hepatocytes and fibroblast(40, 53, 85), and hepatocyte-HUVEC layered hepatic model(55, 58), the 3D liver mimics are comprised entirely of primary cells obtained from rat livers (73, 168). This is the first tissue engineered liver mimics where rLSEC phenotype (typically lost within 72 hours of removal from the liver) could be maintained up to 12 days in culture. CYP enzymatic activity as well as presence of bile canaliculi in the 3D liver mimics suggested that the 3D liver models exhibit significant potential to serve as relevant models for drug and toxicity testing. Accordingly, the information obtained from the liver models can be used to design artificial livers that can provide support to patients suffering from liver diseases.

In order to better understand the physiology of tissue-engineered livers, future goals are to incorporate rat Kupffer cells or stellate cells into the 3D hepatic models to determine if the 3D liver mimics comprised of all the cell types found in liver *in vivo* would perform more optimally than the hepatic models previously designed. Incorporation of these cells may have a synergistic effect on the enhancement and maintenance of hepatic phenotypes.

.

5.2.2 Comprehensive and Temporal Genome-wide Transcriptional Profiles of Primary Rat Hepatocytes in Collagen Sandwich and Monolayer Cultures

To the best of our knowledge this is first such dataset that reported comprehensive genome-wide gene expression profiles of primary hepatocytes in collagen sandwich (CS) and monolayer cultures (HMs). Previous studies have either reported trends for only a few genes in spheroid cultures or measured data for a three-day period (105, 176). The results and trends obtained from our study provide both a comprehensive and temporal genome-wide analysis of the numerous transcriptional changes that take place in conventional hepatocyte cultures. Therefore, these results will provide the essential information to understand the systems biology of 3D tissue-engineered liver models in the future.

5.3 Future Work

5.3.1 Intercellular Signaling between Hepatocytes and Rat Liver Sinusoidal Endothelial Cells: Genome-wide Transcriptional Profiles using DNA Microarrays

In the liver, hepatocytes and LSECs are layered in a stratified configuration (1-3). Optimal hepatic function is dependent upon inter-cellular communications between the parenchymal (hepatocytes) and nonprenchymal (LSECs, Kupffer, stellate) cells. In previous studies, we reported the assembly of the 3D liver sinusoidal mimics that recapitulate key spatial, geometric, and physiological features of the liver (168). Primary rat hepatocytes and LSECs (rLSECs) were assembled in a stratified configuration through the incorporation of a chitosan-hyaluronic acid polyelectrolyte multilayer (PEM) that mimics the Space of Disse. The 3D liver mimetic cellular architectures exhibited the preservation and enhancement of hepatic function.

We hypothesized that the enhanced *in vivo* liver-like features in the hepatic models were a function of inter-cellular communications resulting in transcriptional changes and phenotypic maintenance. Currently, a thorough and comprehensive understanding of the various inter-cellular signals that maintain and promote hepatic phenotype is not available. To better understand the successful enhancement of liver function in the 3D hepatic models reported by our group, our future plan is to measure inter-cellular signaling to obtain insights into which pathways are perturbed. As demonstrated in Chapter 3, the genome-wide gene expression profiles of primary hepatocytes in CS and HM showed that the fate of cellular behavior in two distinctive culture systems is governed by transcriptional changes within each system (177). Likewise, comprehensive gene expression profiles in tissue-engineered hepatic models can provide information on cell-cell interactions that promote the enhancement of hepatic functions.

In 2D co-culture comprised of 50% hepatocytes and 50% fibroblasts, the gene expression profiles of hepatocytes revealed that genes related neural cadherin (N-cadherin), chondroitin sulfate, decorin and VGEF were mainly associated with heterotypic cellular interactions between hepatocytes and fibroblasts (62). This study reported that N-cadherin as a heterotypic junction protein and decorin as a major liver proteoglycan are key candidates that mediate hepatocytes-fibroblasts interactions. Other studies focused on gene expression information in response to drug, toxins and xenobiotics (85, 178). In a micro patterned co-culture of hepatocytes and fibroblasts, the genes related to several cytochrome P450s and phase II enzymes were analyzed. The results showed that the genes were expressed at statistically significant levels in the co-culture as compared to freshly isolated hepatocytes. In another study, the genes in the xenobiotic response category were investigated to understand biological pathways that promote a phenotype. However, since these studies reported only a few numbers of genes involved in transcriptional changes of xenobiotic and immune response genes, they did not provide a sufficiently comprehensive profile of hepatocytes (85, 178).

Since hepatocytes cultured with LSECs exhibited significantly enhanced phenotypic functions in comparison to hepatocyte monolayers, global genome-wide transcriptional profiles of hepatocytes and LSEC in the 3D hepatic constructs can shed lights on understanding key

signaling pathways and molecules that play pivotal roles in the enhancement of *in vivo* liver-like functions.

5.3.2 Western Blots for CYP1A1/2 and CYP3A Proteins

As described in Chapter 4, the 3D hepatic models exhibited increasing CYP1A1/2 and CYP3A activity in comparison to rLSECs-Hepatocytes and HM cultures. In order to verify the presence of these proteins, Western blot measurements for these CYP proteins will be conducted in the future. These measurements will enable the accurate correlation between the presence of CYP proteins in difference *in vitro* hepatic cultures and their enzymatic activity.

5.3.3 Conclusions

The focus of this research project was to design 3D liver sinusoidal mimics comprised of primary rat hepatocytes and human or rat LSECs (hLSECs or rLSECs), and a PEM that mimics the Space of Disse. Through this project, 3D hepatic models that recapitulate key characteristics of hepatic sinusoids found *in vivo* could be assembled. Also, comparative genome-wide transcriptional profiles of primary hepatocytes in CS and HMs could shed light on further investigation into the systems biology of engineered liver tissues. Important areas of future work include understanding intercellular communications between hepatocytes and rat LSECs using DNA microarrays, incorporating Kupffer cells or stellate cells into the 3D liver models, and Western blots for CYP1A1/2 and CYP3A enzymes. Successful completion of these next steps will enable a better understanding of the transcriptional and molecular signatures that govern liver physiology.

REFERENCES

1. Arias, I. M., Boyer, J. L., Chisari, F. V., Fausto, M., Schachter, D., and Shafritz, D. A. (2001) *The Liver: Biology and Pathology* Lippincott Williams and Wilkins, Philadelphia, PA
2. LeCluyse, E. L., Bullock, P. L., and Parkinson, A. (1996) Strategies for restoration and maintenance of normal hepatic structure and function in long-term cultures of rat heaptocytes. *Advanced Drug Delivery Reviews* **22**, 133-186
3. Junqueira, L. C., and Carneiro, J. (2003) *Basic Histology: Text & Atlas,* McGraw-Hill/Appleton & Lange; 10 edition (November 11, 2002), New York, NY
4. Strain, A. J., and Neuberger, J. M. (2002) A bioartificial liver--state of the art. *Science* **295**, 1005-1009
5. Jungermann, K., and Kietzmann, T. (1996) Zonation of parenchymal and nonparenchymal metabolism in liver. *Annu Rev Nutr* **16**, 179-203
6. Jungermann, K., and Kietzmann, T. (2000) Oxygen: modulator of metabolic zonation and disease of the liver. *Hepatology* **31**, 255-260
7. Katz, N. R. (1992) Metabolic heterogeneity of hepatocytes across the liver acinus. *J Nutr* **122**, 843-849
8. Allen, J. W., and Bhatia, S. N. (2003) Formation of steady-state oxygen gradients in vitro: application to liver zonation. *Biotechnol Bioeng* **82**, 253-262
9. Roberts, R. A., Ganey, P. E., Ju, C., Kamendulis, L. M., Rusyn, I., and Klaunig, J. E. (2007) Role of the Kupffer cell in mediating hepatic toxicity and carcinogenesis. *Toxicol Sci* **96**, 2-15
10. Braet, F., and Wisse, E. (2002) Structural and functional aspects of liver sinusoidal endothelial cell fenestrae: a review. *Comp Hepatol* **1**, 1
11. Racanelli, V., and Rehermann, B. (2006) The liver as an immunological organ. *Hepatology* **43**, S54-62
12. Sato, M., Suzuki, S., and Senoo, H. (2003) Hepatic stellate cells: unique characteristics in cell biology and phenotype. *Cell Struct Funct* **28**, 105-112
13. Blomhoff, R., and Wake, K. (1991) Perisinusoidal stellate cells of the liver: important roles in retinol metabolism and fibrosis. *FASEB J* **5**, 271-277
14. March, S., Graupera, M., Rosa Sarrias, M., Lozano, F., Pizcueta, P., Bosch, J., and Engel, P. (2007) Identification and functional characterization of the hepatic stellate cell CD38 cell surface molecule. *Am J Pathol* **170**, 176-187
15. Alberts, B., Johnson, A., Lewis, J., Raff, M., Roberts, K., and Walter, P. (2002) *Molecular biology of the cell* Garland Science, New York, NY
16. Moghe, P. V., Berthiaume, F., Ezzell, R. M., Toner, M., Tompkins, R. G., and Yarmush, M. L. (1996) Culture matrix configuration and composition in the maintenance of hepatocyte polarity and function. *Biomaterials* **17**, 373-385
17. Dunn, J. C., Yarmush, M. L., Koebe, H. G., and Tompkins, R. G. (1989) Hepatocyte function and extracellular matrix geometry: long-term culture in a sandwich configuration. *FASEB J* **3**, 174-177
18. Guguen-Guillouzo, C., Clement, B., Lescoat, G., Glaise, D., and Guillouzo, A. (1984) Modulation of human fetal hepatocyte survival and differentiation by interactions with a rat liver epithelial cell line. *Dev Biol* **105**, 211-220

19. Gershwin, M. E., Vierling, J. M., and Manns, M. P. (2007) *Liver immunology: principles and practice* Humana Press, Totowa, N.J.
20. Smedsrod, B. (2004) Clearance function of scavenger endothelial cells. *Comp Hepatol* **3 Suppl 1**, S22
21. McCourt, P. A., Smedsrod, B. H., Melkko, J., and Johansson, S. (1999) Characterization of a hyaluronan receptor on rat sinusoidal liver endothelial cells and its functional relationship to scavenger receptors. *Hepatology* **30**, 1276-1286
22. Wisse, E., Braet, F., Luo, D., De Zanger, R., Jans, D., Crabbe, E., and Vermoesen, A. (1996) Structure and function of sinusoidal lining cells in the liver. *Toxicol Pathol* **24**, 100-111
23. Smedsrod, B., De Bleser, P. J., Braet, F., Lovisetti, P., Vanderkerken, K., Wisse, E., and Geerts, A. (1994) Cell biology of liver endothelial and Kupffer cells. *Gut* **35**, 1509-1516
24. Smedsrod, B., Pertoft, H., Gustafson, S., and Laurent, T. C. (1990) Scavenger functions of the liver endothelial cell. *Biochem J* **266**, 313-327
25. Elvevold, K., Smedsrod, B., and Martinez, I. (2008) The liver sinusoidal endothelial cell: a cell type of controversial and confusing identity. *Am J Physiol Gastrointest Liver Physiol* **294**, G391-400
26. Hellevik, T., Bondevik, A., and Smedsrod, B. (1996) Intracellular fate of endocytosed collagen in rat liver endothelial cells. *Exp Cell Res* **223**, 39-49
27. Elvevold, K., Simon-Santamaria, J., Hasvold, H., McCourt, P., Smedsrod, B., and Sorensen, K. K. (2008) Liver sinusoidal endothelial cells depend on mannose receptor-mediated recruitment of lysosomal enzymes for normal degradation capacity. *Hepatology* **48**, 2007-2015
28. Nedredal, G. I., Elvevold, K. H., Ytrebo, L. M., Olsen, R., Revhaug, A., and Smedsrod, B. (2003) Liver sinusoidal endothelial cells represents an important blood clearance system in pigs. *Comp Hepatol* **2**, 1
29. Daneker, G. W., Lund, S. A., Caughman, S. W., Swerlick, R. A., Fischer, A. H., Staley, C. A., and Ades, E. W. (1998) Culture and characterization of sinusoidal endothelial cells isolated from human liver. *In Vitro Cell Dev Biol Anim* **34**, 370-377
30. Tokairin, T., Nishikawa, Y., Doi, Y., Watanabe, H., Yoshioka, T., Su, M., Omori, Y., and Enomoto, K. (2002) A highly specific isolation of rat sinusoidal endothelial cells by the immunomagnetic bead method using SE-1 monoclonal antibody. *J Hepatol* **36**, 725-733
31. Ishibashi, H., Nakamura, M., Komori, A., Migita, K., and Shimoda, S. (2009) Liver architecture, cell function, and disease. *Semin Immunopathol* **31**, 399-409
32. Naito, M., Hasegawa, G., and Takahashi, K. (1997) Development, differentiation, and maturation of Kupffer cells. *Microsc Res Tech* **39**, 350-364
33. Peng, Y., and Murr, M. M. (2007) Establishment of immortalized rat Kupffer cell lines. *Cytokine* **37**, 185-191
34. de Leeuw, A. M., Brouwer, A., Barelds, R. J., and Knook, D. L. (1983) Maintenance cultures of Kupffer cells isolated from rats of various ages: ultrastructure, enzyme cytochemistry, and endocytosis. *Hepatology* **3**, 497-506
35. Bouwens, L. (1988) Proliferation and phenotypic expression of non-parenchymal liver cells. *Scand J Gastroenterol Suppl* **151**, 46-51
36. Smedsrod, B., Pertoft, H., Eggertsen, G., and Sundstrom, C. (1985) Functional and morphological characterization of cultures of Kupffer cells and liver endothelial cells

prepared by means of density separation in Percoll, and selective substrate adherence. *Cell Tissue Res* **241**, 639-649
37. Smedsrod, B., Le Couteur, D., Ikejima, K., Jaeschke, H., Kawada, N., Naito, M., Knolle, P., Nagy, L., Senoo, H., Vidal-Vanaclocha, F., and Yamaguchi, N. (2009) Hepatic sinusoidal cells in health and disease: update from the 14th International Symposium. *Liver Int* **29**, 490-501
38. Friedman, S. L. (2008) Hepatic stellate cells: protean, multifunctional, and enigmatic cells of the liver. *Physiol Rev* **88**, 125-172
39. Blaner, W. S., O'Byrne, S. M., Wongsiriroj, N., Kluwe, J., D'Ambrosio, D. M., Jiang, H., Schwabe, R. F., Hillman, E. M., Piantedosi, R., and Libien, J. (2009) Hepatic stellate cell lipid droplets: a specialized lipid droplet for retinoid storage. *Biochim Biophys Acta* **1791**, 467-473
40. Bhatia, S. N., Balis, U. J., Yarmush, M. L., and Toner, M. (1999) Effect of cell-cell interactions in preservation of cellular phenotype: cocultivation of hepatocytes and nonparenchymal cells. *FASEB J* **13**, 1883-1900
41. Dunn, J. C., Tompkins, R. G., and Yarmush, M. L. (1991) Long-term in vitro function of adult hepatocytes in a collagen sandwich configuration. *Biotechnol Prog* **7**, 237-245
42. Lerche, C., Fautrel, A., Shaw, P. M., Glaise, D., Ballet, F., Guillouzo, A., and Corcos, L. (1997) Regulation of the major detoxication functions by phenobarbital and 3-methylcholanthrene in co-cultures of rat hepatocytes and liver epithelial cells. *Eur J Biochem* **244**, 98-106
43. Mesnil, M., Fraslin, J. M., Piccoli, C., Yamasaki, H., and Guguen-Guillouzo, C. (1987) Cell contact but not junctional communication (dye coupling) with biliary epithelial cells is required for hepatocytes to maintain differentiated functions. *Exp Cell Res* **173**, 524-533
44. Morin, O., and Normand, C. (1986) Long-term maintenance of hepatocyte functional activity in co-culture: requirements for sinusoidal endothelial cells and dexamethasone. *J Cell Physiol* **129**, 103-110
45. Nahmias, Y., Schwartz, R. E., Hu, W. S., Verfaillie, C. M., and Odde, D. J. (2006) Endothelium-mediated hepatocyte recruitment in the establishment of liver-like tissue in vitro. *Tissue Eng* **12**, 1627-1638
46. Rojkind, M., Novikoff, P. M., Greenwel, P., Rubin, J., Rojas-Valencia, L., de Carvalho, A. C., Stockert, R., Spray, D., Hertzberg, E. L., and Wolkoff, A. W. (1995) Characterization and functional studies on rat liver fat-storing cell line and freshly isolated hepatocyte coculture system. *Am J Pathol* **146**, 1508-1520
47. Zinchenko, Y. S., and Coger, R. N. (2005) Engineering micropatterned surfaces for the coculture of hepatocytes and Kupffer cells. *J Biomed Mater Res A* **75**, 242-248
48. Zinchenko, Y. S., Schrum, L. W., Clemens, M., and Coger, R. N. (2006) Hepatocyte and kupffer cells co-cultured on micropatterned surfaces to optimize hepatocyte function. *Tissue Eng* **12**, 751-761
49. Shimaoka, S., Nakamura, T., and Ichihara, A. (1987) Stimulation of growth of primary cultured adult rat hepatocytes without growth factors by coculture with nonparenchymal liver cells. *Exp Cell Res* **172**, 228-242
50. Kuri-Harcuch, W., and Mendoza-Figueroa, T. (1989) Cultivation of adult rat hepatocytes on 3T3 cells: expression of various liver differentiated functions. *Differentiation* **41**, 148-157

51. Goulet, F., Normand, C., and Morin, O. (1988) Cellular interactions promote tissue-specific function, biomatrix deposition and junctional communication of primary cultured hepatocytes. *Hepatology* **8**, 1010-1018
52. Griffith, L. G., Wu, B., Cima, M. J., Powers, M. J., Chaignaud, B., and Vacanti, J. P. (1997) In vitro organogenesis of liver tissue. *Ann N Y Acad Sci* **831**, 382-397
53. Bhatia, S. N., Yarmush, M. L., and Toner, M. (1997) Controlling cell interactions by micropatterning in co-cultures: hepatocytes and 3T3 fibroblasts. *J Biomed Mater Res* **34**, 189-199
54. Lee, J., Morgan, J. R., Tompkins, R. G., and Yarmush, M. L. (1993) Proline-mediated enhancement of hepatocyte function in a collagen gel sandwich culture configuration. *FASEB J* **7**, 586-591
55. Hirose, M., Yamato, M., Kwon, O. H., Harimoto, M., Kushida, A., Shimizu, T., Kikuchi, A., and Okano, T. (2000) Temperature-Responsive surface for novel co-culture systems of hepatocytes with endothelial cells: 2-D patterned and double layered co-cultures. *Yonsei Med J* **41**, 803-813
56. Harimoto, M., Yamato, M., Hirose, M., Takahashi, C., Isoi, Y., Kikuchi, A., and Okano, T. (2002) Novel approach for achieving double-layered cell sheets co-culture: overlaying endothelial cell sheets onto monolayer hepatocytes utilizing temperature-responsive culture dishes. *J Biomed Mater Res* **62**, 464-470
57. Ohashi, K., Yokoyama, T., Yamato, M., Kuge, H., Kanehiro, H., Tsutsumi, M., Amanuma, T., Iwata, H., Yang, J., Okano, T., and Nakajima, Y. (2007) Engineering functional two- and three-dimensional liver systems in vivo using hepatic tissue sheets. *Nat Med* **13**, 880-885
58. Ito, A., Takizawa, Y., Honda, H., Hata, K., Kagami, H., Ueda, M., and Kobayashi, T. (2004) Tissue engineering using magnetite nanoparticles and magnetic force: heterotypic layers of cocultured hepatocytes and endothelial cells. *Tissue Eng* **10**, 833-840
59. Ito, A., Ino, K., Hayashida, M., Kobayashi, T., Matsunuma, H., Kagami, H., Ueda, M., and Honda, H. (2005) Novel methodology for fabrication of tissue-engineered tubular constructs using magnetite nanoparticles and magnetic force. *Tissue Eng* **11**, 1553-1561
60. Sechser, A., Osorio, J., Freise, C., and Osorio, R. W. (2001) Artificial liver support devices for fulminant liver failure. *Clin Liver Dis* **5**, 415-430
61. Corlu, A., Ilyin, G., Cariou, S., Lamy, I., Loyer, P., and Guguen-Guillouzo, C. (1997) The coculture: a system for studying the regulation of liver differentiation/proliferation activity and its control. *Cell Biol Toxicol* **13**, 235-242
62. Khetani, S. R., Szulgit, G., Del Rio, J. A., Barlow, C., and Bhatia, S. N. (2004) Exploring interactions between rat hepatocytes and nonparenchymal cells using gene expression profiling. *Hepatology* **40**, 545-554
63. Tilles, A. W., Baskaran, H., Roy, P., Yarmush, M. L., and Toner, M. (2001) Effects of oxygenation and flow on the viability and function of rat hepatocytes cocultured in a microchannel flat-plate bioreactor. *Biotechnol Bioeng* **73**, 379-389
64. Zaret, K. S. (2002) Regulatory phases of early liver development: paradigms of organogenesis. *Nat Rev Genet* **3**, 499-512
65. Cleaver, O., and Melton, D. A. (2003) Endothelial signaling during development. *Nat Med* **9**, 661-668
66. Matsumoto, K., Yoshitomi, H., Rossant, J., and Zaret, K. S. (2001) Liver organogenesis promoted by endothelial cells prior to vascular function. *Science* **294**, 559-563

67. Ross, M. A., Sander, C. M., Kleeb, T. B., Watkins, S. C., and Stolz, D. B. (2001) Spatiotemporal expression of angiogenesis growth factor receptors during the revascularization of regenerating rat liver. *Hepatology* **34**, 1135-1148
68. Nahmias, Y., Casali, M., Barbe, L., Berthiaume, F., and Yarmush, M. L. (2006) Liver endothelial cells promote LDL-R expression and the uptake of HCV-like particles in primary rat and human hepatocytes. *Hepatology* **43**, 257-265
69. Shimizu, T., Yamato, M., Kikuchi, A., and Okano, T. (2003) Cell sheet engineering for myocardial tissue reconstruction. *Biomaterials* **24**, 2309-2316
70. Shimizu, T., Yamato, M., Isoi, Y., Akutsu, T., Setomaru, T., Abe, K., Kikuchi, A., Umezu, M., and Okano, T. (2002) Fabrication of pulsatile cardiac tissue grafts using a novel 3-dimensional cell sheet manipulation technique and temperature-responsive cell culture surfaces. *Circ Res* **90**, e40
71. Wilson, W. C., and Boland, T. (2003) Cell and organ printing 1: Protein and cell printers. *Anatomical Record Part a-Discoveries in Molecular Cellular and Evolutionary Biology* **272A**, 491-496
72. Boland, T., Mironov, V., Gutowska, A., Roth, E. A., and Markwald, R. R. (2003) Cell and organ printing 2: Fusion of cell aggregates in three-dimensional gels. *Anatomical Record Part a-Discoveries in Molecular Cellular and Evolutionary Biology* **272A**, 497-502
73. Rajagopalan, P., Shen, C. J., Berthiaume, F., Tilles, A. W., Toner, M., and Yarmush, M. L. (2006) Polyelectrolyte nano-scaffolds for the design of layered cellular architectures. *Tissue Eng* **12**, 1553-1563
74. Chung, T. W., Yang, J., Akaike, T., Cho, K. Y., Nah, J. W., Kim, S. I., and Cho, C. S. (2002) Preparation of alginate/galactosylated chitosan scaffold for hepatocyte attachment. *Biomaterials* **23**, 2827-2834
75. Park, I. K., Yang, J., Jeong, H. J., Bom, H. S., Harada, I., Akaike, T., Kim, S. I., and Cho, C. S. (2003) Galactosylated chitosan as a synthetic extracellular matrix for hepatocytes attachment. *Biomaterials* **24**, 2331-2337
76. Park, I. K., Kim, T. H., Park, Y. H., Shin, B. A., Choi, E. S., Chowdhury, E. H., Akaike, T., and Cho, C. S. (2001) Galactosylated chitosan-graft-poly(ethylene glycol) as hepatocyte-targeting DNA carrier. *J Control Release* **76**, 349-362
77. Joddar, B., and Ramamurthi, A. (2006) Elastogenic effects of exogenous hyaluronan oligosaccharides on vascular smooth muscle cells. *Biomaterials* **27**, 5698-5707
78. Remuzzi, A., Mantero, S., Colombo, M., Morigi, M., Binda, E., Camozzi, D., and Imberti, B. (2004) Vascular smooth muscle cells on hyaluronic acid: culture and mechanical characterization of an engineered vascular construct. *Tissue Eng* **10**, 699-710
79. Sauerbrey, G. (1959) Verwendung von Schwingquarzen zur Wägung Dünner Schichten und zur Mikrowägung. *Zeitschrift für Physik A Hadrons and Nuclei* **155**, 206-222
80. Voinova, M. V., Rodahl, M., Jonson, M., and Kasemo, B. (1999) Viscoelastic acoustic response of layered polymer films at fluid-solid interfaces: Continuum mechanics approach. *Physica Scripta* **59**, 391-396
81. de Kerchove, A. J., and Elimelech, M. (2007) Formation of polysaccharide gel layers in the presence of Ca2+ and K+ ions: Measurements and mechanisms. *Biomacromolecules* **8**, 113-121

82. Munro, J. C., and Frank, C. W. (2004) Polyacrylamide adsorption from aqueous solutions on gold and silver surfaces monitored by the quartz crystal microbalance. *Macromolecules* **37**, 925-938
83. Behnia, K., Bhatia, S., Jastromb, N., Balis, U., Sullivan, S., Yarmush, M., and Toner, M. (2000) Xenobiotic metabolism by cultured primary porcine hepatocytes. *Tissue Eng* **6**, 467-479
84. Green, D. W., and Perry, R. H. (2008) *Perry's Chemical Engineers' Handbook*, McGraw-Hill, New York, NY
85. Khetani, S. R., and Bhatia, S. N. (2008) Microscale culture of human liver cells for drug development. *Nat Biotechnol* **26**, 120-126
86. Liu, X., LeCluyse, E. L., Brouwer, K. R., Gan, L. S., Lemasters, J. J., Stieger, B., Meier, P. J., and Brouwer, K. L. (1999) Biliary excretion in primary rat hepatocytes cultured in a collagen-sandwich configuration. *Am J Physiol* **277**, G12-21
87. Hwa, A. J., Fry, R. C., Sivaraman, A., So, P. T., Samson, L. D., Stolz, D. B., and Griffith, L. G. (2007) Rat liver sinusoidal endothelial cells survive without exogenous VEGF in 3D perfused co-cultures with hepatocytes. *FASEB J* **21**, 2564-2579
88. Smedsrod, B., Melkko, J., Araki, N., Sano, H., and Horiuchi, S. (1997) Advanced glycation end products are eliminated by scavenger-receptor-mediated endocytosis in hepatic sinusoidal Kupffer and endothelial cells. *Biochem J* **322 (Pt 2)**, 567-573
89. Seternes, T., Sorensen, K., and Smedsrod, B. (2002) Scavenger endothelial cells of vertebrates: a nonperipheral leukocyte system for high-capacity elimination of waste macromolecules. *Proc Natl Acad Sci U S A* **99**, 7594-7597
90. Elvevold, K. H., Nedredal, G. I., Revhaug, A., and Smedsrod, B. (2004) Scavenger properties of cultivated pig liver endothelial cells. *Comp Hepatol* **3**, 4
91. Nava, A., Mazza, E., Furrer, M., Villiger, P., and Reinhart, W. H. (2008) In vivo mechanical characterization of human liver. *Med Image Anal* **12**, 203-216
92. Sandrin, L., Fourquet, B., Hasquenoph, J. M., Yon, S., Fournier, C., Mal, F., Christidis, C., Ziol, M., Poulet, B., Kazemi, F., Beaugrand, M., and Palau, R. (2003) Transient elastography: a new noninvasive method for assessment of hepatic fibrosis. *Ultrasound Med Biol* **29**, 1705-1713
93. Chen, A. A., Khetani, S. R., Lee, S., Bhatia, S. N., and Van Vliet, K. J. (2009) Modulation of hepatocyte phenotype in vitro via chemomechanical tuning of polyelectrolyte multilayers. *Biomaterials* **30**, 1113-1120
94. Pa, J. H., and Yu, T. L. (2001) Light scattering study of chitosan in acetic acid aqueous solutions. *Macromolecular Chemistry and Physics* **202**, 985-991
95. Lee, S. B., Lee, Y. M., Song, K. W., and Park, M. H. (2003) Preparation and properties of polyelectrolyte complex sponges composed of hyaluronic acid and chitosan and their biological behaviors. *Journal of Applied Polymer Science* **90**, 925-932
96. Omiecinski, C. J., Remmel, R. P., and Hosagrahara, V. P. (1999) Concise review of the cytochrome P450s and their roles in toxicology. *Toxicological Sciences* **48**, 151-156
97. Thummel, K. E., and Wilkinson, G. R. (1998) In vitro and in vivo drug interactions involving human CYP3A. *Annual Review of Pharmacology and Toxicology* **38**, 389-430
98. Rendic, S., and DiCarlo, F. J. (1997) Human cytochrome P450 enzymes: A status report summarizing their reactions, substrates, inducers, and inhibitors. *Drug Metabolism Reviews* **29**, 413-580

99. Rahman, A., Korzekwa, K. R., Grogan, J., Gonzalez, F. J., and Harris, J. W. (1994) Selective Biotransformation of Taxol to 6-Alpha-Hydroxytaxol by Human Cytochrome-P450 2c8. *Cancer Research* **54**, 5543-5546
100. Nahmias, Y., Schwartz, R. E., Verfaillie, C. M., and Odde, D. J. (2005) Laser-guided direct writing for three-dimensional tissue engineering. *Biotechnology and Bioengineering* **92**, 129-136
101. Nahmias, Y., and Odde, D. J. (2006) Micropatterning of living cells by laser-guided direct writing: application to fabrication of hepatic-endothelial sinusoid-like structures. *Nat Protoc* **1**, 2288-2296
102. Arias, I. M., Boyer, J. L., Chisari, F. V., Fausto, M., Schachter, D., and Shafritz, D. A. (2001) *The liver: biology and pathobiology*, Lippincott Williams and Wilkins
103. Dunn, J. C., Tompkins, R. G., and Yarmush, M. L. (1992) Hepatocytes in collagen sandwich: evidence for transcriptional and translational regulation. *J Cell Biol* **116**, 1043-1053
104. Chang, T. T., and Hughes-Fulford, M. (2008) Monolayer and Spheroid Culture of Human Liver Hepatocellular Carcinoma Cell Line Cells Demonstrate Distinct Global Gene Expression Patterns and Functional Phenotypes. *Tissue Eng Part A* **15**, 559-567
105. Baker, T. K., Carfagna, M. A., Gao, H., Dow, E. R., Li, Q., Searfoss, G. H., and Ryan, T. P. (2001) Temporal gene expression analysis of monolayer cultured rat hepatocytes. *Chem Res Toxicol* **14**, 1218-1231
106. Li, Z., Srivastava, S., Yang, X., Mittal, S., Norton, P., Resau, J., Haab, B., and Chan, C. (2007) A hierarchical approach employing metabolic and gene expression profiles to identify the pathways that confer cytotoxicity in HepG2 cells. *BMC Syst Biol* **1**, 21
107. Subramanian, A., Tamayo, P., Mootha, V. K., Mukherjee, S., Ebert, B. L., Gillette, M. A., Paulovich, A., Pomeroy, S. L., Golub, T. R., Lander, E. S., and Mesirov, J. P. (2005) Gene set enrichment analysis: a knowledge-based approach for interpreting genome-wide expression profiles. *Proc Natl Acad Sci U S A* **102**, 15545-15550
108. Dinu, I., Potter, J. D., Mueller, T., Liu, Q., Adewale, A. J., Jhangri, G. S., Einecke, G., Famulski, K. S., Halloran, P., and Yasui, Y. (2009) Gene-set analysis and reduction. *Brief Bioinform* **10**, 24-34
109. Abatangelo, L., Maglietta, R., Distaso, A., D'Addabbo, A., Creanza, T. M., Mukherjee, S., and Ancona, N. (2009) Comparative study of gene set enrichment methods. *BMC Bioinformatics* **10**, 275
110. Gentleman, R. C., Carey, V. J., Bates, D. M., Bolstad, B., Dettling, M., Dudoit, S., Ellis, B., Gautier, L., Ge, Y., Gentry, J., Hornik, K., Hothorn, T., Huber, W., Iacus, S., Irizarry, R., Leisch, F., Li, C., Maechler, M., Rossini, A. J., Sawitzki, G., Smith, C., Smyth, G., Tierney, L., Yang, J. Y., and Zhang, J. (2004) Bioconductor: open software development for computational biology and bioinformatics. *Genome Biol* **5**, R80
111. Smyth, G. K. (2005) Limma: linear models for microarray data. In *Bioinformatics and Computational Biology Solutions Using R and Bioconductor* (Gentlemen, R., Carey, V., Dudoit, S., Irizarry, R., and Huber, W., eds) pp. 397-420, Springer, New York
112. Knuth, D. E. (1998) *The Art of Computer Programming, Vol 2: Seminumerical Algorithms*, Addison Wesley, Reading, MA
113. Hsiao, L. L., Dangond, F., Yoshida, T., Hong, R., Jensen, R. V., Misra, J., Dillon, W., Lee, K. F., Clark, K. E., Haverty, P., Weng, Z., Mutter, G. L., Frosch, M. P., Macdonald, M. E., Milford, E. L., Crum, C. P., Bueno, R., Pratt, R. E., Mahadevappa, M., Warrington,

J. A., Stephanopoulos, G., and Gullans, S. R. (2001) A compendium of gene expression in normal human tissues. *Physiol Genomics* **7**, 97-104
114. Su, A. I., Cooke, M. P., Ching, K. A., Hakak, Y., Walker, J. R., Wiltshire, T., Orth, A. P., Vega, R. G., Sapinoso, L. M., Moqrich, A., Patapoutian, A., Hampton, G. M., Schultz, P. G., and Hogenesch, J. B. (2002) Large-scale analysis of the human and mouse transcriptomes. *Proc Natl Acad Sci U S A* **99**, 4465-4470
115. Angrand, P. O., Rousset, J. P., and Weiss, M. C. (1992) Cell phenotype, binding affinity and promoter structure modulate transactivation by HNF1 and LAP. *J Cell Sci* **103 (Pt 4)**, 1083-1092
116. Wu, K. J., Wilson, D. R., Shih, C., and Darlington, G. J. (1994) The transcription factor HNF1 acts with C/EBP alpha to synergistically activate the human albumin promoter through a novel domain. *J Biol Chem* **269**, 1177-1182
117. Chawla, A., Repa, J. J., Evans, R. M., and Mangelsdorf, D. J. (2001) Nuclear receptors and lipid physiology: opening the X-files. *Science* **294**, 1866-1870
118. Chiang, J. Y. (2003) Bile acid regulation of hepatic physiology: III. Bile acids and nuclear receptors. *Am J Physiol Gastrointest Liver Physiol* **284**, G349-356
119. Ory, D. S. (2004) Nuclear receptor signaling in the control of cholesterol homeostasis: have the orphans found a home? *Circ Res* **95**, 660-670
120. Kalaany, N. Y., and Mangelsdorf, D. J. (2006) LXRS and FXR: the yin and yang of cholesterol and fat metabolism. *Annu Rev Physiol* **68**, 159-191
121. Russell, D. W. (1999) Nuclear orphan receptors control cholesterol catabolism. *Cell* **97**, 539-542
122. Zelcer, N., and Tontonoz, P. (2006) Liver X receptors as integrators of metabolic and inflammatory signaling. *J Clin Invest* **116**, 607-614
123. Lefebvre, P., Cariou, B., Lien, F., Kuipers, F., and Staels, B. (2009) Role of bile acids and bile acid receptors in metabolic regulation. *Physiol Rev* **89**, 147-191
124. Lu, T. T., Makishima, M., Repa, J. J., Schoonjans, K., Kerr, T. A., Auwerx, J., and Mangelsdorf, D. J. (2000) Molecular basis for feedback regulation of bile acid synthesis by nuclear receptors. *Mol Cell* **6**, 507-515
125. Goodwin, B., Jones, S. A., Price, R. R., Watson, M. A., McKee, D. D., Moore, L. B., Galardi, C., Wilson, J. G., Lewis, M. C., Roth, M. E., Maloney, P. R., Willson, T. M., and Kliewer, S. A. (2000) A regulatory cascade of the nuclear receptors FXR, SHP-1, and LRH-1 represses bile acid biosynthesis. *Mol Cell* **6**, 517-526
126. Wolfrum, C., Borrmann, C. M., Borchers, T., and Spener, F. (2001) Fatty acids and hypolipidemic drugs regulate peroxisome proliferator-activated receptors alpha - and gamma-mediated gene expression via liver fatty acid binding protein: a signaling path to the nucleus. *Proc Natl Acad Sci U S A* **98**, 2323-2328
127. Gervois, P., Torra, I. P., Fruchart, J. C., and Staels, B. (2000) Regulation of lipid and lipoprotein metabolism by PPAR activators. *Clin Chem Lab Med* **38**, 3-11
128. Willson, T. M., Brown, P. J., Sternbach, D. D., and Henke, B. R. (2000) The PPARs: from orphan receptors to drug discovery. *J Med Chem* **43**, 527-550
129. Francis, G. A., Fayard, E., Picard, F., and Auwerx, J. (2003) Nuclear receptors and the control of metabolism. *Annu Rev Physiol* **65**, 261-311
130. Tugwood, J. D., Issemann, I., Anderson, R. G., Bundell, K. R., McPheat, W. L., and Green, S. (1992) The mouse peroxisome proliferator activated receptor recognizes a

response element in the 5' flanking sequence of the rat acyl CoA oxidase gene. *EMBO J* **11**, 433-439
131. Bardot, O., Aldridge, T. C., Latruffe, N., and Green, S. (1993) PPAR-RXR heterodimer activates a peroxisome proliferator response element upstream of the bifunctional enzyme gene. *Biochem Biophys Res Commun* **192**, 37-45
132. Hashimoto, T., Fujita, T., Usuda, N., Cook, W., Qi, C., Peters, J. M., Gonzalez, F. J., Yeldandi, A. V., Rao, M. S., and Reddy, J. K. (1999) Peroxisomal and mitochondrial fatty acid beta-oxidation in mice nullizygous for both peroxisome proliferator-activated receptor alpha and peroxisomal fatty acyl-CoA oxidase. Genotype correlation with fatty liver phenotype. *J Biol Chem* **274**, 19228-19236
133. Kersten, S., Seydoux, J., Peters, J. M., Gonzalez, F. J., Desvergne, B., and Wahli, W. (1999) Peroxisome proliferator-activated receptor alpha mediates the adaptive response to fasting. *J Clin Invest* **103**, 1489-1498
134. Brandt, J. M., Djouadi, F., and Kelly, D. P. (1998) Fatty acids activate transcription of the muscle carnitine palmitoyltransferase I gene in cardiac myocytes via the peroxisome proliferator-activated receptor alpha. *J Biol Chem* **273**, 23786-23792
135. Gyamfi, M. A., Kocsis, M. G., He, L., Dai, G., Mendy, A. J., and Wan, Y. J. (2006) The role of retinoid X receptor alpha in regulating alcohol metabolism. *J Pharmacol Exp Ther* **319**, 360-368
136. Lieber, C. S. (2000) ALCOHOL: its metabolism and interaction with nutrients. *Annu Rev Nutr* **20**, 395-430
137. Nagy, L. E. (2004) Molecular aspects of alcohol metabolism: transcription factors involved in early ethanol-induced liver injury. *Annu Rev Nutr* **24**, 55-78
138. Liu, C., Russell, R. M., Seitz, H. K., and Wang, X. D. (2001) Ethanol enhances retinoic acid metabolism into polar metabolites in rat liver via induction of cytochrome P4502E1. *Gastroenterology* **120**, 179-189
139. Lieber, C. S. (1997) Cytochrome P-4502E1: its physiological and pathological role. *Physiol Rev* **77**, 517-544
140. Cariou, B., Duran-Sandoval, D., Kuipers, F., and Staels, B. (2005) Farnesoid X receptor: a new player in glucose metabolism? *Endocrinology* **146**, 981-983
141. Stayrook, K. R., Bramlett, K. S., Savkur, R. S., Ficorilli, J., Cook, T., Christe, M. E., Michael, L. F., and Burris, T. P. (2005) Regulation of carbohydrate metabolism by the farnesoid X receptor. *Endocrinology* **146**, 984-991
142. Konno, Y., Negishi, M., and Kodama, S. (2008) The roles of nuclear receptors CAR and PXR in hepatic energy metabolism. *Drug Metab Pharmacokinet* **23**, 8-13
143. Claudel, T., Staels, B., and Kuipers, F. (2005) The Farnesoid X receptor: a molecular link between bile acid and lipid and glucose metabolism. *Arterioscler Thromb Vasc Biol* **25**, 2020-2030
144. Yamagata, K., Daitoku, H., Shimamoto, Y., Matsuzaki, H., Hirota, K., Ishida, J., and Fukamizu, A. (2004) Bile acids regulate gluconeogenic gene expression via small heterodimer partner-mediated repression of hepatocyte nuclear factor 4 and Foxo1. *J Biol Chem* **279**, 23158-23165
145. Desvergne, B., Michalik, L., and Wahli, W. (2006) Transcriptional regulation of metabolism. *Physiol Rev* **86**, 465-514
146. Morris, S. M., Jr. (2002) Regulation of enzymes of the urea cycle and arginine metabolism. *Annu Rev Nutr* **22**, 87-105

147. Schimke, R. T. (1962) Adaptive characteristics of urea cycle enzymes in the rat. *J Biol Chem* **237**, 459-468
148. Krebs, H. A. (1935) Metabolism of amino-acids: The synthesis of glutamine from glutamic acid and ammonia, and the enzymic hydrolysis of glutamine in animal tissues. *Biochem J* **29**, 1951-1969
149. Haussinger, D. (1990) Nitrogen metabolism in liver: structural and functional organization and physiological relevance. *Biochem J* **267**, 281-290
150. Saheki, T., and Katunuma, N. (1975) Analysis of regulatory factors for urea synthesis by isolated perfused rat liver. I. Urea synthesis with ammonia and glutamine as nitrogen sources. *J Biochem* **77**, 659-669
151. Omiecinski, C. J., Remmel, R. P., and Hosagrahara, V. P. (1999) Concise review of the cytochrome P450s and their roles in toxicology. *Toxicol Sci* **48**, 151-156
152. Thummel, K. E., and Wilkinson, G. R. (1998) In vitro and in vivo drug interactions involving human CYP3A. *Annu Rev Pharmacol Toxicol* **38**, 389-430
153. Rendic, S., and Di Carlo, F. J. (1997) Human cytochrome P450 enzymes: a status report summarizing their reactions, substrates, inducers, and inhibitors. *Drug Metab Rev* **29**, 413-580
154. Wang, X. J., Hodgkinson, C. P., Wright, M. C., and Paine, A. J. (1997) Temperature-sensitive mRNA degradation is an early event in hepatocyte de-differentiation. *Biochem J* **328 (Pt 3)**, 937-944
155. Tuschl, G., and Mueller, S. O. (2006) Effects of cell culture conditions on primary rat hepatocytes-cell morphology and differential gene expression. *Toxicology* **218**, 205-215
156. Benjamini, Y., and Hochberg, Y. (1995) Controlling the false discovery rate: a practical and powerful approach to multiple testing. *Journal of the Royal Statistical Society, Series B (Methodological)* **57**, 289-300
157. Fraser, R., Dobbs, B. R., and Rogers, G. W. (1995) Lipoproteins and the liver sieve: the role of the fenestrated sinusoidal endothelium in lipoprotein metabolism, atherosclerosis, and cirrhosis. *Hepatology* **21**, 863-874
158. McCuskey, R. S. (2006) Sinusoidal endothelial cells as an early target for hepatic toxicants. *Clin Hemorheol Microcirc* **34**, 5-10
159. LeCouter, J., Moritz, D. R., Li, B., Phillips, G. L., Liang, X. H., Gerber, H. P., Hillan, K. J., and Ferrara, N. (2003) Angiogenesis-independent endothelial protection of liver: role of VEGFR-1. *Science* **299**, 890-893
160. Wisse, E., Braet, F., and Dianzhong, I. (1999) *Endothelial cells of the hepatic sinusoids: a review. liver diseases and hepatic sinusoidal cells*, Springer-Verlag, Tokyo
161. Rieder, H., Meyer zum Buschenfelde, K. H., and Ramadori, G. (1992) Functional spectrum of sinusoidal endothelial liver cells. Filtration, endocytosis, synthetic capacities and intercellular communication. *J Hepatol* **15**, 237-250
162. Gao, W., Bentley, R. C., Madden, J. F., and Clavien, P. A. (1998) Apoptosis of sinusoidal endothelial cells is a critical mechanism of preservation injury in rat liver transplantation. *Hepatology* **27**, 1652-1660
163. Sellaro, T. L., Ranade, A., Faulk, D. M., McCabe, G. P., Dorko, K., Badylak, S. F., and Strom, S. C. (2010) Maintenance of human hepatocyte function in vitro by liver-derived extracellular matrix gels. *Tissue Eng Part A* **16**, 1075-1082

164. McGuire, R. F., Bissell, D. M., Boyles, J., and Roll, F. J. (1992) Role of extracellular matrix in regulating fenestrations of sinusoidal endothelial cells isolated from normal rat liver. *Hepatology* **15**, 989-997
165. Sellaro, T. L., Ravindra, A. K., Stolz, D. B., and Badylak, S. F. (2007) Maintenance of hepatic sinusoidal endothelial cell phenotype in vitro using organ-specific extracellular matrix scaffolds. *Tissue Eng* **13**, 2301-2310
166. March, S., Hui, E. E., Underhill, G. H., Khetani, S., and Bhatia, S. N. (2009) Microenvironmental regulation of the sinusoidal endothelial cell phenotype in vitro. *Hepatology* **50**, 920-928
167. DeLeve, L. D., Wang, X., Hu, L., McCuskey, M. K., and McCuskey, R. S. (2004) Rat liver sinusoidal endothelial cell phenotype is maintained by paracrine and autocrine regulation. *Am J Physiol Gastrointest Liver Physiol* **287**, G757-763
168. Kim, Y., Larkin, A. L., Davis, R. M., and Rajagopalan, P. (2010) The design of in Vitro liver sinusoid mimics using chitosan-hyaluronic acid polyelectrolyte multilayers. *Tissue Eng Part A* **16**(9), 2731-41.
169. Wang, S., Nagrath, D., Chen, P. C., Berthiaume, F., and Yarmush, M. L. (2008) Three-dimensional primary hepatocyte culture in synthetic self-assembling peptide hydrogel. *Tissue Eng Part A* **14**, 227-236
170. Ohmura, T., Enomoto, K., Satoh, H., Sawada, N., and Mori, M. (1993) Establishment of a novel monoclonal antibody, SE-1, which specifically reacts with rat hepatic sinusoidal endothelial cells. *J Histochem Cytochem* **41**, 1253-1257
171. Rajagopalan, P., Berthiaume, F., Tilles, A. W., Toner, M., and Yarmush, M. L. (2005) Selective enhancement of cytochrome p-450 activity in rat hepatocytes by in vitro heat shock. *Tissue Eng* **11**, 1527-1534
172. Thomas, C., Pellicciari, R., Pruzanski, M., Auwerx, J., and Schoonjans, K. (2008) Targeting bile-acid signalling for metabolic diseases. *Nat Rev Drug Discov* **7**, 678-693
173. Hofmann, A. F., and Hagey, L. R. (2008) Bile acids: chemistry, pathochemistry, biology, pathobiology, and therapeutics. *Cell Mol Life Sci* **65**, 2461-2483
174. Deo, A. K., and Bandiera, S. M. (2008) Identification of human hepatic cytochrome p450 enzymes involved in the biotransformation of cholic and chenodeoxycholic acid. *Drug Metab Dispos* **36**, 1983-1991
175. Zimniak, P., Holsztynska, E. J., Radominska, A., Iscan, M., Lester, R., and Waxman, D. J. (1991) Distinct forms of cytochrome P-450 are responsible for 6 beta-hydroxylation of bile acids and of neutral steroids. *Biochem J* **275 (Pt 1)**, 105-111
176. Chang, T. T., and Hughes-Fulford, M. (2009) Monolayer and Spheroid Culture of Human Liver Hepatocellular Carcinoma Cell Line Cells Demonstrate Distinct Global Gene Expression Patterns and Functional Phenotypes. *Tissue Engineering Part A* **15**, 559-567
177. Kim, Y., Lasher, C. D., Milford, L. M., Murali, T. M., and Rajagopalan, P. A Comparative Study of Genome-Wide Transcriptional Profiles of Primary Hepatocytes in Collagen Sandwich and Monolayer Cultures. *Tissue Eng Part C Methods*. Epub of Ahead
178. Natsoulis, G., Pearson, C. I., Gollub, J., B, P. E., Ferng, J., Nair, R., Idury, R., Lee, M. D., Fielden, M. R., Brennan, R. J., Roter, A. H., and Jarnagin, K. (2008) The liver pharmacological and xenobiotic gene response repertoire. *Mol Syst Biol* **4**, 175